LOAD TESTING OF DEEP FOUNDATIONS

USING

OSTERBERG CELL (O-CELL)

TEST METHOD

Interim Report

Dr. Dan A. Brown

Ms. Lijun Shi

Highway Research Center
Harbert Engineering Center
Auburn University, Alabama 36849-5337

Sept. 2001

Load Testing of Deep Foundations

Using

Osterberg Cell (O-cell)

Test Method

Interim Report

Dr. Dan A. Brown

Ms. Lijun Shi

Sept. 2001

Load Testing of Deep Foundations Using

Osterberg Cell (O-cell) Test Method

Interim Report

Abstract:

The attached report is published as an internal report of the Auburn University Highway Research Center. This report is a portion of the interim report on NCHRP Project 21-08, Innovative Load Testing Systems, and represents the AU HRC contribution to the overall project report through Geosciences Testing and Research, Inc. (GTR) of N. Chelmsford, MA.

OSTERBERG CELL (O-CELL) LOAD TESTING

INTRODUCTION

This portion of the research describes the work related to a critical assessment of the Osterberg Cell (O-cell) load testing technology. Named for its inventor, Dr. Jorj Osterberg, the O-cell load testing method involves the use of an embedded expendable jack which is cast within the test foundation. Although the method has occasionally been used with driven piles, the primary use of the technology is for drilled shaft foundations. As shown on Figure 1, this embedded jack is used to load one part of the shaft against the other so as to conduct a loading test without the need for independent reaction piles. In many cases (and increasingly in recent years), cells have been placed at multiple levels within the shaft in order to conduct loading tests of different isolated portions of the test shaft

The objectives of this interim report are to:

1. Review the current state of practice with respect to O-cell testing technology,

2. Perform an initial critical assessment of the test method, the interpretation of the results, and the use of the test results in design, and

3. Develop a revised work plan for phase II of the research.

The current state of practice is reviewed with emphasis on the use of the test method by state DOT's for highway project. This work has included telephone conversations with many state DOT geotechnical engineers as well as a search of the engineering literature.

The critical assessment of the method includes an effort toward identifying load test projects where comparative test methods have been used as well as a theoretical study of the O-cell testing method using nonlinear finite element models.

BACKGROUND

A review of the O-cell testing method and technology is provided by Osterberg, (1) which describes the test method and equipment. The use of O-cell testing for drilled shafts for highway bridges is also summarized by O'Neill and Reese, (2). The cell itself is composed of a large diameter pressure cell which contains a pressurized fluid (usually water or oil). The large diameter of the cell compared to conventional hydraulic jacks allows relatively large forces to be generated for a given pressure. Typical pressures of up to 10,000 psi are used although devices are now reportedly capable of up to 15,000 psi. Standard sizes are typically up to 32 inches diameter, and these may be used in parallel within a large diameter shaft (the writer is aware of a cloverleaf arrangement of 4 cells at a given elevation) to generate very large forces. The cell(s) are typically attached to the base of the rebar cage and tack-welded to hold the cell together until testing (at which time an initial loading to break the tack welds is required). With the multi-level approach, it is necessary to weld the upper cell(s) sufficiently to support the cage below to the lower cell level during installation. It is also necessary to provide a tremie bypass line so that concrete placement between and around the cells can be accomplished.

Embedded LVDT's are used to measure the relative displacement across the cell and have largely replaced the earlier practice of using telltales extending to the surface. Strain gauges are also commonly used to interpret the distribution of resistance along the

4

shaft. Vibrating-wire type instrumentation is generally used for O-cell testing, with monitoring by a computer-based data logger.

In the current practice in the United States, O-cell load testing is performed exclusively by Loadtest, Inc. as a turnkey operation. For highway projects, the actual location of cells, magnitudes of anticipated loads, and many other details of the load test setup are commonly specified by state DOT's or their consultants. Loadtest may sometimes provide input into the details of the test setup, but more often their input is either not sought or is very limited. Loadtest, Inc. is usually subcontracted as a specialty sub to the general contractor on the project.

State DOT Use

A number of interviews were conducted with geotechnical professionals employed with state DOT agencies in order to develop a general sense of the use of O-cell load testing technology. Not every state was contacted, but emphasis was placed on those states where the technology is known to be employed. The most widespread use appears to be in the southeastern states. Of these, Mississippi notably appears to be the largest user with O-cell testing routinely on perhaps 50 or more projects in the last 10 years. Most other southeastern (e.g., FL, GA, KY, NC, SC, VA) states have used O-cell testing on select larger projects involving drilled shafts. Several states (AL, NM, MN) have used O-cell testing rarely or only on a very few projects and do not consider its use routine. Some states have used O-cells in production shafts. A number of state geotech engineers perceive the use of O-cells for rock-socket drilled shafts to be an important use in light of the difficulty in quantifying the performance of such shafts. However, most

5

tests have actually been performed on sites in coastal deposits where large bridge projects and heavily loaded foundations are more common.

Most state geotech engineers who have utilized O-cell testing have tended to accept the measurements as indicative of axial performance of drilled shafts in conventional top down loading. Almost no comparative tests have been performed. New Mexico performed comparative tests on two shafts at a single location in dense sands; these test results will be discussed subsequently. Florida has and is currently sponsoring a research study at the University of Florida relating to O-cell and other test methods, but this research has generated no new comparative tests of O-cell and conventional top down static testing (there are some tests involving O-cell and statnamic measurements).

Comparative Test Data

There are numerous references to O-cell testing in the technical literature, most of the type which describe the technology as an innovative new method for testing with a subsequent case history of use on a project. The emphasis in this research was to search for published cases where comparative test data are available between O-cell testing and conventional testing, or where other critical examinations of the O-cell testing method have been described. Very few such papers exist, although several of interest are described below.

Hong Kong Railway (3), 2000.

Littlechild, Hill, Plumbridge, and Lee (3) describe a load test of shafts in Hong Kong which were socketed into rock as a part of a large scale load testing program on the Kowloon-Canton Railway. Five of these tests combined a kentledge top down test of a

shaft with an embedded O-cell (stage 1), followed by loading via the O-cell at the toe with the kentledge removed (stage 2), followed by loading via the O-cell plus the kentledge (stage 3) to fully engage the end bearing.

Two of these five shafts fully mobilized the side shear of the socket during stage 2, and one of these two had also fully mobilized the side shear of the socket during stage 1 prior to the stage 2 loading. Shaft TWW1 had a 2 m long socket within a highly fractured and weathered granodiorite (RQD = 0). Stage 1 loading via kentledge mobilized 800 KPa (about 8.4 tsf) of unit side shear at a displacement of approximately 50 mm after which a stage 2 loading upward from the O-cell mobilized a unit side shear of 1000 KPa (about 10.4 tsf) at a displacement of approximately 90 mm. The kentledge was then engaged to perform the stage 3 loading. Shaft TSW1 had a 1.5 m socket into a moderately strong, moderately to slightly weathered metasandstone (RQD = 35-74%). Stage 1 loading via kentledge mobilized 4200 KPa (about 44 tsf) of unit side shear at a displacement of only 8 mm; this was not considered to have produced yielding at the pile/soil interface. The stage 2 loading via O-cell mobilized 6000 KPa (about 63 tsf) of side resistance at a displacement of 10 mm and was observed to fail the socket as the resistance dropped dramatically to only about 2000 KPa (about 21 tsf) at a displacement of 18 mm. The authors attributed the strain softening behavior to break-out of a fractured rock cone around the socket due to the uplift loading. None of the other test shafts fully mobilized the side shear resistance.

In end bearing, only shaft TWW1 mobilized large displacements at the shaft base for both kentledge and O-cell loadings. The stage 1 kentledge loading of this shaft mobilized a base resistance of 12.9 Mpa (about 135 tsf) at a displacement of 62 mm (5%

7

of the shaft diameter), and stage 3 O-cell loading mobilized a maximum base resistance of 16Mpa (about 167 tsf) at a displacement of 86 mm (7% of the shaft diameter). The 86 mm displacement appears to have been measured with respect to the start of the stage 3 test, as a plot of the total movement (Fig. 7 in the paper) suggests that the load vs deflection response at the shaft base from the stage 3 loading provided an extension of the load vs deflection response from the stage 1 loading.

Downtown Hong Kong (4)

Ng, Rigby, Li, Yau, and Tang (4) report the results of tests in Hong Kong for some downtown buildings founded on weathered igneous and granitic rocks in which side shear values are measured and reported. Several of these load tests included both top down loading and O-cell loading.

One test in decomposed granite is reported in which a 1.5 m diameter shaft was loaded from the top down to mobilize large downward side shear, after which an embedded O-cell was expanded to mobilize side shear of the same shaft in the opposite direction. For the completely decomposed granite (avg SPT = 75 b/f), 60 kPa side shear (0.6 tsf) was mobilized during the downward loading at a displacement of around 6 mm. The O-cell loading mobilized approximately 105 kPa (1.1 tsf) at a similar absolute displacement upward, about 80% higher. However, the downward loading resulted in a permanent set in the shaft and if the displacement in the O-cell loading is considered with respect to the zero position at the start of the O-cell test rather than the absolute zero, then the O-cell loading mobilized a similar side shear at a similar displacement. The same is true for the lower portion of the shaft in the somewhat less highly decomposed granite

8

(avg SPT > 200 b/f), at somewhat higher values of mobilized unit side shear. The side shearing resistance of this shaft did not exhibit strain softening behavior.

Four shafts were tested using both top down and O-cell loading in weathered rocks. Only two of these shafts (both in granitic rock) achieved displacements in side shear exceeding 10 mm in both directions. Of the four shafts, three were loaded first by top down loading followed by O-cell, the fourth was loaded first by O-cell followed by top down. In each case, the second loading stage appeared to have been influenced by the first, in which the stiffness and stress-strain behavior differed from the initial loading. The authors concluded that the initial loading in these weathered rocks caused a loss of bond in the socket and the breaking off of asperities at the shaft/socket wall interface. The loss of bonding produced a hysteresis-induced softening related to the cyclic loading.

Ng, et al conclude that for the drilled shaft in granitic soil, the stiffness and mobilized side shear at the first and second stage loading is similar. However, for the drilled shafts in weathered rocks, both the stiffness and mobilized side shear is substantially lower during the second stage of a two-stage test due to the loss of bond produced during the initial stage of loading. These data suggest that direct comparisons of O-cell and top down loading from multi-directional tests on a single shaft can be problematic.

New Mexico (5)

The unpublished results of loading tests on two shafts for a bridge in New Mexico are reported by Meyer (5), and include top down loading followed by O-cell loading in the opposite direction. These two tests are at a single site and part of a study to compare drilling fluids (bentonite vs polymer). Each shaft was 30" diameter and 45 feet deep and

9

was constructed in the very dense saturated alluvium of the Rio Grande channel (sand/gravel/cobble). Standard penetration test values averaged around 50 b/6" over most of the length of the shafts. In each shaft the O-cell was placed at approximately the 2/3 depth point of the shaft. The testing sequence in each case was to conduct a top down loading to a displacement of at least 1.5 inches (5% of the shaft diameter), unload, perform a second top down loading to a total displacement of about 3 inches, unload, perform the O-cell loading. In both cases the O-cell produced failure of the upper 2/3 of the shaft in side shear with very small downward movement of the bottom 1/3 of the shaft (less than ½"). The O-cell was pumped to achieve an upward movement of the shaft of around 6 inches in each case.

Based on the interpreted strain gauge data, the top down loading of the upper shaft segment (upper 2/3 of the shaft) produced a maximum load transfer in side shear of around 440 and 550 tons in the bentonite and polymer shafts, respectively. The side shear vs displacement response was very nonlinear after about ½ inch of movement but was observed to increase in a strain-hardening manner to the maximum downward displacement at between 1.5 and 2 inches.

The O-cell loading in the upward direction indicated much lower maximum values of side shear, with totals of around 200 and 270 tons in the bentonite and polymer shafts, respectively. Values at displacements of between 1.5 and 2 inches were even lower; however, the load deflection curves clearly demonstrated the effect of the loading history as each curve exhibited an "S" shape with a local peak at around ½" of upward movement followed by additional hardening at 2 to 4 inches of upward movement as the earlier downward displacements were recovered. This behavior suggests that the top

down loading history had a substantial effect on the response of the shaft to the upward directed loading.

Singapore (6)

An unpublished project report prepared by Molnit and Lee (6) has been provided by Loadtest, Inc. in support of this research. This report provides a comparison between two 1.2 m diameter by 38 m long test shafts in a deep deposit of silty clay/clayey silt soil. The majority of capacity of these shafts is derived from side shear. One of these shafts was loaded to failure using a kentledge (dead weight) loading from the top down and the other was loaded via a multi-stage O-cell system. The load settlement response for this test was developed using load increments of approximately 10% of the maximum load and 1 hour hold periods at each load increment. Several increments were held for longer periods and the maximum load was maintained for 24 hours. The O-cell testing was performed using the normal procedure in which each of many smaller load increments are held for a period of 4 minutes. Thus, there is a potential for the kentledge test to exhibit somewhat softer response due to creep in the clayey bearing soils.

The kentledge system loaded shaft PTP15 to a total load of approximately 28 MN and developed a displacement at the top of the shaft of around 120 mm (10% of shaft diameter). The O-cell test produced a failure of the upper 27 m (above the upper O-cell level) and of the tip resistance (at the 38 m depth), but not of the lower portion of the shaft between the two O-cell levels between the depths of 27 m and 38 m. Assuming that this lower section of shaft was at a state of incipient failure, the projected top-down response from the O-cell testing reportedly indicates a displacement of around 100 mm at a total equivalent load of 28 MN. Even if this lower portion of the shaft were able to

11

support some additional load (which seems likely), it appears that the two tests produce reasonably similar results. Equivalent top-down load settlement curves were very similar, both showing the onset of large deformations at a load of around 20 MN and a displacement of around 25 mm. A portion of the increased settlement from the kentledge loading test is undoubtedly due to the longer sustained loading in these clay soils.

In spite of the differences relating to soil creep and possible lack of fully developing a small portion of the shaft resistance in the O-cell test, the Singapore tests probably provide the most direct comparison data available between the top-down and O-cell method. For this soft soil site, it appears reasonable to conclude that any differences between the two test methods (top-down vs O-cell) are likely to be less than 10% and this magnitude of difference between two different shafts can easily be attributed to site variability.

Osaka, Japan

Comparative tests at another deep soft soil site are reported by Kishida, Tsubakihara, and Ogura (7). These tests are on shafts of 1.2 m diameter and 38.5 m length, almost identical in size to the Singapore data. The soils are interbedded silts and clays in the upper 29 m, with significant dense sand layers interbedded with clay below that depth.

One test shaft was subjected to vertical compression loading (top-down), and had a "friction-cut" within the top 17 m. This appears to have been performed using an oversized hole with a casing inside, but some small amount of load transfer was still mobilized within this zone. A total top-down load of approximately 20 MN was applied to this shaft, producing a downward displacement of around 150 mm. Interpretation of

12

strain gauge instrumentation suggests that the pile tip mobilized just over 6 Mpa of unit end bearing at a tip displacement of around 75 mm (6% of the shaft diameter).

Two shafts were tested using an embedded O-cell placed very near the shaft base. One of these shafts had the "friction cut" in the upper 17 m as per the top-down test shaft and the other had no reduction in side shear. Both of the O-cell tests failed in end bearing without fully mobilizing the side shear capacity of these shafts. The two O-cell tip resistances were similar, and matched very closely with the interpreted response of the base of the top-down test (approximately 5.5 and 6.2 Mpa at a displacement equal to 7% of the shaft diameter). Unfortunately, the O-cell tests mobilized only 2 to 3 mm of displacement in side shear; unit side shear at these small displacements was in general agreement with the side shear at very small displacements in the top-down test, but full side resistance cannot be compared.

In summary, the Osaka tests suggest that the tip resistance mobilized during two O-cell tests in soil compare closely with that interpreted from a conventional top-down test of a similar shaft.

Tests in Florida Limestone

Knight, Puckett, Bennett, Robertson, and Spears (8) describe two projects in Florida in which both O-cell tests and top-down rapid loading tests are performed. All of the top-down tests were performed using the Statnamic device. There are no conventional static loading tests described in this paper. Tests were performed at a site near Tampa and another site in the Florida Panhandle. All of the shafts described are in Florida limestone, a notoriously variable bearing material which has solution cavities and extremely variable strength properties over small distances. Most of the tests described

13

in this paper have complicating factors that preclude a direct comparison of results. In some cases the O-cell test failed the side shear of the socket without mobilizing full end bearing, in others the end bearing failed without mobilizing side shear. Only one of the rapid top-down loading tests fully mobilized the ultimate shaft capacity (which would require mobilizing both end bearing and side shear, since these are developed simultaneously in a top down test). The authors described the highly variable nature of the limestone conditions in Florida, which suggests that even two shafts constructed very nearby are likely to have significantly different behavior. Side shear response in the limestone was also observed to yield in a very brittle fashion in some of the O-cell tests, an observation which suggests that multiple tests of a single test shaft in such material would be affected by load history.

The one test in which the Statnamic loading appeared to fully mobilize the shaft capacity was at the Gandy Bridge site near Tampa. This shaft was 48 inches diameter with a socket extending about 15 feet into limerock. The rapid loading of this shaft achieved over one inch of peak displacement with a permanent set of around 0.3 inches at the top of the shaft. Interpretation of strain gauge instrumentation suggests that an ultimate side shear resistance of around 11 tons per sq.ft. was mobilized. An O-cell test was performed on a similar 48 inch diameter shaft about 12 feet away. The O-cell test shaft encountered a layer of soft clayey soil within the intended "socket" and was interpreted to have an effective rock socket length of 10.6 feet. Tilting of the cell was noted during the test, suggesting an uneven resistance of either the socket or the base or both. The O-cell test indicated a maximum side shear of approximately 11 tons per sq. ft. at an upward movement of the socket of around 1 inch.

14

These results would appear to be in reasonably good agreement. However, caution should be exercised, as comparisons are difficult under such variable subsurface and construction conditions.

Summary of Comparative Field Test Data

Presented on Table 1 is a summary of the field test data described above. These data include a very few reports which are encouraging comparisons of O-cell loadings and top down loadings. Some data appear to indicate differences in behavior. However, it appears that much of the comparative side shear data from multi-directional tests on a single shaft (e.g., top down loading followed by O-cell loading in the opposite direction or vice versa) should be considered suspect because of possible hysteresis effects. It is not clear that such effects are problematic in all types of soils, but at least some of the discrepancies between top down and O-cell loadings can be attributed to this source. Of the three case histories which include comparative tests on separate shafts, the Singapore test was a multi-level O-cell with part of the O-cell loading directed downward (and not fully mobilizing all of the side shear), the Osaka tests did not achieve full mobilization of side shear, and the Tampa tests involve rapid loading rather than conventional static loading in a limestone formation which is known to be highly variable and difficult to characterize.

The available field data appear to be inadequate to draw definitive conclusions regarding the comparison of an upward directed O-cell loading and a conventional top down static test.

Finite Element Models of O-cell Testing

A significant part of the ongoing research is directed toward a comprehensive model of the O-cell using the finite element technique. This effort is intended to provide insight into the fundamental aspects of any potential differences between loading using the O-cell method and a conventional top down load, and to allow parametric study of some of the variables that may influence the results. The following sections provide a summary of the modeling work to date. A more detailed description of the model and results are provided in Appendix A.

Previous FE Models of O-cell Testing

McVay, Huang, and Casper (8) have performed numerical simulations of O-cell and conventional static axial load testing in Florida limestone. These simulations include the use of a finite element code developed by the authors to model Florida limestone using an elastic-plastic constitutive model with a capped yielding (Drucker-Prager) surface and a tension cutoff. The FE model is an axisymmetric model with the shaft bound to the limestone without the use of a contact surface. Thus failure at the shaft/rock interface is exclusively modeled as failure of the rock material itself, a characteristic the authors thought to be representative of shafts in this rough limestone material.

Comparisons of this model between a top down loading and an O-cell loading lead the authors to conclude that the limiting side shear in the limestone was similar where failure occurs at the shaft/rock interface. Near the top of the rock socket in the upward loading case, a cone breakout failure was observed in which the failure propagated away from the shaft/rock interface to produce tensile failure in the surrounding rock. This condition results in lower "measured" side resistance from the O-

16

cell loading compared to a conventional top down loading, but is always on the conservative side. The authors conclude that this condition is most influential for relatively short sockets with length/diameter ratios on the order of 1.75 or less.

Fellenius, et al (9) reported the use of FE analysis to model an O-cell test of a rectangularly shaped, 2.4-m^2 cross section by 28 m long barrette in a deep deposit of residual soil. This analysis was performed using an elastic-plastic soil with a thin (0.1 m thick) layer of soil at the barrette/soil interface used in an attempt to model a slurry film at the interface. The FE model was back-calibrated to the results of the O-cell test (also utilizing some strain gauge data) in order to back fit effective-stress soil properties. Pore water pressures were taken as zero over most of the length of the foundation, as groundwater levels were at a depth of 26 m. The FE model was then used to simulate a conventional top down test of the barrette. The authors conclude that there was generally very little difference between the computed unit side shear values for the two types of tests and no appreciable difference between the two methods of loading in the soils below the barrette.

Description of FE Model for Current Research

The current research utilizes the general purpose code ABAQUS for analysis. This code is widely used in many fields of engineering and is particularly powerful for nonlinear problems. The model includes elastic-plastic soil behavior using an extended Drucker-Prager yield surface model as well as frictional contact surfaces at the shaft/soil interface. Particular attention has been focused upon the initial in-situ stress conditions in the soil. MSC/Patran is used as a pre- and post-processor for generating the mesh and presenting results graphically.

17

The axi-symmetric mesh developed for this research is shown on Fig. 2. The geometry shown is used for all of the results presented in this interim report; the relative influence of length/diameter ratio and other geometric configurations will be considered in phase II. The interface between the shaft and the soil is modeled as a frictional contact surface, with friction coefficient properties that have been adjusted for different runs. The shaft (pile) is modeled as an elastic material with a modulus approximating that of concrete. The O-cell is modeled as a contact surface, internal within the shaft, upon which a pressure boundary condition is imposed to generate the O-cell loading. The shaft itself is 30 feet long with a radius of 1.5 feet, thus a length/diameter ratio of 10 is maintained. The bottom boundary of the mesh is at a distance of 10 diameters below the base and the far field boundary is at a radial distance of 15 diameters. The far field boundary is modeled as a pressure boundary so that the in-situ horizontal stresses (and thus K_o) can be controlled prior to loading the shaft. The bottom boundary is modeled as a rough base.

The loading sequence used to construct the model is critical to development of a realistic state of in-situ stress. The following sequence was used in this research:

1. Simultaneously apply gravity (gravity turn-on) and horizontal pressure on the far boundary using K_o=0.43. This value of K_o is representative of a normally consolidated condition for the value of Poisson's ratio used for this soil (0.3) and produces a stress state equal to that of a displacement constraint on the far boundary. During this loading phase, the shaft/soil interface is set as frictionless to simulate the placement of fluid concrete

and avoid residual stresses from differing unit weight and elastic modulus between the shaft and the soil.

2. Increase the horizontal pressure on the far boundary to simulate overconsolidated soil conditions as required for the particular analysis. Several different values of K_o have been used in the analyses performed to date, ranging from 0.43 (normally consolidated, in which this step is skipped) to 2.0 (heavily overconsolidated). K_o was taken as constant with depth for purposes of these analyses.

3. Apply the external loads, either to the top of the shaft for the top down loading or to the contact surface at 1 diameter above the base for the O-cell loading.

In the case of the O-cell loading, a soft spring was added to the top of the shaft to allow convergence at loads which approach and slightly exceed failure in uplift; otherwise the limit load at which the shaft pushes from the ground cannot be accurately determined. The force in this spring has been subsequently deducted from the net O-cell force on the shaft in uplift. Similarly, forces have been adjusted to account for shaft weight as per conventional practice in evaluating O-cell field test results. The procedures outlined in the standard appendix to the Loadtest, Inc. reports entitled "Construction of the Equivalent Top-Loaded Load-Settlement Curve from the Results of an O-cell" have been followed in comparing the equivalent top load response as would be done for a field test. Elastic shortening of the shaft is included, although the magnitude of elastic shortening was very small relative to the total movements.

The soil properties used for analysis include elastic modulus, $E = 14$ ksi, Poisson's ratio $\nu = 0.3$, angle of internal friction $\beta = 31°$, cohesion intercept $d = 8$ psi. Note that these parameters are for a Drucker-Prager yield surface; they represent the angle of the shear surface and intercept of the octahedral shear stress with respect to the mean principal stress rather than the conventional Mohr-Coulomb relations (which work poorly for a three dimensional stress state). The concrete is modeled using $E = 5000$ ksi, Poisson's ratio $\nu = 0.3$ and the rock (where used) is modeled using $E = 1400$ ksi (100 times that of soil, but still less than the concrete), Poisson's ratio $\nu = 0.3$. The contact surface between the shaft and soil is modeled as a frictional interface with a friction angle of either $31°$ or $50°$; the former generally produced failure at the interface and the higher value often produced failure in the soil elements adjacent to the shaft.

Results

Presented on Figure 3 are the computed load vs deflection comparisons for the four cases analyzed involving shafts embedded within soil. Note that this soil is representative of a fairly competent material with significant cohesion such as a cemented sand or stiff silty clay. Figures 3a) through 3c) illustrate cases with an extreme range of in-situ horizontal stress ranging from $K_o = 0.43$ to 2.0; case b) with $K_o = 1$ is likely to be more representative of typical conditions in stiff or dense soil. These data suggest that the O-cell method tends to produce excellent comparisons for the cases where K_o was relatively low and tends to be increasingly conservative as K_o becomes large. Note that for these cases, failure tended to be at the frictional interface between the shaft and soil. Figure 3d) illustrates the case for $K_o = 1$ but with a much increased interface friction so that the failure tended to be in the adjacent soil elements over much of the length of the

20

shaft. This case indicated a somewhat closer agreement than the similar case (b) with a smaller interface friction angle although still slightly conservative.

An examination of the differences in behavior is instructive, and will be focused on the $K_o = 1$ case for purposes of this discussion; details of all of the other runs are provided in Appendix A. Presented on Figure 4 are comparisons of the load vs deflection for tip resistance and side shear for the case of $K_o = 1$, interface friction = 31°. The tip resistance from the two loading conditions is seen to be nearly identical, with the O-cell loading somewhat conservative in the side shear with respect to the top down loading. Thus, almost all of the differences between the top down and O-cell loading is attributed to differences in side shear from pushing up vs pushing down.

The differences related to load direction appear to be related to differences in the normal stresses on the shaft/soil interface related to direction of loading. Presented on Figure 5 are plots of the stress history at selected nodes along the interface for the two cases with $K_o = 1$; Figure 5a) presents the results for interface friction (δ) = 31°, Figure 5b) presents the results for $\delta = 50°$. The normal stresses at the interface are seen to decrease slightly for the upward directed (O-cell) loading, while normal stresses tended to remain almost constant or increase slightly for the top down loading. The result of these differences in normal stress is most notable for the $\delta = 31°$ case, where the initial contact with the yield surface is shifted slightly to the right and thus mobilizes a higher shear stress at yield. Note that the yield surface in this case is clearly represented by the $\delta = 31°$ line, indicating failure at the frictional interface. For the $\delta = 50°$ case, the differences are much smaller and the yield surface at failure corresponds to the shear strength properties of the soil rather than the interface for all except the most shallow

21

depth. Note the indication of cohesion by the points tracking on the yield surface. Only the 5 foot depth for the O-cell loading appears to contact the $\delta = 50°$ line. Thus the failure in the soil is indicated and the cohesive nature of the soil makes differences in normal stress at the interface much less significant.

Results for Rock Model

The model used for the rock case uses the same mesh as described previously with the upper 15 feet composed of soil as in previous models ($K_o = 1$, $\delta = 31°$) and the material below the 15 foot depth composed of rock. With the O-cell placed at 3 feet above the base, the effective socket length tested is therefore 12 feet, with a length/diameter ratio of 4. The rock includes a frictional interface with a relatively high friction angle between the shaft and rock of $\delta = 50°$, with the rock considered to be a sufficiently strong material to force failure at the interface. Thus, this model includes no provisions for "cone breakout" as was the case in the models analyzed by McVay, et al (8). For the top down loading, a "soft base" was constructed by defining a row of elements immediately below the tip of the shaft to have a very low modulus. This approach is considered similar to that which would be used to conduct a full scale physical test in the field in which a compressible material might be placed into the base of the shaft excavation. For both the top down and O-cell loading case models, only failure in side shear is observed.

Presented on Figure 6 is a plot of the load in side shear vs displacement for the top down and O-cell loadings of the rock-socketed drilled shaft. Note that the O-cell loading is seen to be relatively conservative for this condition in terms of overall side shear capacity.

More insight into the behavior in these FE models is available from the shear stress data plotted vs depth along the shaft on Figure 7. Normal stresses follow an identical pattern. These data suggest that the relative distribution of side shear along the shaft is quite dramatically different between the two loading cases, even though the average might be reasonably similar. In each case the highest shear stresses coincide with the highest normal stresses, which in turn are biased towards the end of the rock socket which is feeling the most intense axial load in the shaft. The magnitude of this effect is related to the Poisson's ratio in the shaft and rock; in soil the modulus of the soil is so much lower that the Poisson's effect is insignificant. In this case the modulus of the rock was around 28% of the shaft concrete modulus and the effect is quite dramatic.

It is thought that there are a number of case histories of O-cell loading in which strain gauges indicate a strong bias of higher unit side shear in the portion of the socket nearest the O-cell. This pattern is consistent with the behavior observed in this model. More investigation of such case histories is warranted.

Note that this pattern of shear stress in a rock socket is associated with a frictional shaft/rock interface. If the failure mode of the socket in side shear is better represented by a shearing failure through a material which is considered to have strength that is independent of the confining stress, the pattern of maximum side shear stress would tend to be more uniform at failure. Further investigation of this behavior is warranted, although it is considered by the writer that the confining stress plays a strong role in the maximum shear stress which can be developed (even concrete strength is strongly influenced by confining stress).

Summary

The FE analysis of a limited range of conditions suggests that the O-cell method of load testing is likely to be conservative in estimating shaft capacity under most instances with respect to conventional top down load testing techniques. The most significant differences relate to the side shear response of the shaft to upward directed loading in lieu of downward directed loading. The relative difference is small in instances where side shear is dominated by cohesion in the soil or where the ratio of horizontal to vertical stress (K_o) in the soil around the shaft is small. Relative differences are more significant in cases where K_o is high and in rock sockets where the rock modulus is of the same order of magnitude as the concrete modulus and the side shearing resistance is influenced by the normal stress at the shaft/rock interface.

Need for Additional Analysis Using FE Models

The range of conditions evaluated to date is limited and a more complete range of models need to be analyzed to identify the most important variables. In particular, well-documented case histories of rock socket shafts need to be considered. Multi-level O-cell tests in which sockets between the two O-cell levels are loaded in the down direction vs another similar test in the same or similar rock formation with the socket loaded in the up direction might prove particularly useful in further examination.

RESEARCH PLAN FOR PHASE II

Phase II of the research will perform the following tasks:

- Work to collect and review additional test data comparing O-cell and conventional top down testing. In addition, it is considered instructive to obtain

comparative data from multi-stage O-cell tests in which tests of the middle socket have been performed in different directions. It is also desirable to obtain well-documented and instrumented tests in rock sockets where the site characterization is good so that modeling of such foundation types may be performed. Selected field tests of this type will serve as a basis for additional FE model studies

- Conduct additional FE model studies for a broader range of conditions in order to clarify the effect of variables thought to be important and to utilize field tests for model calibration purposes.

- Assess the applicability and reliability of the O-cell method for a range of possible conditions to identify those conditions where the method offers the most compelling advantages and to identify those conditions where the interpretation of the test results may require more in-depth evaluation than is currently performed. Recommendations for use and interpretation of the O-cell test results are included in this task.

- Prepare and submit a final report documenting the entire research effort and the need for any additional research or testing.

REFERENCES

1. Osterberg, J.O., 1995. "The Osterberg Cell for Load Testing Drilled Shafts and Driven Piles," Report No. FHWA-SA-94-035, Federal Highway Administration, Feb., 1995, 92 p.

2. O'Neill, M.W. and Reese, L.C., 1999. "Drilled Shafts: Construction Procedures and Design Methods," Report No. FHWA-IF-99-025, Federal Highway Administration, Aug., 1999, 758 p.

3. Littlechild, B.D., Hill, S.J., Plumbridge, G.D., and Lee, S.C., 2000. "Load Capacity of Foundations on Rock," Geotechnical Special Publication 100, ASCE, pp. 140-157.

4. Ng, C.W.W., Rigby, D.B., Li, J.H.M., Yau, T.L.Y. and Tang, W.H., 2001. "Side Shear of Large Diameter Drilled Shafts in Weathered Geomaterials," Geotechnical Special Publication 113, ASCE, pp. 758-772.

5. Meyer, R., 1996. "A Comparison of Two Shafts between Polymer and Bentonite Slurry Construction and between Conventional and Osterberg Cell Load Testing," presentation given at the SW Transportation Geotechnical Engineers Conference, Little Rock, AR, unpublished.

6. Molnit, T., and Lee, J.S., 1998. "Comparison Report, Osterberg Cell Test Method (PTP14) versus Kentledge Test Method (PTP15), MRT C701, Singapore," Loadtest, Inc., report to Hyundai Construction, April, 1998.

7. Kishida, H., Tsubakihara, Y., and Ogura, H., ??? "Pile Loading Tests at Osaka Amenity Park Project," unpublished report to Mitsubishi Corp.

8. McVay, M., Huang, S. and Casper, R., 2001. "Numerical Simulation of Drilled Shafts for Osterberg, Pullout, and Axial Compression Loading in Florida Limestone," internal Univ. of Florida Report.

9. Fellenius, B.H., Altaee, A., Kulesza, R., and Hayes, J., 1999. "O-Cell Testing and FE Analysis of 28-m-Deep Barrette in Manila, Philippines," *Journal of Geotechnical & Geoenvironmental Engineering*, ASCE, v 125 n 7, pp 566-575.

Location	Shaft/Soil Conditions	Loading Conditions	Results
Hong Kong Railway	2 m socket in weathered granodiorite	Top down followed by O-cell upward on same shaft	O-cell unit shear (10tsf) about 25% higher; end bearing compared well
	1.5 m socket into slightly weathered metasandstone	Top down followed by O-cell upward on same shaft	Top down did not yield at 8mm, O-cell yield at 40% higher unit side shear at 10 mm w/ brittle failure
Downtown Hong Kong	1.2 m diam. Shaft in decomposed granite	Top down followed by O-cell upward on same shaft	Similar side shear at similar displacement w.r.t. start position, but not at similar displacement w.r.t. absolute displacement
	1-1.3 m diam. Shafts in weathered rock	3 shafts w/ top down followed by O-cell upward; one shaft w/ O-cell upward followed by top down	Loss of bond observed during initial loading, w/ subsequent softening; Authors conclude that comparison of multi-directional tests are problematic due to hysteresis
New Mexico	30" diam. Shaft in very dense sand	2 shafts w/ top down to 3" displ. followed by O-cell up to 6" displ.	O-cell loading yielded in side shear (up) at about ½ the side shear from the top down loading
Singapore	1.2 m by 38 m shafts in deep clay/silt	2 separate shafts, one top down, one multi-level O-cell	Very close in side shear; portion of O-cell side shear not fully mobilized
Osaka	1.2 m by 38 m shafts in deep clay/silt/sand	2 O-cell shafts, one top down shaft	O-cell didn't fully mobilize side shear, end bearing compared very well
Tampa	48" shafts in limerock	1 O-cell shaft, one statnamic shaft	Very close in unit side shear

Table 1 Summary of Comparative Field Load Test Data

O-cell (typ)

Single O-cell Test

Multi Level O-cell Test
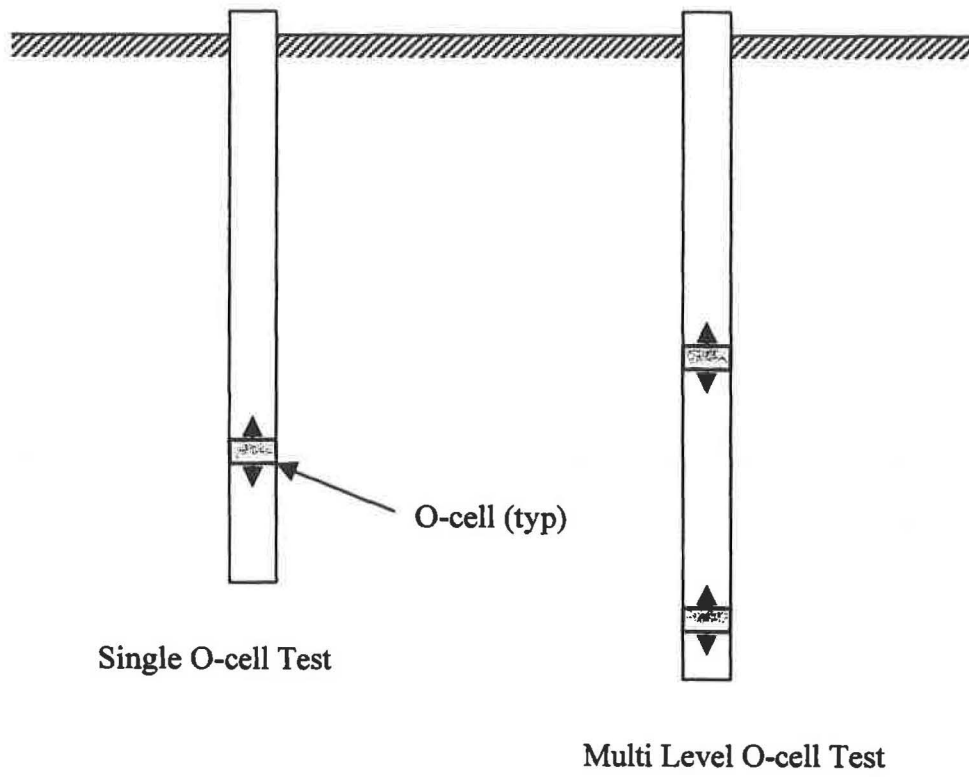
Figure 1 Schematic Diagram of O-cell Testing
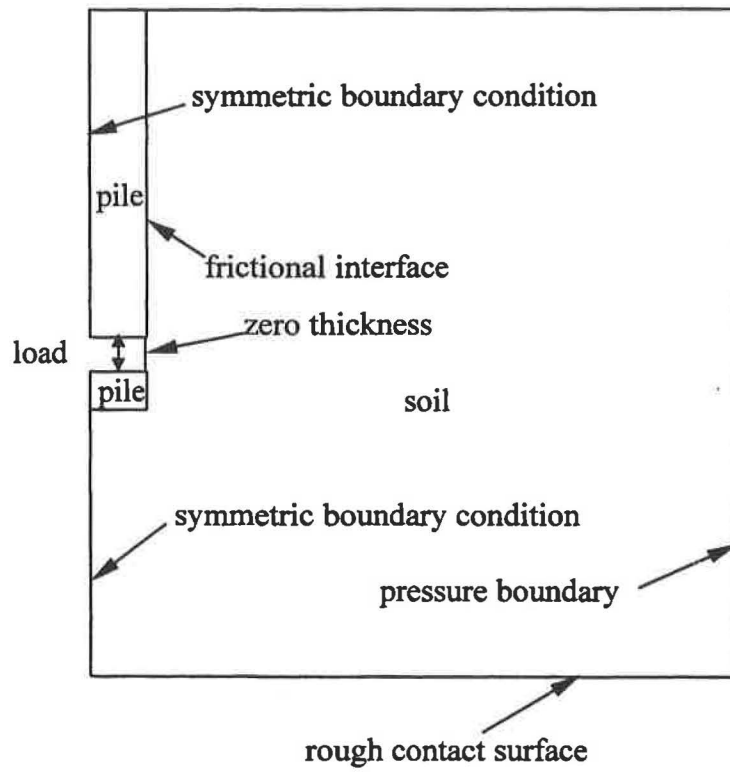
Figure 2 Schematic Diagram of Axi-symmetric FE Model
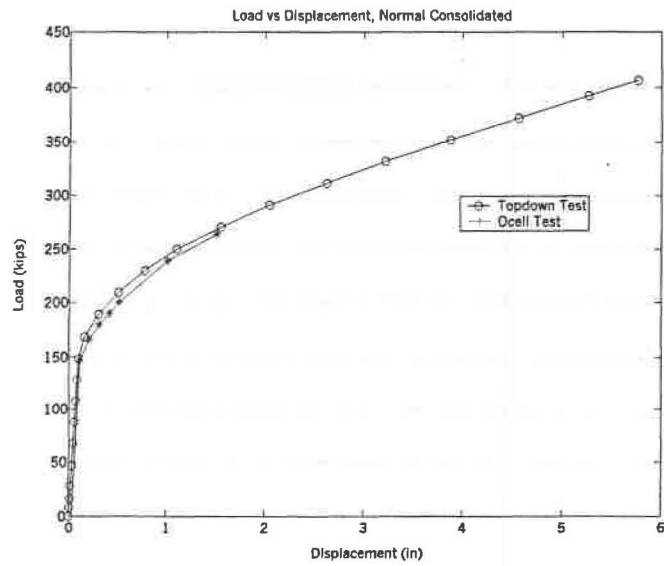
a) $K_o = 0.43$, Shaft/Soil friction = 31°
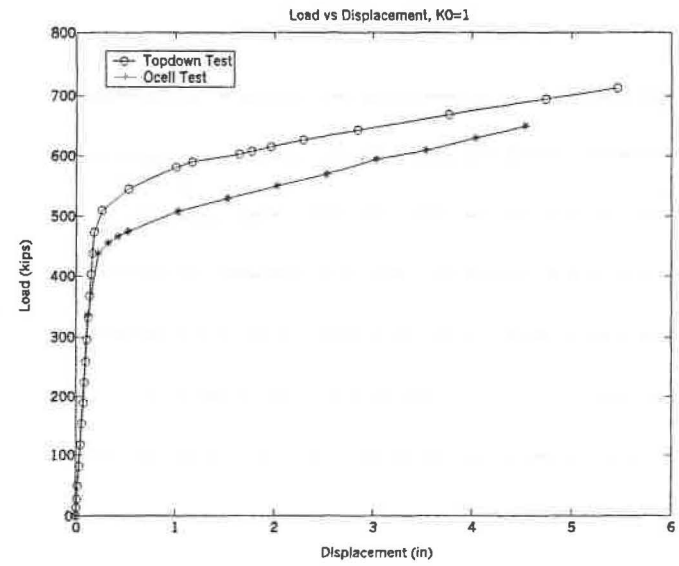
b) $K_o = 1$, Shaft/Soil friction = 31°
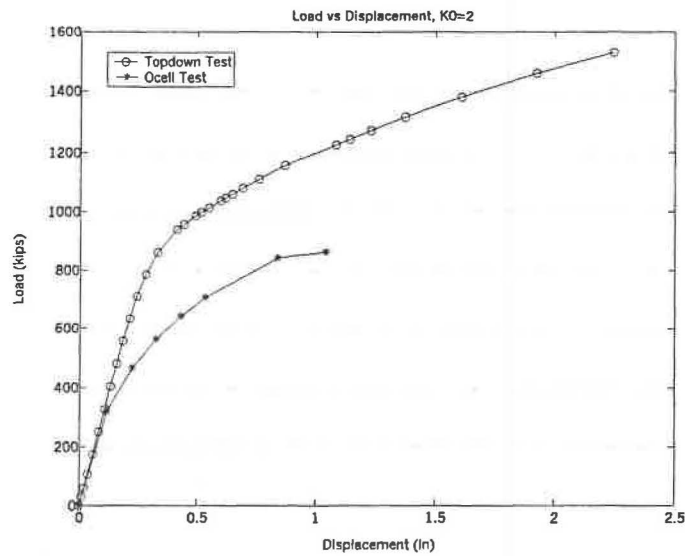
c) $K_o = 2$, Shaft/Soil friction = 31°
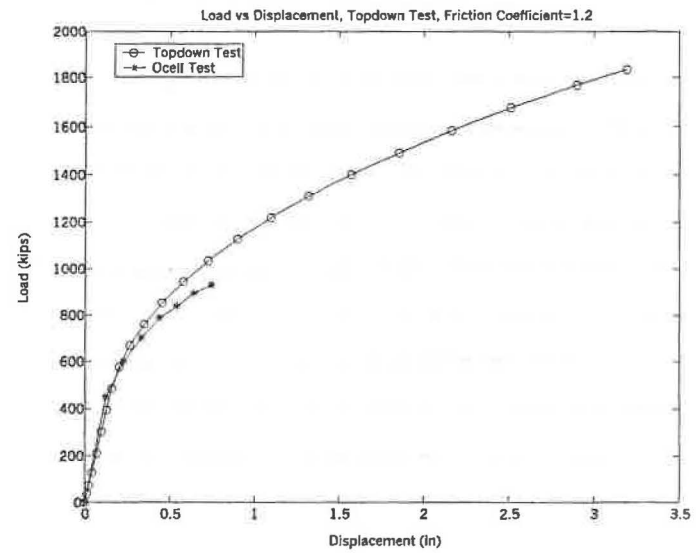
d) $K_o = 1$, Shaft/Soil friction = 50°

Figure 3 Top Down vs O-cell Computed Load-Deflection for Soils
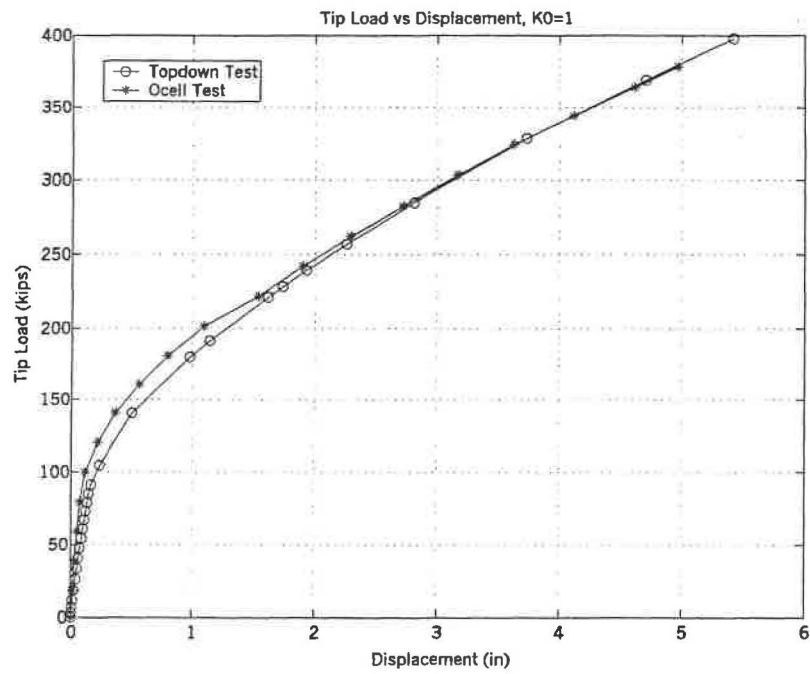
a) tip resistance
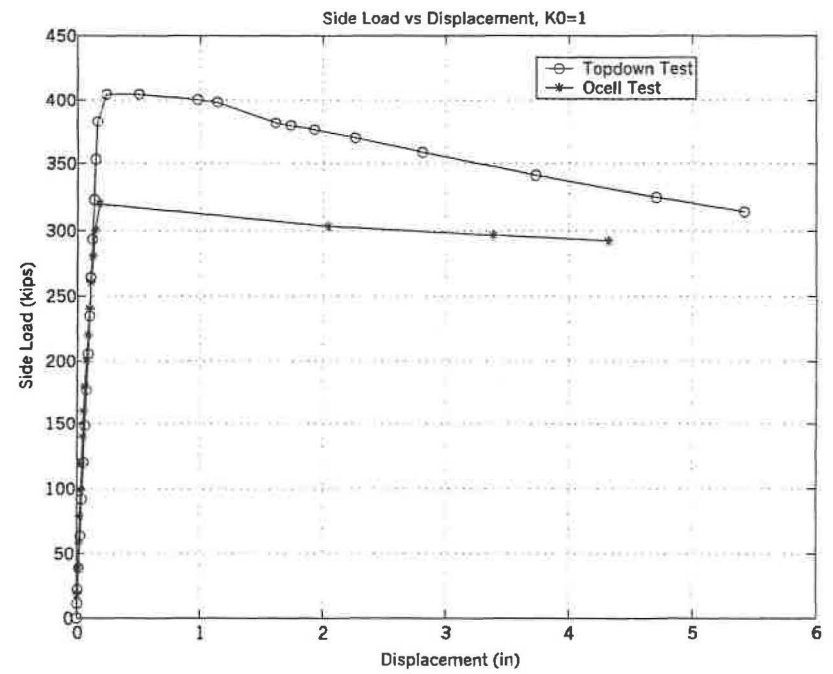
b) side shear

Figure 4 Tip Resistance and Side Shear for $K_o=1$, $\delta=31°$

a) $K_o=1, \delta=31^o$

b) $K_o=1, \delta=50^o$
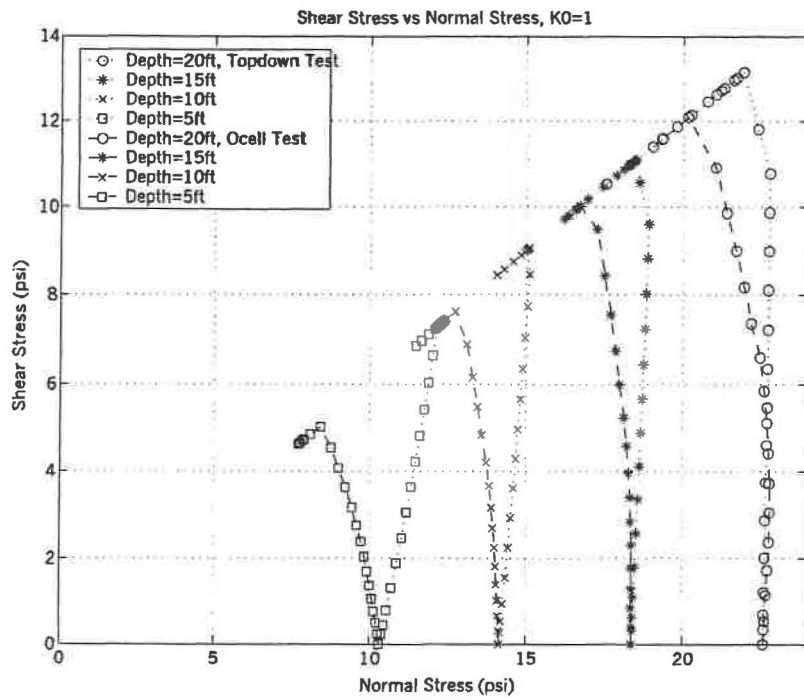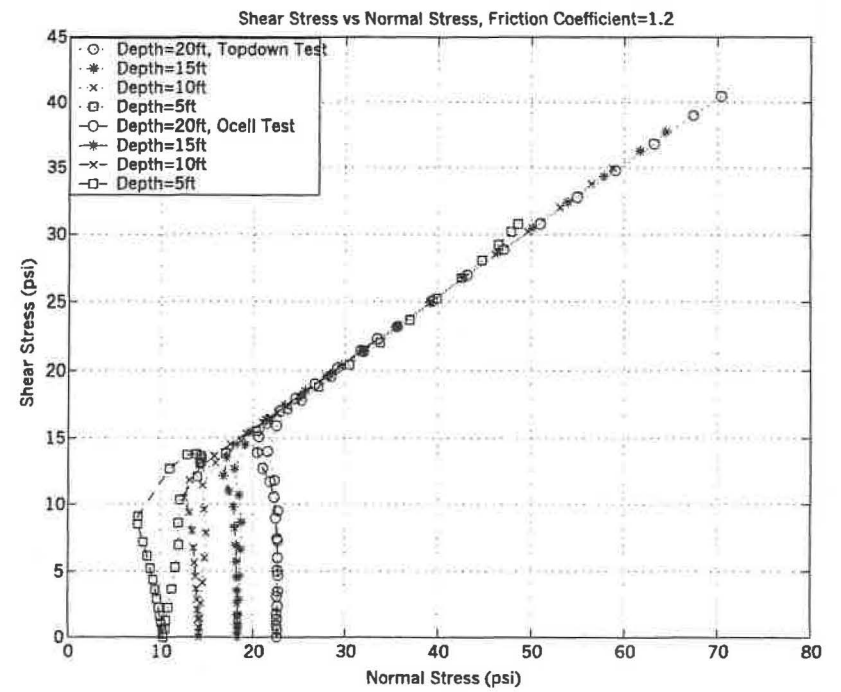
Figure 5 Stress Path at Points Along the Shaft/Soil Interface
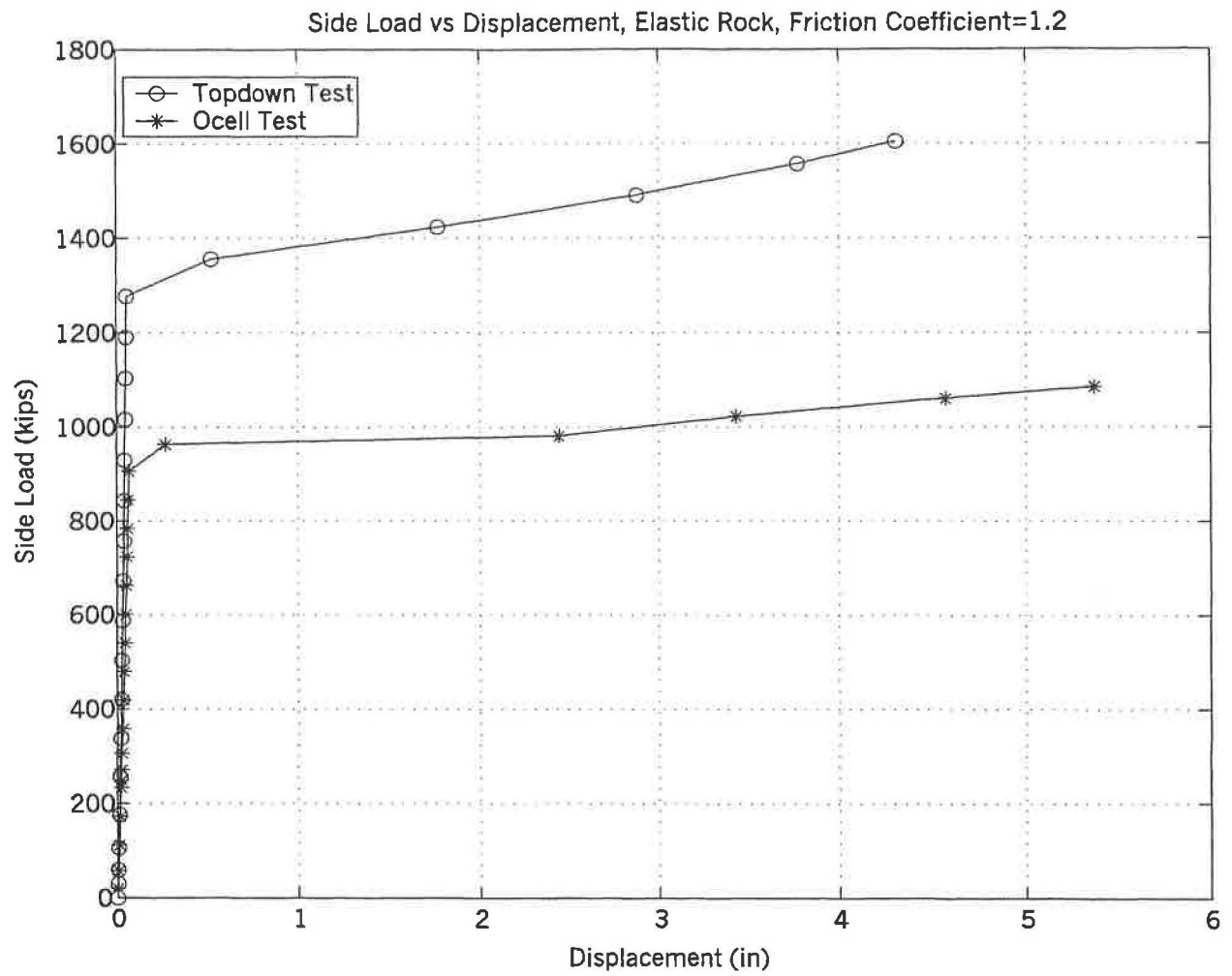
Figure 6 Comparison of Side Shear vs Displacement for Rock Models

Shear Stress vs Depth on Pile-Soil Interface, Topdown Test, Elastic Rock, Friction Coefficient=1.

Shear Stress vs Depth on Pile-Soil Interface, Ocell Test, Elastic Rock, Friction Coefficient=1.2
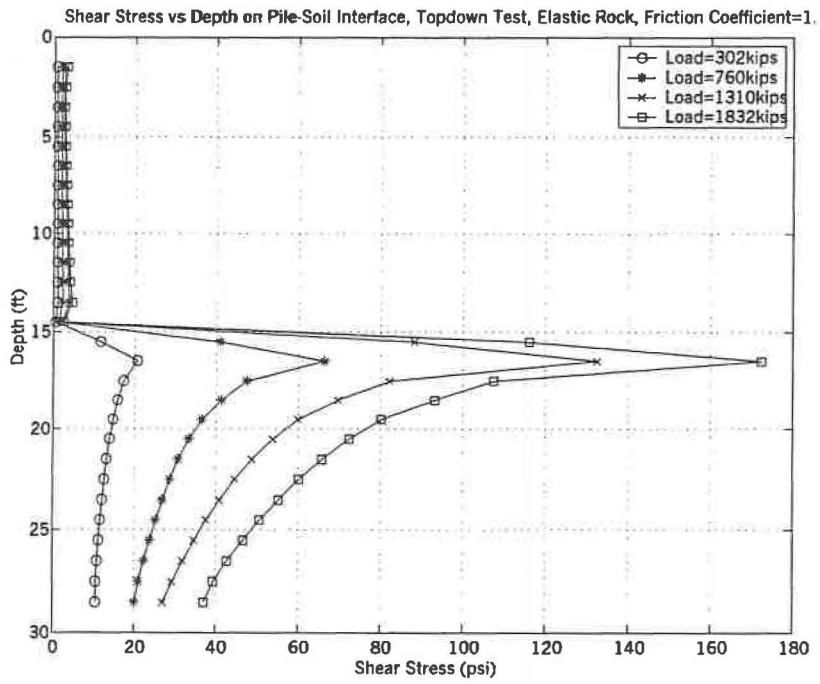
a) Top Down Model
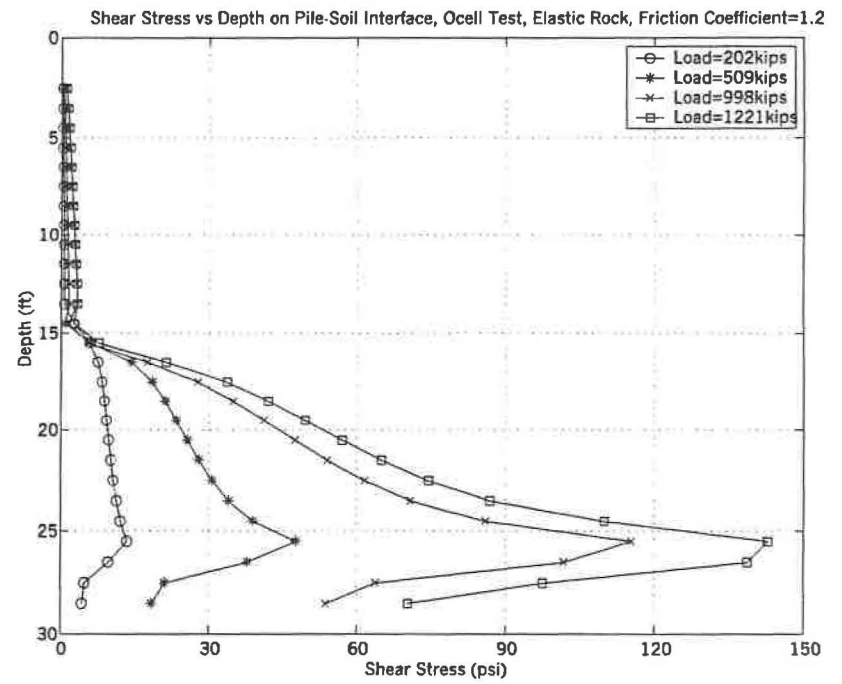
b) O-cell Model

Figure 7 Rock Socket Shear Stresses

Appendix A

Interim Report

for

Finite Element Modeling Osterberg Load Test

INTRODUCTION

This portion of the research describes the development of a finite element model for the Osterberg load test. In the Osterberg (O-cell) load test, an Osterberg load cell is embedded at the bottom of the test shaft. When it is pressurized, a pair of forces in the opposite direction will be generated. The downward force from the bottom of the cell is resisted by the bearing stratum while the upward force from the top of the cell is resisted by the weight of the pier and by the skin friction along the sides of the shaft. The O-cell load test can therefore directly separate end bearing and side friction. In order to compare the Osterberg load test with conventional load tests, the topdown test is also simulated using finite element method. In topdown test, load is applied to the top of the pile so that pile and the surrounding soil will settle, which will be resisted by both end bearing and side friction.

The finite element model allows a parametric study to be conducted by changing some properties to analyze the influence of these properties on the final capacity and load transfer, etc. For example, soil over-consolidation ratio, soil properties and roughness of soil surface play an important roll in pile capacity. In this project, several cases with different properties mentioned above were calculated and results were compared with respect to topdown test versus O-cell test and different cases.

FINITE ELEMENT CODE—ABAQUS & MSC/PATRAN

ABAQUS was used to perform the finite element analysis since it provides a large number of capabilities for analyzing different problems, including many nonstructural applications. And it is also powerful to model material properties, including some models

particularly for soil, such as Drucker-Prager model used in this project, which are very common in geotechnical engineering. ABAQUS is used throughout the world for stress, heat transfer, and other types of analysis in mechanical, structural, civil, and related engineering applications.

It can deal with general analysis including

- Static stress/displacement analysis

- Viscoelastic/viscoplastic response

- Transient dynamic stress/displacement analysis

- Transient or steady-state heat transfer analysis

- Transient or steady-state mass diffusion analysis

- Steady-state transport analysis

- Coupled problems

and linear perturbation analysis which includes

- Static stress/displacement analysis

- Dynamic stress/displacement analysis

Model for material includes metals, cast iron, rubber, plastics, composites, resilient and crushable foam, concrete, sand, clay, and jointed rock. The material response for each of these models may be highly nonlinear. General elastic, elastic-plastic, and elastic-viscoplastic behaviors are provided. Both isotropic and anisotropic behavior can be modeled. User-defined materials can also be created with a subroutine interface.

MSC/PATRAN is used as preprocessor and postprocessor in this project, which is compatible with ABAQUS. Finite element model and mesh can be generated easily by

drawing and PATRAN will generate the input file for ABAQUS automatically. After running ABAQUS, results may be read by PATRAN, so displacements and stresses can be presented very clearly so that the critical point or element can be located very quickly by just looking at the displacement and stress fringe results. Different useful kinds of graphs can be plotted in PATRAN such as load-displacement curve.

MODEL DESCRIPTION

The brief diagram of models for topdown test and O-cell test are shown in Figure A-1 and Figure A-2 respectively. The details of finite element modeling are described as follows.

Geometry, Element Type and Boundary of Mesh

A two dimensional axis-symmetric model was used for both topdown and O-cell load tests, which reduced the problem size thus the computing time significantly. ABAQUS includes both first-order and second-order elements with fully and reduced integration method. In this axis-symmetric model, fully integrated 4 nodes (first-order) quadrilateral axis-symmetric elements were used for both soil and pile.

Figure A-3 shows the finite element mesh, the dimension of which is 60ft deep by 45ft radial. Soil below the pile tip is 10 times of the pile diameter and the width of the mesh is 15 times of the pile diameter. As shown in Figure A-3, finite element is finer near the pile than that far away from the pile.

Boundary conditions are very important in the modeling. The model used in this project was simulated as close to the real case as possible. On the symmetric boundary (left side of the mesh), symmetric boundary condition was applied, which means only

vertical displacement is permitted and horizontal displacement is constrained. At far side of the model (boundary far away from the shaft or right side of the mesh), horizontal pressure boundary condition was used. Horizontal pressure that is proportional to depth was applied to this boundary. By doing this, the in-situ ratio of horizontal to vertical stress may be controlled. At the bottom of the model, a rough contact surface was used. On this surface, friction can develop and no relative displacement will occur. This is used to prevent horizontal displacement of the bottom boundary.

Constitutive Model

Soil

An elastic-plastic (Drucker-Prager) constitutive model was used to simulate soil properties, which has Von Mises yield surface as its yielding criteria. The yield surface can be expressed as

$$F = t - p \tan \beta - d = 0$$

where

d=cohesion;

β=friction angle;

t=Octahedral shear stress, $t = \sqrt{\frac{1}{3}[(\sigma_1 - \sigma_2)^2 + (\sigma_2 - \sigma_3)^2 + (\sigma_3 - \sigma_1)^2]}$;

p=Octahedral normal stress, $p = \frac{1}{3}(\sigma_1 + \sigma_2 + \sigma_3)$.

Figure A-4 shows the failure envelope in p-t plane. In this model, there is a regime of purely elastic response, after which some of the material deformation is not recoverable and can be idealized as being plastic. Plastic deformation has been modeled

using an associative flow rule, which implies that dilation occurs during plastic yield. Such behavior is thought to be appropriate for dense granular soils.

Rock

Rock has a much higher stiffness than soil, so its deformation is relatively small and it's difficult to fail the rock. Therefore, for the research performed to date, rock was simply modeled as linear elastic material.

Concrete Shaft

Concrete shaft was modeled as linear elastic material and its stiffness is much higher than that of soil.

Contact Surface Between Soil and Pile

The interaction surface between the pile and soil is described as a frictional contact surface, which allows slip. When the shear stress on that surface exceeds some value, soil and pile will not stick with each other and slip will occur. Coulomb friction theory is used in the model so that maximum frictional shear stress on the interaction surface is proportional to the normal pressure by a friction coefficient. The failure envelope is shown in Figure A-5, where δ is the friction angle and the friction coefficient is $\mu = \tan \delta$. Once the shear stress exceeds the maximum frictional shear stress, slip will occur. For this friction model, an interface stiffness is applied to allow small relative deformation prior to slip, so the contact stiffness is not infinity even if slip is not developing.

Topdown Load Test

In topdown test, load is applied to the top of the pile as a pressure load. The whole test was divided into three steps which are described as follows.

Step 1: Apply gravity force, and at the same time, apply horizontal pressure on far side boundary with $K_0 = 0.43$ (normal consolidated);

Step 2: Add additional horizontal pressure for over-consolidated case, skip this step for normal consolidated case;

Step 3: Apply external load to the top of the pile.

In order to avoid residual stresses, the contact surface between soil and pile was modeled as frictionless in the first two steps so that the pile can settle down without any obstruction. In step 3, friction coefficient was changed to the desired value to provide side shear. In all cases, the end of step 2 is the base state of step 3, so this base state was deducted from the final results to get the response under the external load.

O-cell Load Test

In O-cell load test, O-cell was embedded 3ft above the base of the shaft as a contact surface without thickness. O-cell pressure will generate forces with same magnitude in opposite direction. The interaction between two parts of shaft was modeled as contact surface so that the load can be transferred between two parts of pile when gravity force was applied. Similar to the topdown load test, there are three steps during calculation.

Step 1: Apply gravity force, and at the same time, apply horizontal pressure on far side boundary with $K_0 = 0.43$ (normal consolidated);

Step 2: Add additional horizontal pressure for over-consolidated case, skip this step for normal consolidated case;

Step 3: Apply O-cell pressure.

As in topdown load test, the friction coefficient of contact surface between soil and shaft is zero in the first two steps and changed to the desired value in the last step. Since the upper part of pile will move upward without any constraint after contact surface between soil and pile fails, soft springs were added to the top of the pile to allow a convergent solution as the load approaches and exceeds the shaft uplift capacity. When dealing with the results, this soft spring force is deducted from the total load.

In order to compare the results from topdown load test and O-cell load test, an equivalent topdown load versus settlement curve was generated from O-cell load test using the method described as follows. On O-cell test load-displacement curve, select a specified movement and then find the corresponding side load and ending bearing load. Adding these two loads will give the equivalent topdown load corresponding to the movement. Refer to "Construction of the Equivalent Top-Loaded Load-Settlement Curve from the Results of an O-cell" for details. When doing this, elastic shortening of the shaft was also considered although the magnitude of this elastic shortening was very small relative to the total settlement.

PROPERTIES COMMON TO ALL

In all cases for both Osterberg load test and topdown test, 3ft diameter concrete shaft was used, which is 30ft deep. For O-cell load test, Osterberg load cell is embedded 3ft above the bottom of the shaft with zero thickness. The following are properties and each material.

Concrete shaft: $E = 5000ksi$, $v = 0.3$;

Soil: $E = 14ksi$, $v = 0.3$, $\beta = 31°$, $d = 8psi$;

Rock: $E = 1400ksi$, $v = 0.3$;

In calculation, soil was modeled as fully associated, which means the dilation angle equals the friction angle.

CASES ANALYZED

Several cases in terms of different over-consolidation ratio and friction coefficient of soil-pile interface were calculated for both topdown load test and O-cell load test. The following presents results case by case and also compares results of topdown load test and O-cell load test. For the following, μ refers to the friction coefficient of the contact surface between soil and pile and δ refers to the corresponding friction angle. K_0 is the ratio of horizontal stress to vertical stress.

Case I: All Soil, $K_0 = 0.43$, (Normal Consolidated), $\mu = 0.6$ ($\delta = 31°$)

In this case, all soil is normal consolidated with the properties described before. Figure A-6 and A-7 show the load-displacement curve for topdown test and O-cell test respectively. As shown in the plots, stiffness decreases with the increase of the applied load. For topdown test, the whole system failed at about 170kips of applied load, after which the stiffness decreases rapidly. In Figure A-7, node 2378 represents the upper part of the shaft and node 2502 represents the lower part of the shaft. For the O-cell test, the load for the upper part of the pile has been adjusted for the soft spring force at the top of the pile, which enables the downward force to mobilize additional end bearing. It's obvious that side shear failed first at about 130kips applied load. At the beginning of applying O-cell pressure, there's almost no movement because there's initial stress in the system due to the self weight of soil and pile, and this stress needs to be overcome before

significant displacement occurs. Note that the "end bearing" includes side shear on the 3ft shaft below the O-cell, which is also true for following cases.

The equivalent topdown load vs displacement generated from O-cell test is shown in Figure A-8, comparing with the result from topdown test. It is indicated that the two curves match well for this case and the O-cell slightly underestimates the capacity. Figure A-9 and Figure A-10 show the tip load vs displacement curve and side load vs displacement curve for both tests respectively. For topdown test, the tip load was calculated from the vertical stress at O-cell level and side load was calculated by subtracting tip load from total load. Comparing these two figures, it can be concluded that most of the applied load is resisted by end bearing, which can also seen from the load-displacement curve for O-cell test shown in Figure A-7. As shown in figures, tip load vs displacement curve and the first part of side load vs displacement curve for two tests match well. But the topdown test shows more strain softening than the O-cell test.

Figure A-11 is the comparison of stress path (shear stress vs normal stress) at different nodes along the contact surface between soil and pile from the topdown test and the O-cell test. At the beginning of the test, deeper node was at a higher stress than the lower node due to the overburden pressure. The initial stress state at the same node is the same for topdown and O-cell tests, and the shear stress for all nodes starts from zero because the contact surface is frictionless before top loads or O-cell pressures are applied. The stress paths for the topdown test and the O-cell test are somewhat different, with more significant differences at shallow depths. As the applied load is increasing, slip will occur after overcoming the surface frictional stress. This can be seen from the sudden change of the slope of each curve. After slip occurs, stress path follows the contact

surface property defined, i.e. $\mu = 0.6$. Connecting the failure envelope will result in a straight line with a slope of 0.6. These plots suggest that the failure occurred at the contact rather than within the soil. As a general trend, the normal stresses along the interface tended to decrease during O-cell loading and increase slightly for topdown loading.

Figure A-12 and Figure A-13 are normal stress and shear stress at different loads on soil-pile interface changing with the depth in topdown test respectively. As shown in the figures, normal stress and shear stress curves are very similar in shape. Normal stress and shear stress increase with the depth at the beginning of the test, but with the increase of the applied load, both normal stress and shear stress curves become totally different. It's indicated in Figure A-12 that at some depths normal stress decreases with the increase of the applied load, this is because the contact surface tends to open. Similarly, normal stress and shear stress versus depth curves at different loads in O-cell test are shown in Figure A-14 and Figure A-15. The maximum normal stress is not at the bottom of the shaft, but at a depth of from about 27.5ft at load=54kips to 22.5ft at load=204kips. Similar to the topdown test, the shear stress curve is very similar to normal stress curve except at depth around O-cell where the contact nodes tends to open which result in zero normal stress and shear stress.

Figure A-16 and Figure A-17 show comparison of stress path (octahedral shear stress vs octahedral normal stress) of different soil elements below the pile toe. Element 1062 in topdown test and 62 in O-cell test are at the same location, as are element 1065 and 65. The soil almost failed from the beginning of applied due to initial stress state because of large deviatoric stress in this normally consolidated condition, and the straight

line corresponds to soil yield surface envelope. It is also shown that the stress path in topdown test and O-cell test is almost same.

For this case, it's obvious that side friction is easier to fail than end bearing and end bearing provides most of the resistance to the applied load. This holds true for both topdown and O-cell load test. Results from topdown and O-cell test are consistent and match fairly well, but O-cell test tends to overestimate pile capacity a little. Also, soil is easy to fail because the horizontal pressure is small which leads to high deviatoric or shear stress.

Case II: All Soil, $K_0 = 1$, $\mu = 0.6$ $(\delta = 31°)$

For the same soil and other conditions, over-consolidated cases were calculated with a higher ratio of in-situ horizontal to vertical stress (K_0). This case is probably more representative of typical soil conditions for drilled shafts. For $K_0 = 1$, Figure A-18 and Figure A-19 show the load vs displacement curve for topdown and O-cell test respectively. It is obvious that the capacity was much higher compared to normal consolidated case for both tests. In the O-cell test, it's hard to tell whether side shear or end bearing failed first as shown in Figure A-19. But it is clear that the contact surface between soil and pile failed at a load of about 350 kips. Similar to normal consolidated case, there's very small movement at the beginning of the O-cell test due to the self weight of the upper part of the shaft, and side shear is mobilized at less than ¼ inch of displacement.

Figure A-20 shows the match between the load vs displacement curve of topdown test and equivalent topdown load vs displacement curve generated from O-cell test. It is indicated that the O-cell test is conservative compared with the topdown test. For

instance, at 1in displacement, the corresponding load from the topdown test is about 580kips, while load from the O-cell test is around 500kips. This can be also concluded from the side load vs displacement curve shown in Figure A-22. Figure A-21 is the plot of tip load vs displacement curve for both the topdown test and the O-cell test, which shows that the results of two tests match well. Comparing Figure A-21 and Figure A-22, it can be found that side load is a little higher than tip load, indicating that end bearing and side friction almost have same capacity.

Similar to normal consolidated case, shear stress vs normal stress curves at different nodes along the interface between soil and pile were plotted in Figure A-23 for both topdown test and O-cell test. There's no difference between topdown test and O-cell test at the beginning of the test, but the upward directed O-cell loading tends to reduce the effective normal stress compared to the topdown loading. After slip, all nodes tended towards slight strain-softening along the yield surface that defines the contact surface properties.

Figure A-24 to Figure A-27 show normal stress and shear stress changing with along the length of the pile for topdown and O-cell test respectively. The maximum value for both normal stress and shear stress is not at the bottom of the shaft, which reflects the shadowing effect of the mobilization of end bearing. For both the topdown test and O-cell test, normal stress decreases with the increase of the applied load. While shear stress increases first and then decreases with the increase of the applied load in topdown test, but increases in O-cell test. This corresponds to the different stress path which is shown in Figure A-23.

Figure A-28 to Figure A-29 are plots showing the comparison of stress path of different soil elements below the pile toe for both the topdown test and O-cell test. For each element, the stress path is almost same for topdown and O-cell test, starting from a low Octahedral shear stress with both shear stress and normal stress increasing until reaching the failure envelope or yielding. After yielding, all nodes followed the path specified for the soil properties.

Case III: All Soil, $K_0 = 2$, $\mu = 0.6$ ($\delta = 31°$)

This case represents a heavily consolidated soil with large locked-in horizontal stresses, $K_0 = 2$. The results in terms of load vs displacement curve, stress path for soil-pile interface and soil elements, etc, are presented as follows.

Figure A-30 shows the load vs displacement curve for topdown load test. With the capacity increasing as compared to $K_0 = 1$ case, pile began to yield at a load of approximately 1000kips. For the O-cell test, the load vs displacement curves are plotted on Figure A-31, showing that end bearing failed before the failure of side shear. Note that a relatively large movement was required to mobilize side shear.

The equivalent topdown load vs displacement curve generated from O-cell test is shown in Figure A-32 comparing the load vs displacement curve from the topdown test. It can be seen easily that O-cell test is relatively conservative. For example, it will require a load of 1000kips to produce 0.5in displacement for the topdown test as compared to about 700kips for the O-cell test. Figure A-33 and Figure A-34 present tip load vs displacement curve and side vs displacement curve respectively. For topdown test, no more than 30% of the applied load was transferred to pile tip and most was resisted by

the side shear. Comparing the results from topdown and O-cell test, it's not difficult to find that O-cell test is conservative which is also shown in Figure A-32.

As before, Figure A-35 shows shear stress vs normal stress curves at different nodes along the soil-pile interface for both topdown test and O-cell test. Again, shear stress started from zero for all nodes and initial stress states for topdown test and O-cell test are same. Each node follows its own stress path for different test until reaching failure envelope. At a depth of 15ft, normal stress increases after failure in topdown test but decreases in O-cell test. At depths of 5ft and 10ft, normal stress decreases after slip occurs. But at a depth of 20ft, normal stress increases after slip occurs. So different nodes have different stress path and post failure behavior.

Normal stress and shear stress changing along the depth of the pile for topdown test and O-cell test are shown in Figure A-36 through Figure A-39 respectively. Similar to the above two cases, different nodes have different stress path, so it's hard to tell how normal stress and shear stress change with the applied load as a whole.

Figure A-40 and Figure A-41 compare the stress path of different soil elements below the pile toe for the topdown test and O-cell test. For this case, all four elements start with a state close to the failure envelope, with horizontal stress greater than vertical stress. However, with the increasing of the applied load (or vertical stress), the difference between the vertical stress and horizontal stress decreases, which leads the shear stress to decrease. But the average normal stress (or Octahedral normal stress) increases. After reaching some point, vertical stress becomes the first principal stress. Then with the increase of the applied load, shear stress increases until failure.

For this case, pile capacity increases compared with Case II, so does side friction. It can be seen that end bearing fails first for this case and most of the applied load is resisted by side friction. Comparing topdown and O-cell tests shows that the O-cell test tends to be conservative for these conditions of high lateral stress. Another important point is stress path of soil element, which is different from the previous two cases. This is because horizontal stress is greater than the vertical stress at the beginning of the test, thus horizontal stress is the first principal stress. But vertical stress becomes the first principal stress with the increasing of applied load. This results in shear stress decreasing first and then increasing.

Case IV: All Soil, $K_0 = 1$, $\mu = 1.2$ $(\delta = 50°)$

Roughness of soil-pile interface can affect side resistance directly, so it's necessary to analyze how friction coefficient of soil-pile interface influence the results in topdown and O-cell test. This case can be compared with Case II with same conditions except twice of friction coefficient was used to define a very rough soil-pile interface.

Load-displacement curve for topdown test was plotted in Figure A-42. Compared to Case II, capacity increases greatly. For this case, about 1160kips applied load is required to produce 1in settlement, while in Case II, only about 580kips is needed to have 1in displacement occur. This is also shown in load vs displacement curve for O-cell test plotted in Figure A-43. For Case II, side shear failed at an O-cell load of about 350kips, but side shear did not fail even at around 700kips O-cell load for this case. Note also that larger displacement is required to mobilize side shear. It is also apparent that the rough base and differing stress conditions mobilize greater end bearing than for case II.

However, note that this "end bearing" includes side shear on the lower 3ft socket below the O-cell.

Figure A-44 shows the equivalent topdown load vs displacement curve generated from the O-cell test as compared with load vs displacement curve from the topdown test. The two curves match fairly well and the O-cell test tends to underestimate the capacity slightly for this case. Tip load vs displacement and side load vs displacement curve are shown in Figure A-45 and Figure A-46 respectively. Similar to Case III, most of the applied load goes to side shear indicating end bearing is weak compared with side shear, which can be seen from the load vs displacement curve shown in Figure A-43. This is due to the high friction coefficient of the soil-pile interface. For tip load, O-cell test overestimates the capacity while underestimating capacity for side load.

Figure A-47 is a stress path plot for different nodes along soil-pile interface for topdown and O-cell test as before. Since the contact surface friction coefficient is very high, surrounding soil yielded before the contact surface. This can be seen from the envelope of stress path at depths of 10ft, 15ft and 20ft, which is close to the soil failure envelope. It's also shown that soil at all depths tends to dilate because normal stress increases with the increase of applied load.

As before, Figure A-48 to Figure A-51 are plots of normal stress and shear stress versus depth curves at different loads for topdown test and O-cell test. For this case, in topdown test, both normal stress and shear stress increase with the increasing of the applied load, and from the magnitude of the shear stress as compared to the normal stress, the contact won't fail. In O-cell test, shear stress increases with the increase of the applied load, but normal stress does not.

Stress path of different soil elements below the pile toe are plotted in Figure A-52 and Figure A-53. Similar to other cases, stress path is almost same for topdown test and O-cell test. Each element followed specific stress path until soil yielding.

For this case, side friction improves greatly as compared to Case II indicating that roughness of soil surface is important for pile capacity. Therefore, the total pile capacity improves significantly. Because of high friction coefficient, it's hard to fail the contact surface resulting in the failure of the surrounding soil. This can be seen from the stress path curves at different nodes along the soil-pile interface.

Case V: Soil Over Rock, $K_0 = 1$, $\mu = 1.2$ For Rock And $\mu = 0.6$ For Soil

In this case, soil deposit is composed of two layers: 15ft soil over rock. Different contact surface friction coefficients were used, 1.2 for rock-pile interface and 0.6 for soil-pile interface. For the topdown test, in order to fail the side shear, a false base was used under the pile tip as might be done with a physical test in rock. This false base is thin layer with a very low Young's modulus (1.4ksi) and zero Poisson's ratio.

Figure A-54 shows load-displacement curve for the topdown test, which is similar to other cases but with a much higher capacity. As shown in the figure, pile failed at a load of about 1400kips after which displacement increases rapidly. The generated tip load vs displacement curve and side load vs displacement curve are shown in Figure A-55 and Figure A-56 respectively. Obviously, only a very small part of the applied load goes to pile tip because of low stiffness of the false base. Figure A-56 also compares the result from the topdown test and the O-cell test, showing that the O-cell test is conservative in this case. Figure A-57 is the load-displacement curve for the O-cell test. As shown in

figure, the downward displacement of pile tip is almost nothing due to the high stiffness of rock. Side shear failed at about 1000kips O-cell load.

Figure A-58 and Figure A-59 show the stress path at different nodes along contact surface in soil and rock respectively. Comparing these two figures, it can be seen that stresses in rock are much higher than in soil because of different stiffness. And they have different failure envelope with a slope of 0.6 and 1.2 respectively. Soil tends to dilate (normal stress increase) at all depth. In the O-cell test, it's very difficult to fail the contact surface at depth of 28ft as shown in Figure A-59 that the stress path at that depth is far from the failure envelope.

Figure A-60 to Figure A-63 show the change of normal stress and shear stress along the length of pile for topdown and O-cell tests respectively. As shown in figures, both normal stress and shear stress in the topdown test and the O-cell test increase with the increase of the applied load. Normal stress curves are similar shear stress curves. It is also shown that stress in rock is much high than in soil which is also concluded from Figure A-58 and Figure A-59, and this is because rock has a much higher stiffness than soil.

For this case, pile capacity increases greatly due to the high stiffness of rock deposit. Because of its high stiffness, it's very difficult to fail the end bearing, which can be found from the load-displacement curve of the O-cell test. Furthermore, rock accounts for most of the side shear as shown in the plot of shear stress vs depth. The O-cell test is conservative in estimating side friction for this case.

SUMMARY

Finite element models for both topdown test and O-cell test were built up using ABAQUS and MSC/PATRAN. Different boundary conditions were applied to simulate the real situation in the load test. Several cases were calculated and results were analyzed and compared between the topdown test and the O-cell test. From the above analysis, several conclusions can be drawn described as follows.

1) In general, the O-cell test seems to underestimate pile capacity more or less;

2) The ratio of in-situ horizontal to vertical stress affects capacity significantly. With the increase of K_0, pile capacity improves;

3) Roughness of the soil surface plays an important roll in improving pile capacity. The increase of friction coefficient will improve side resistance directly.

4) Rock improves capacity in both end bearing and side friction;

5) Stress path for soil element is almost same for the topdown test and the O-cell test, but the stress path for contact surface is different for the topdown test and the O-cell test although they start from the same stress state.

6) From the normal stress and shear versus depth curves, it is indicated that the maximum normal stress or shear stress is not always at the bottom of the pile. There's no a simple relation between the curves and the applied load which is because every node has a different stress path.
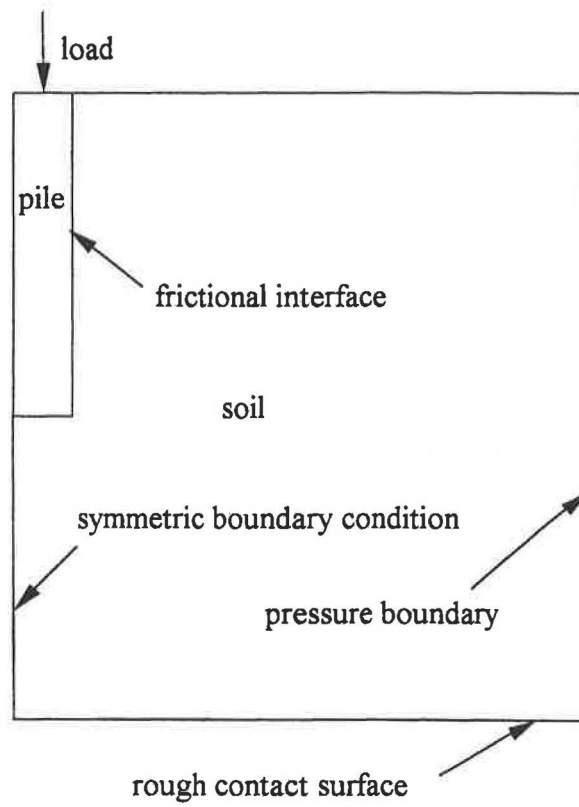
Figure A-1   Topdown Load Test Model
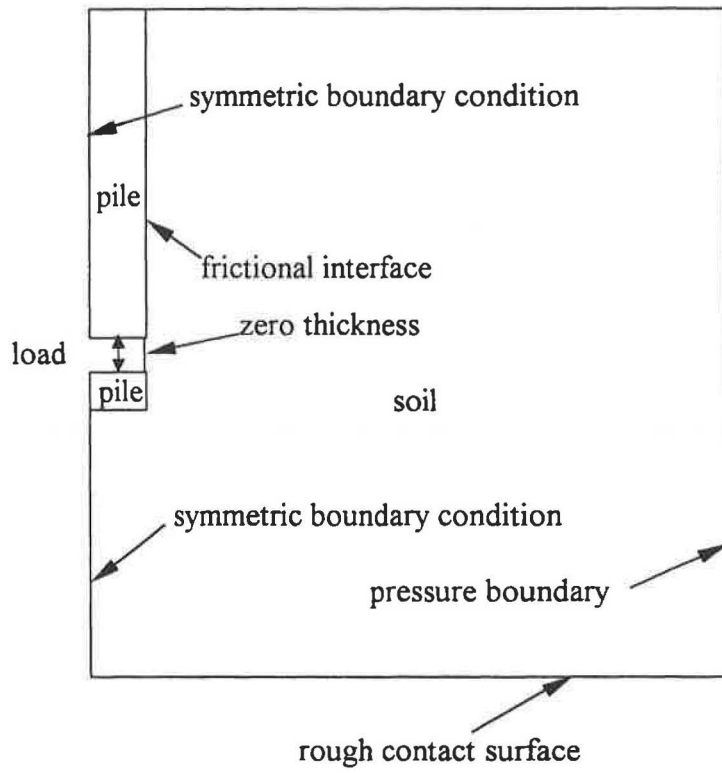
Figure A-2 O-cell Load Test Model
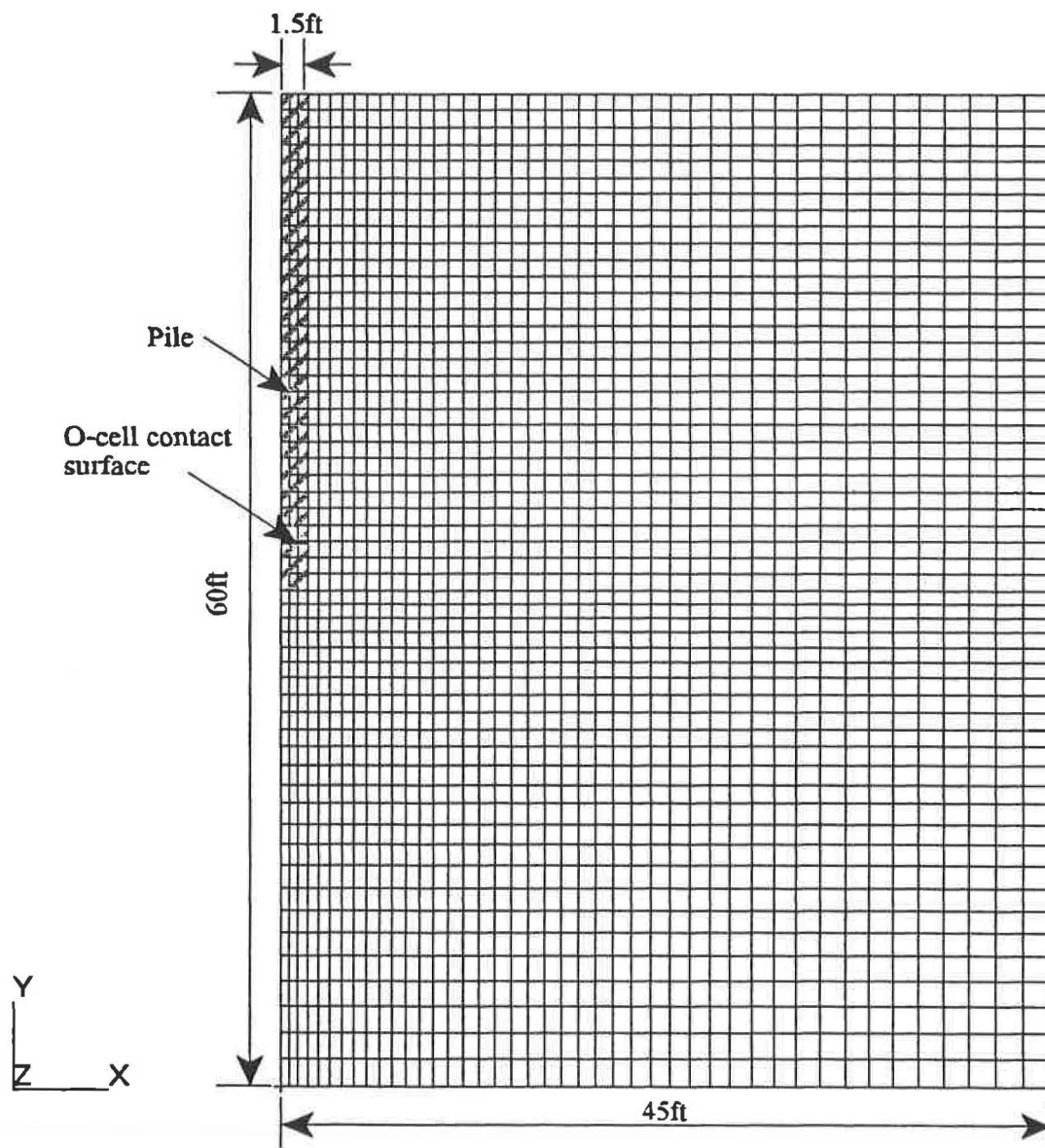
Figure A-3 Finite Element Mesh
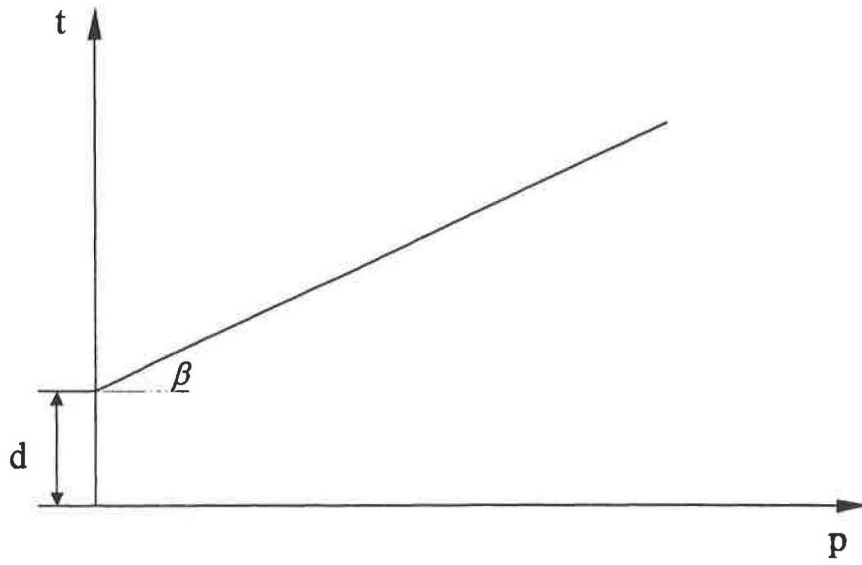
Figure A-4 Linear Drucker-Prager Model
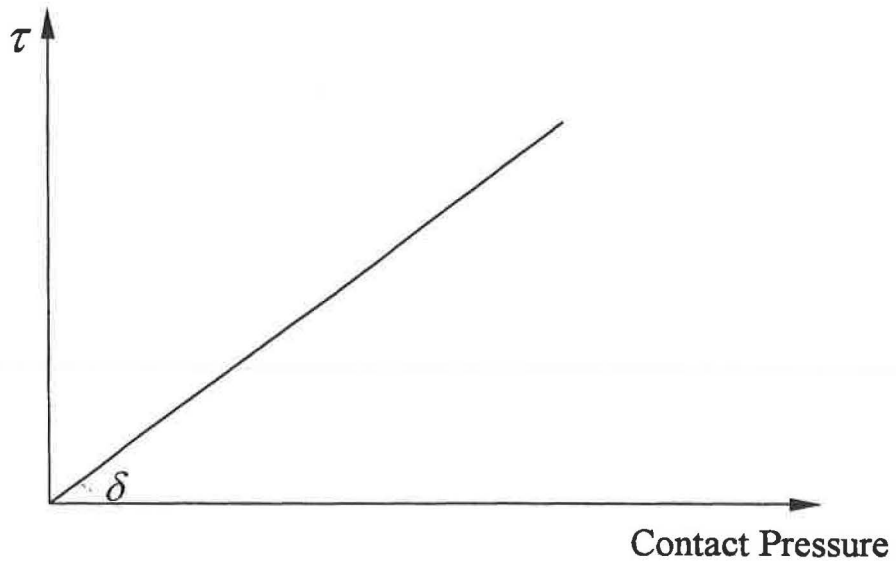
Figure A-5 Frictional Contact Surface
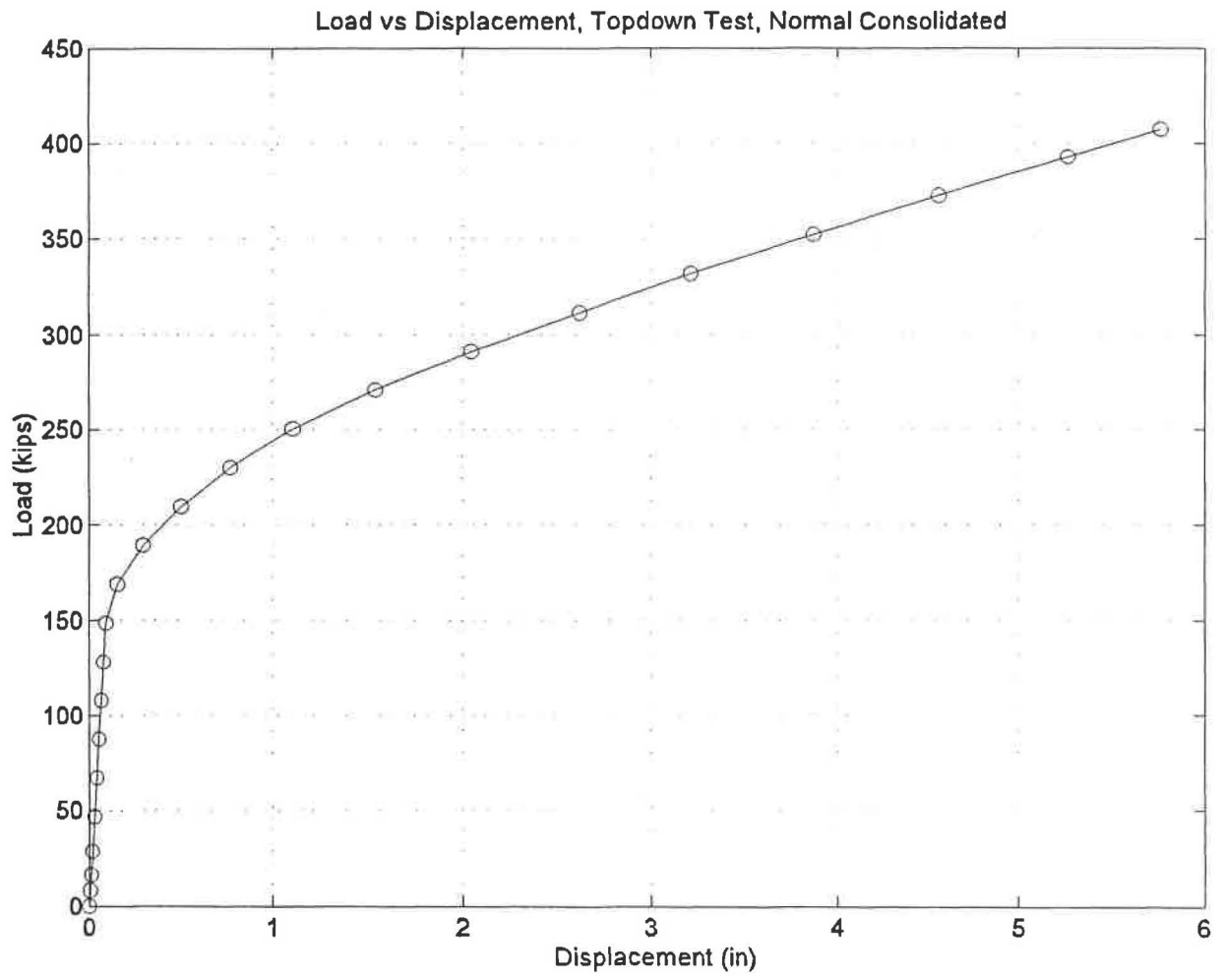
Figure A-6 Load-Displacement Curve, Topdown Test, Normal Consolidated
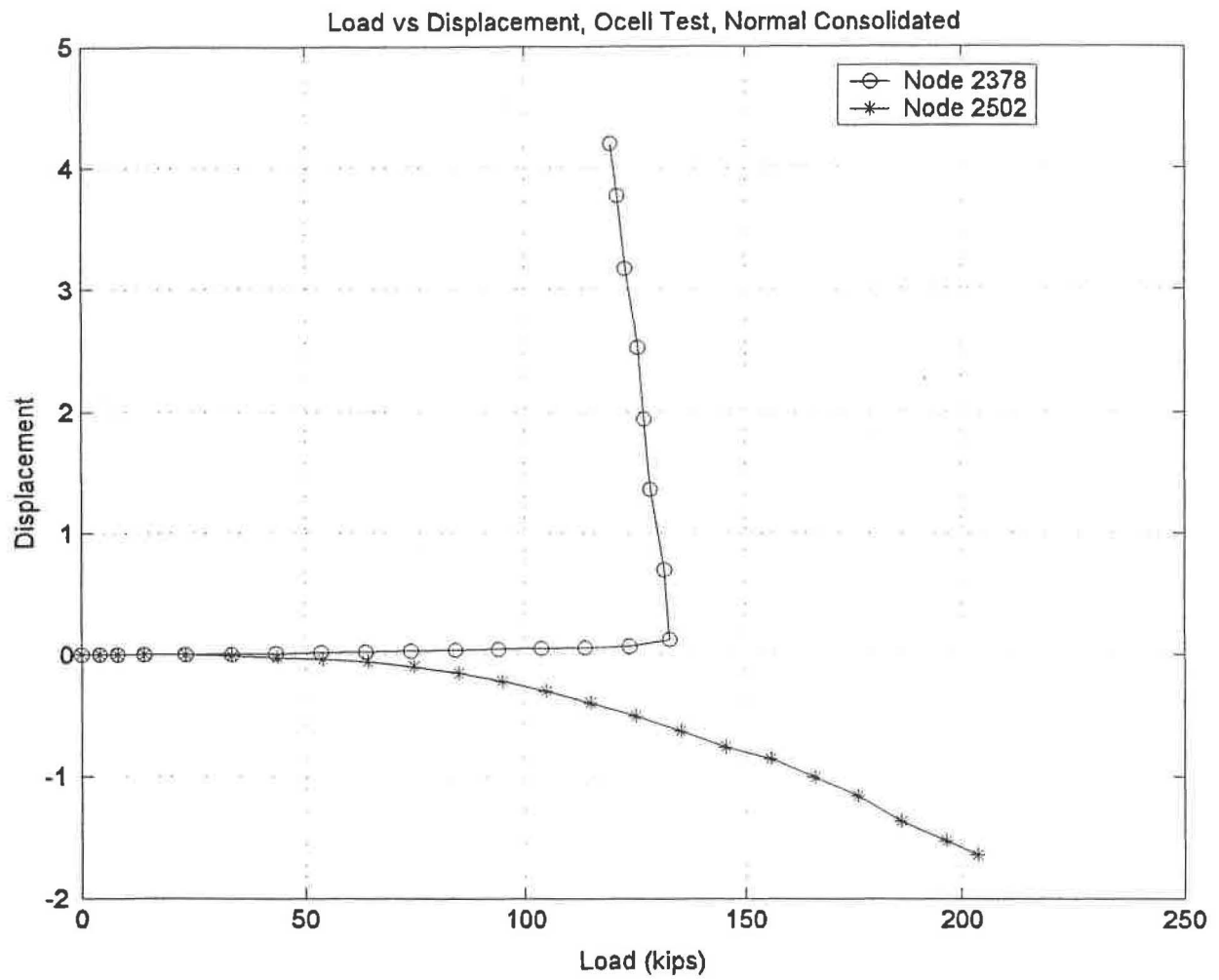
Figure A-7 Load-Displacement Curve, O-cell Test, Normal Consolidated
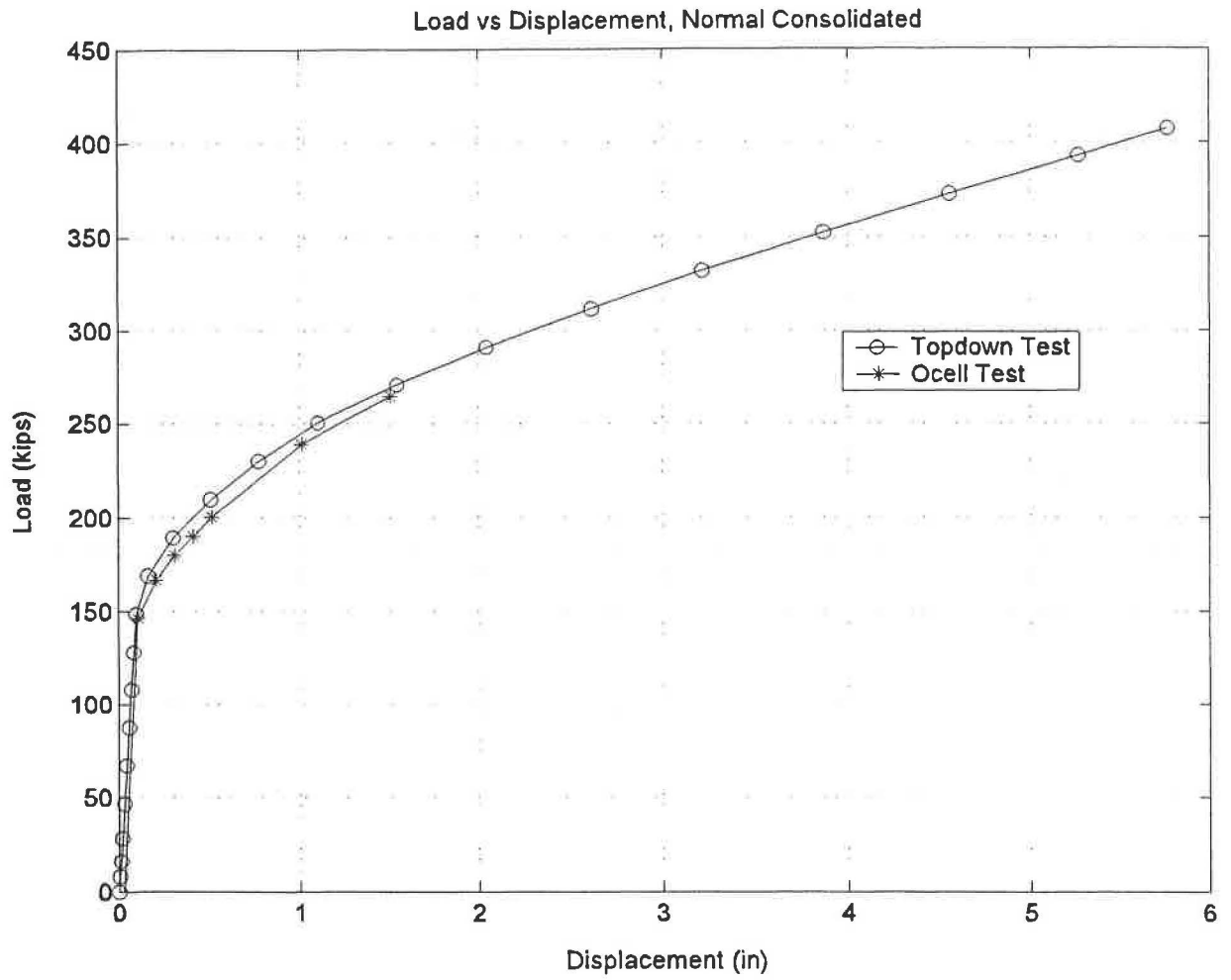
Figure A-8 Comparison of Topdown Test and O-cell Test, Normal Consolidated
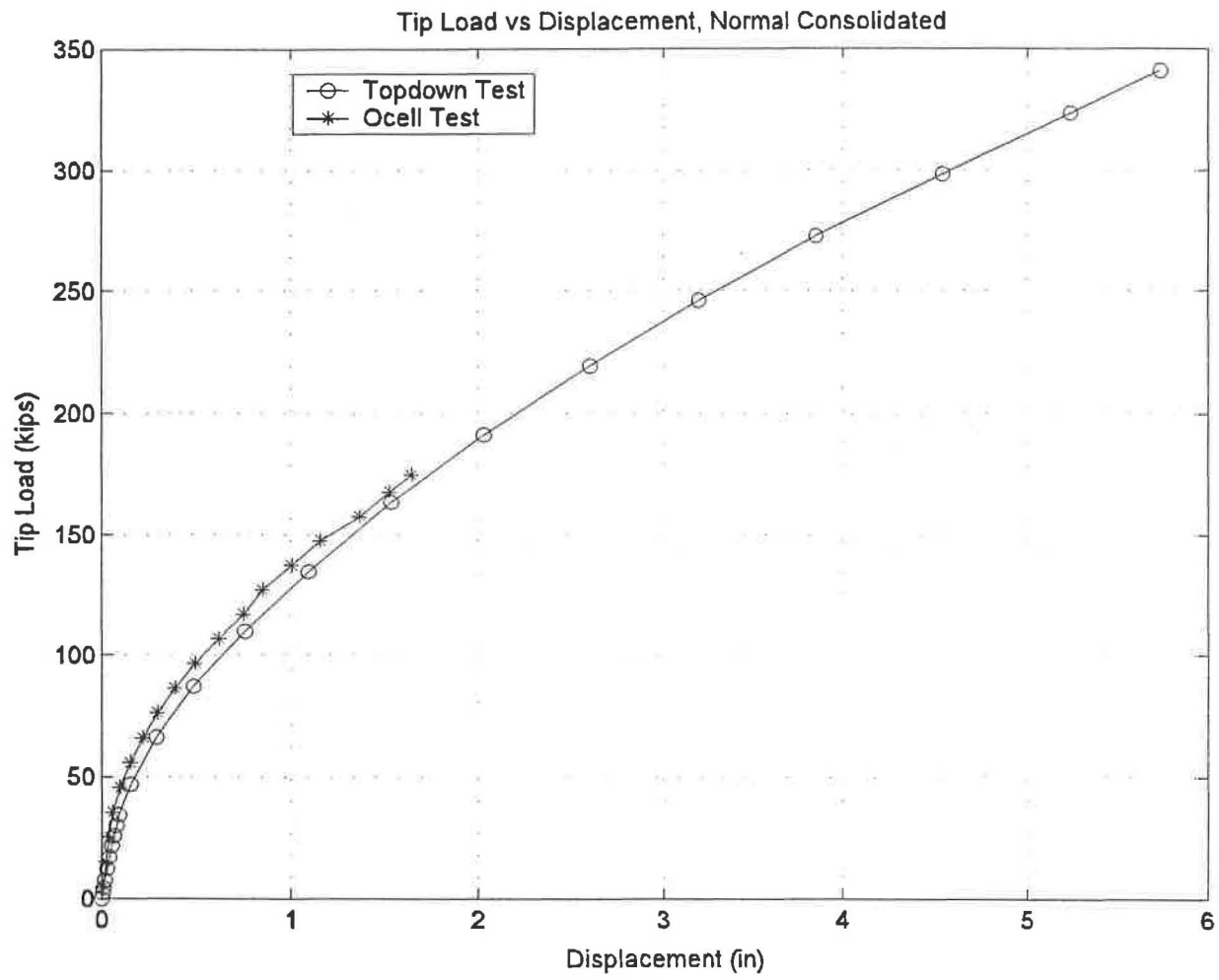
Figure A-9 Tip Load vs Displacement Curve, Normal Consolidated
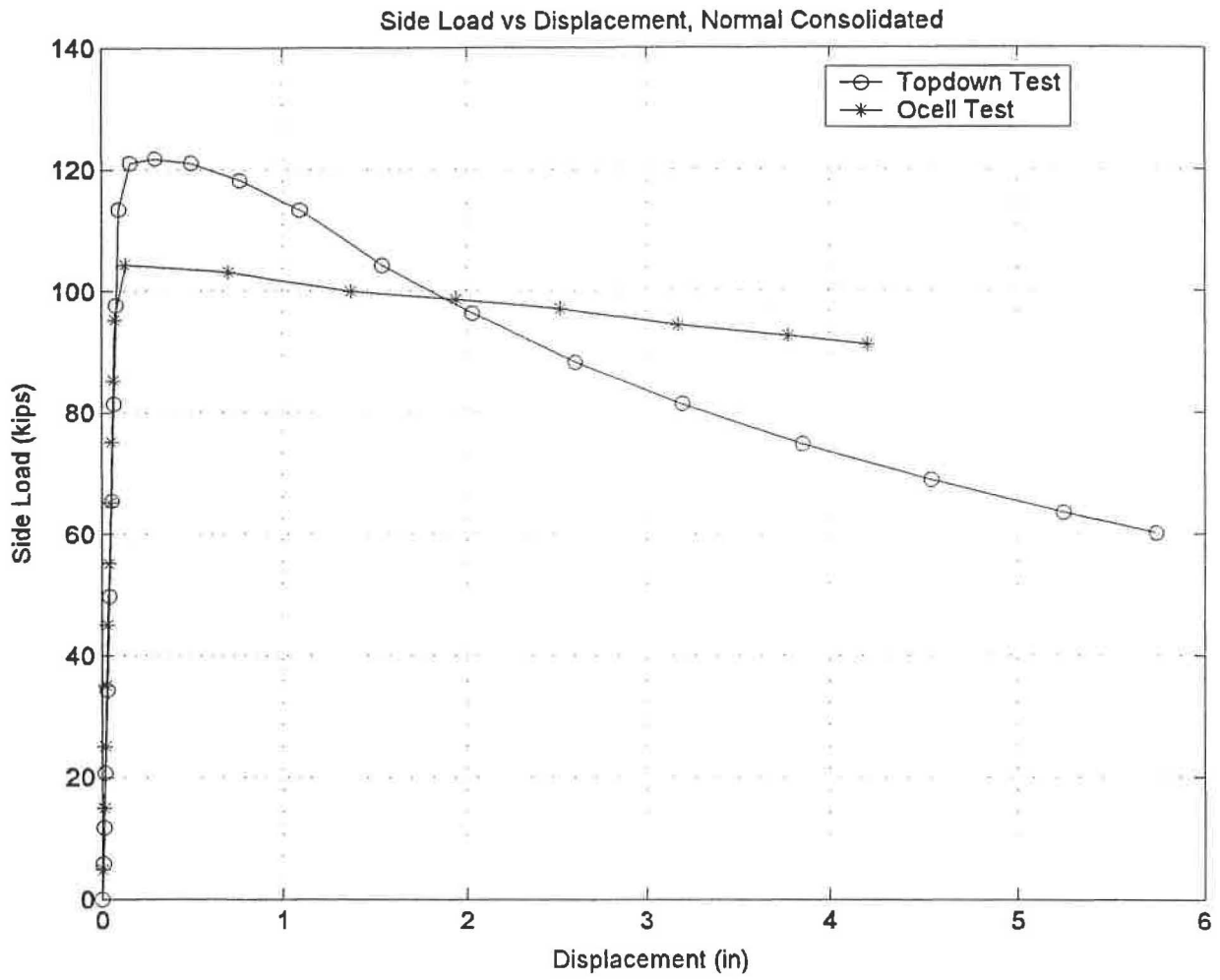
Figure A-10 Side Load vs Displacement Curve, Normal Consolidated
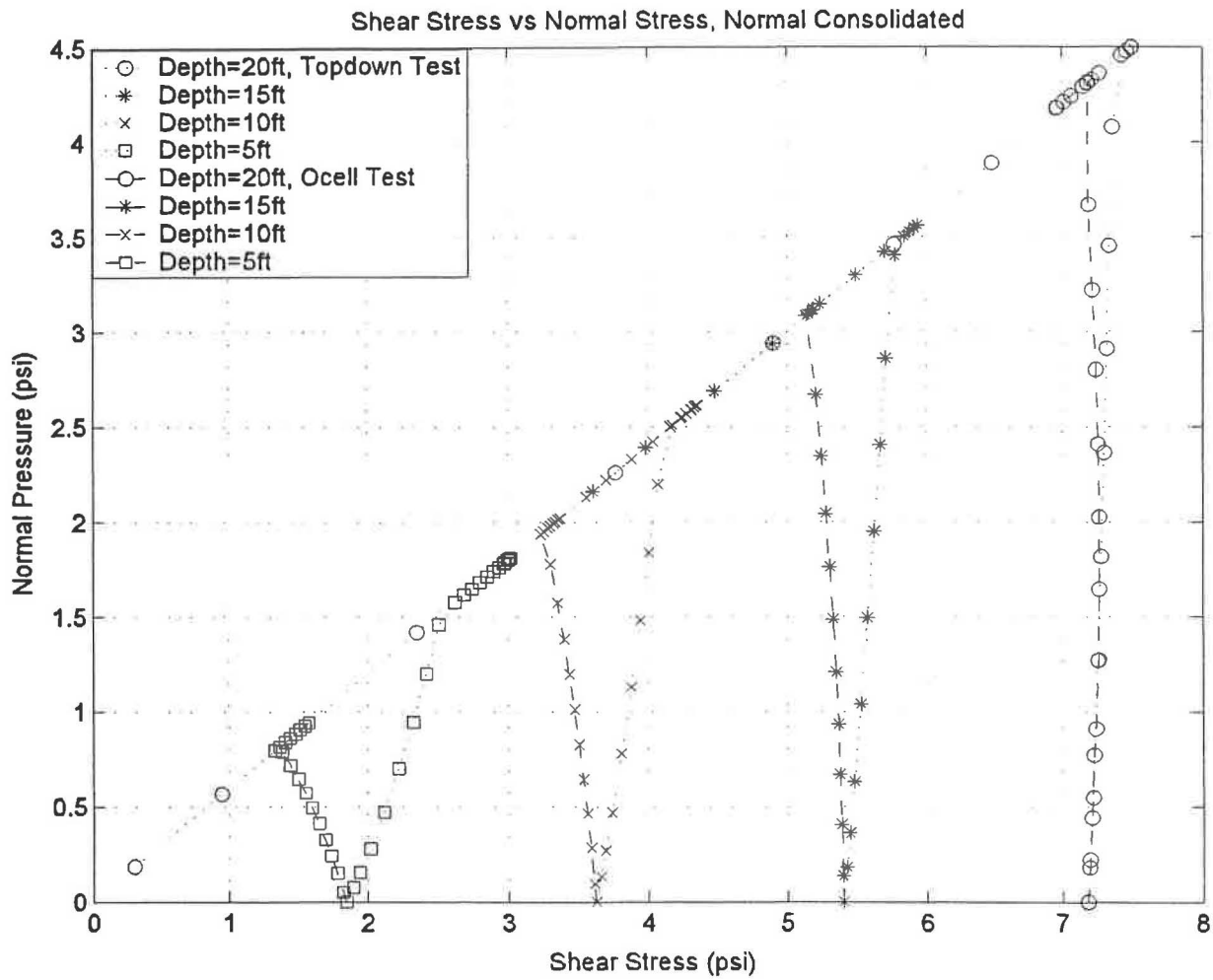
Figure A-11 Stress Path at Different Nodes on Soil-Pile Interface,
Normal Consolidated

A-29
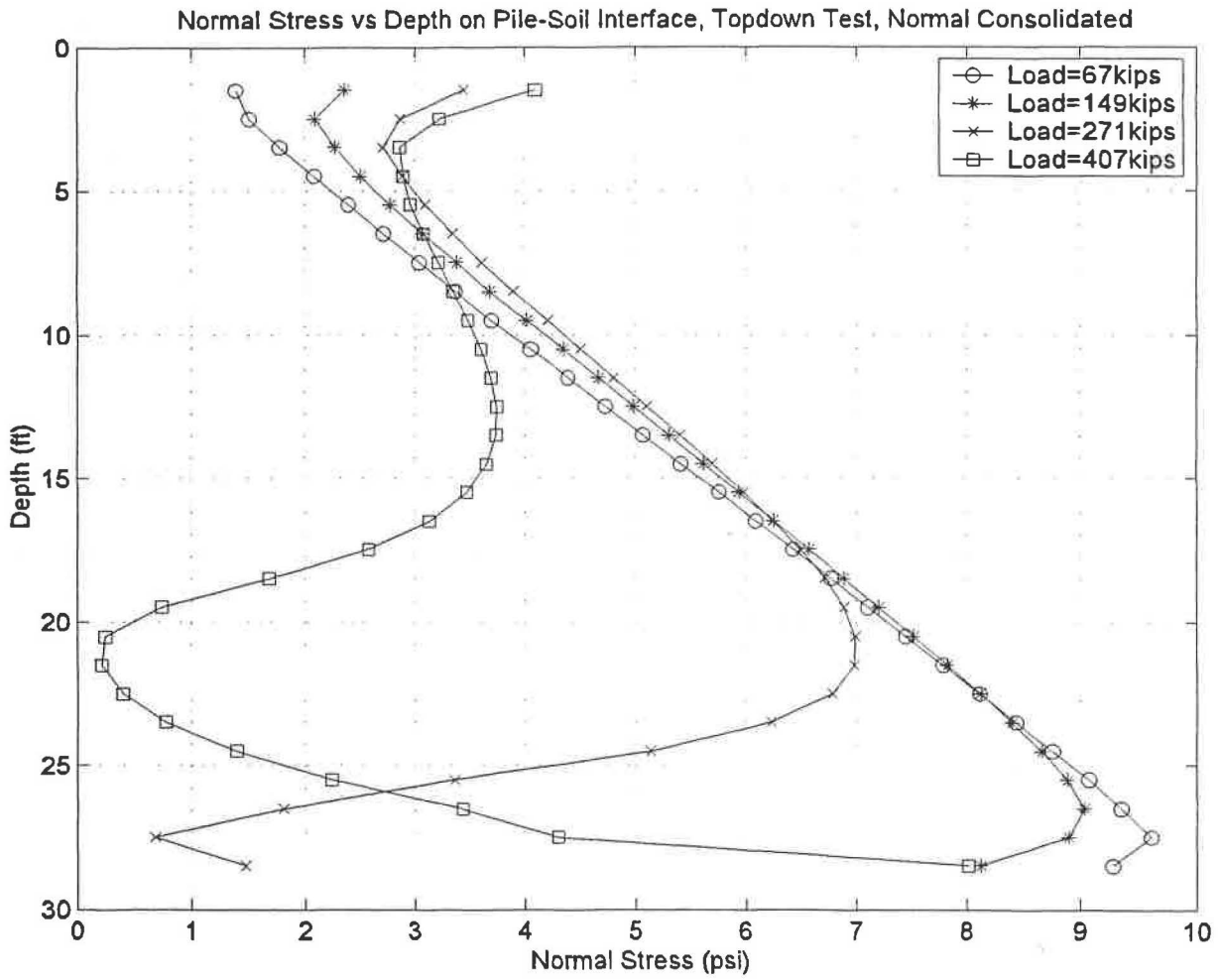
Figure A-12 Normal Stress vs Depth Curve, Topdown Test, Normal Consolidated
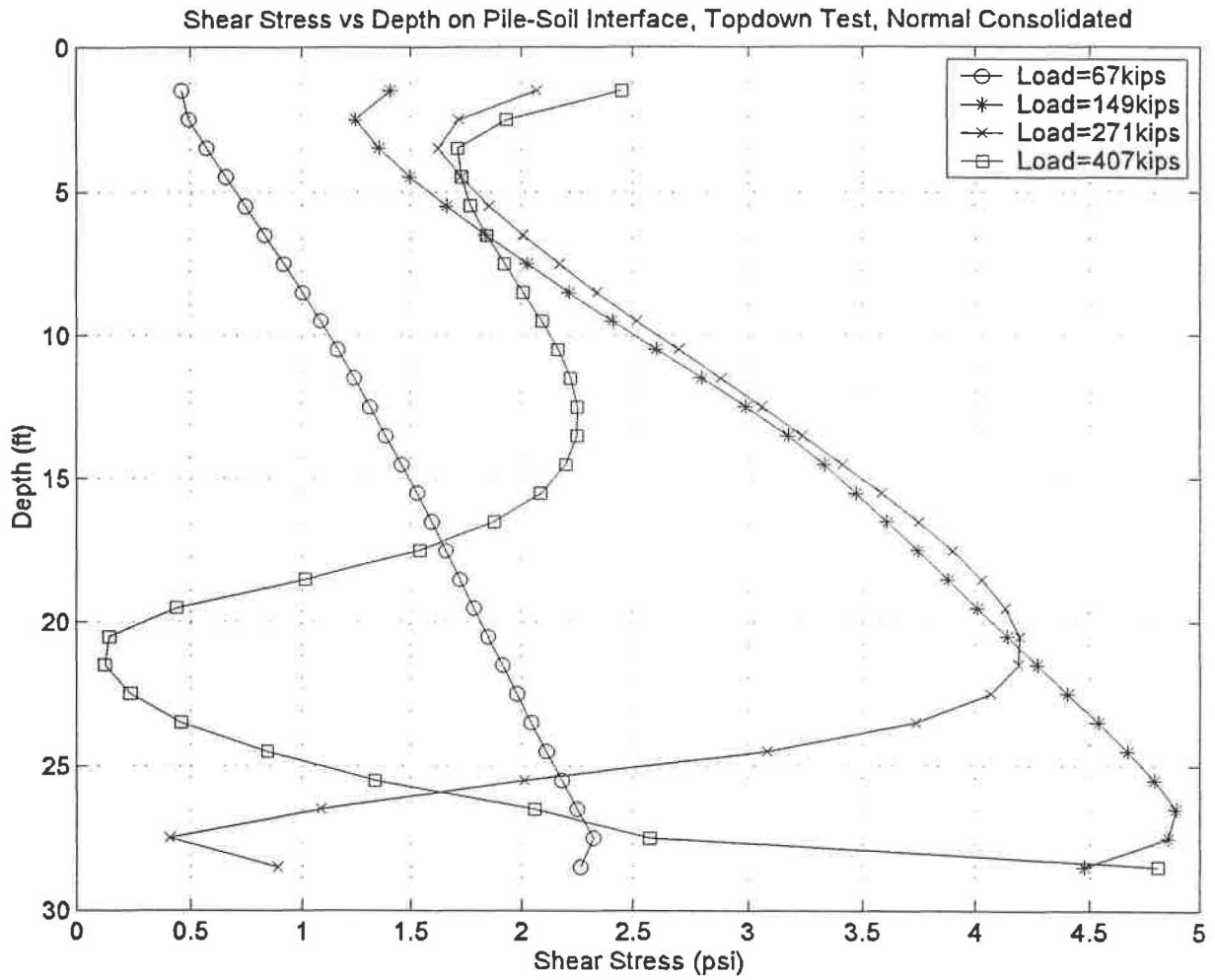
Figure A-13 Shear Stress vs Depth Curve, Topdown Test, Normal Consolidated
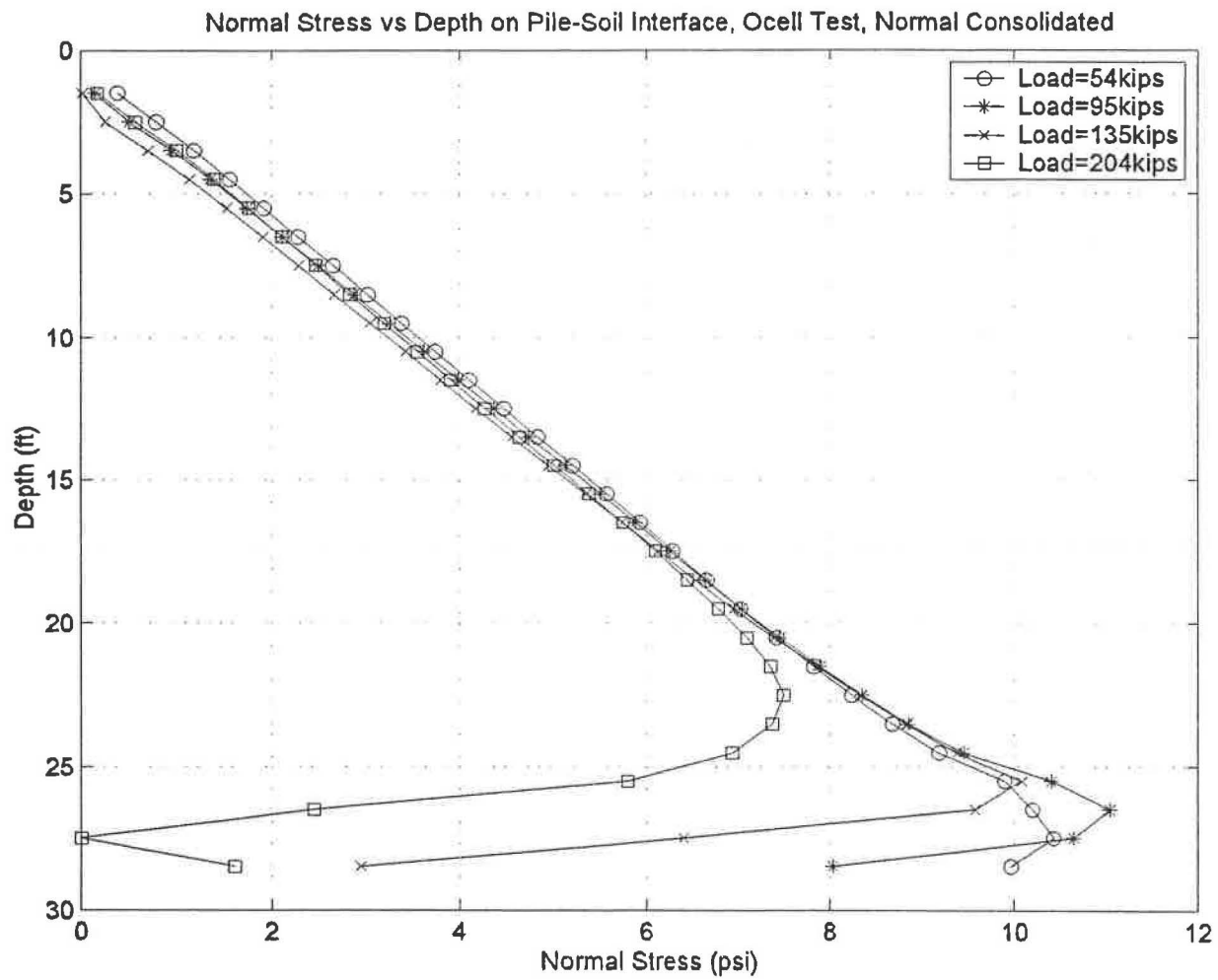
Figure A-14 Normal Stress vs Depth Curve, O-cell Test, Normal Consolidated
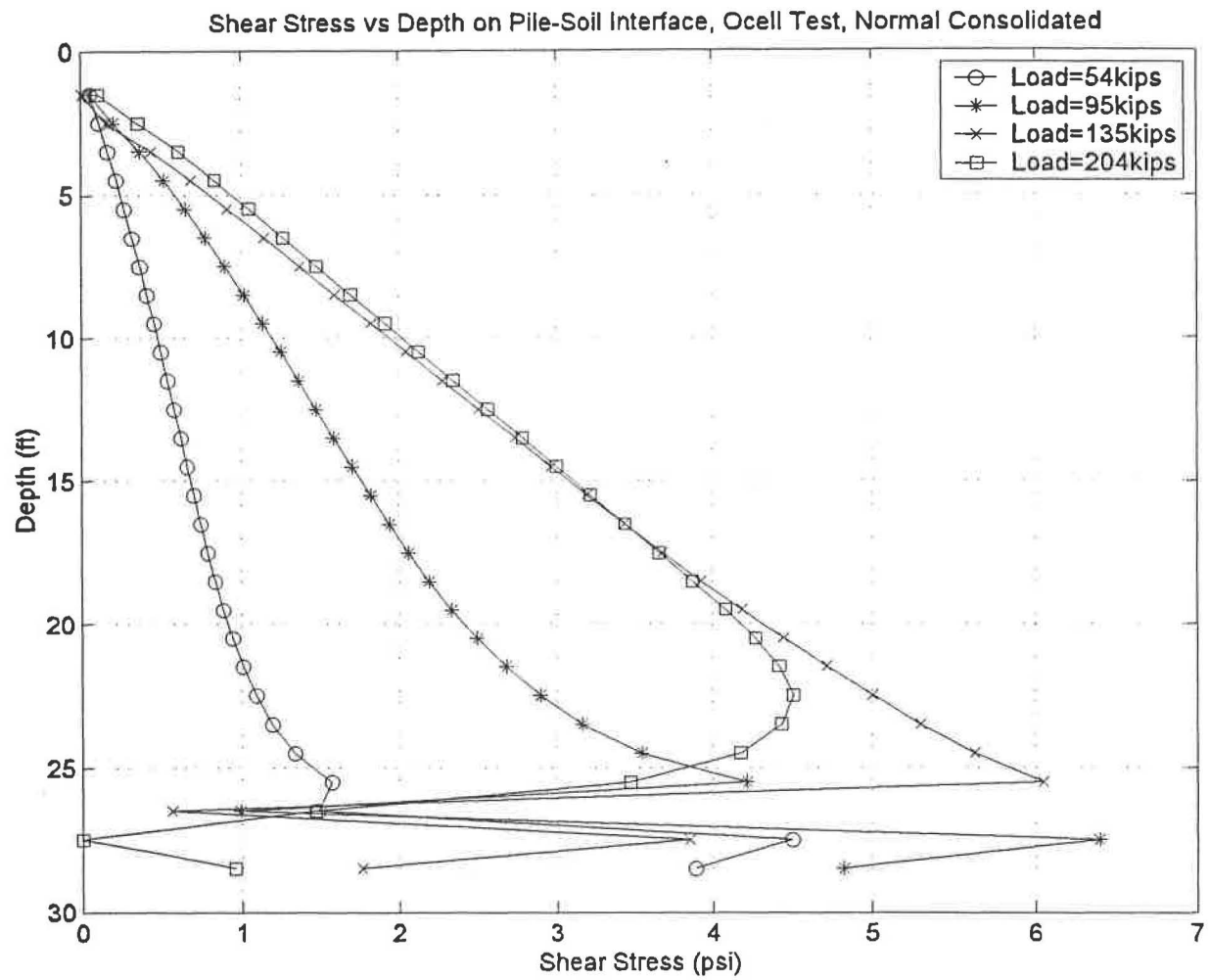
Figure A-15 Shear Stress vs Depth Curve, O-cell Test, Normal Consolidated
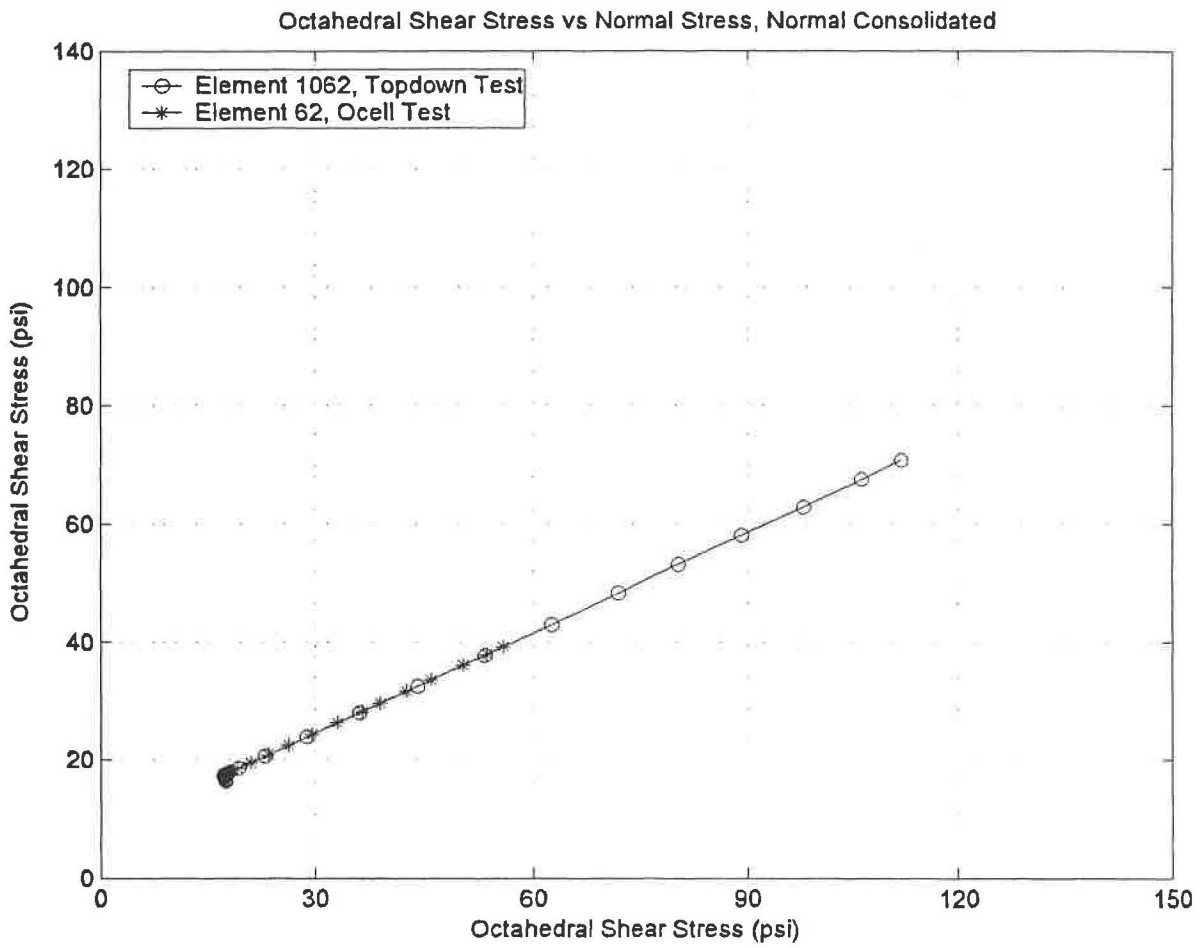
Figure A-16 Stress Path of Soil Element, Normal Consolidated

Octahedral Shear Stress vs Normal Stress, Normal Consolidated
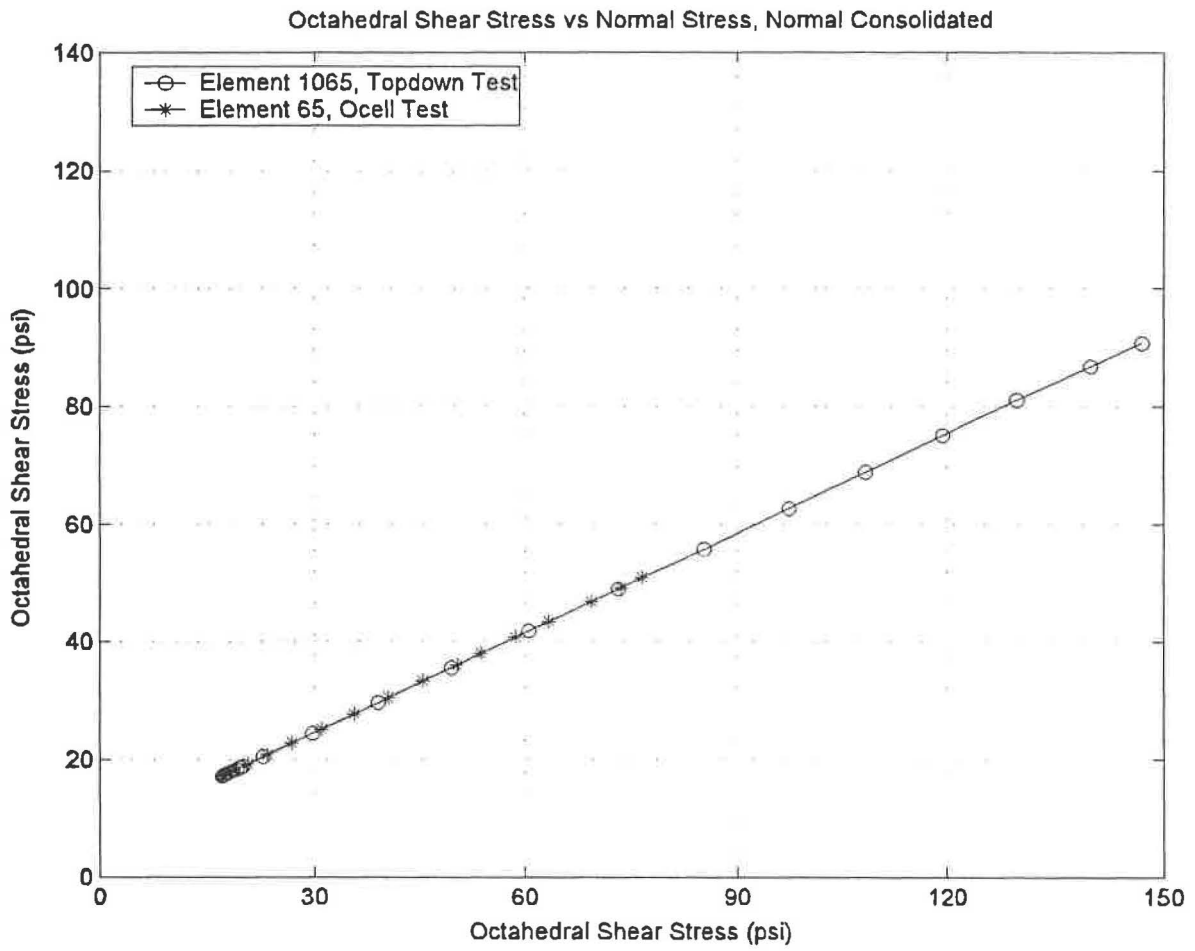
Figure A-17 Stress Path of Soil Element, Normal Consolidated
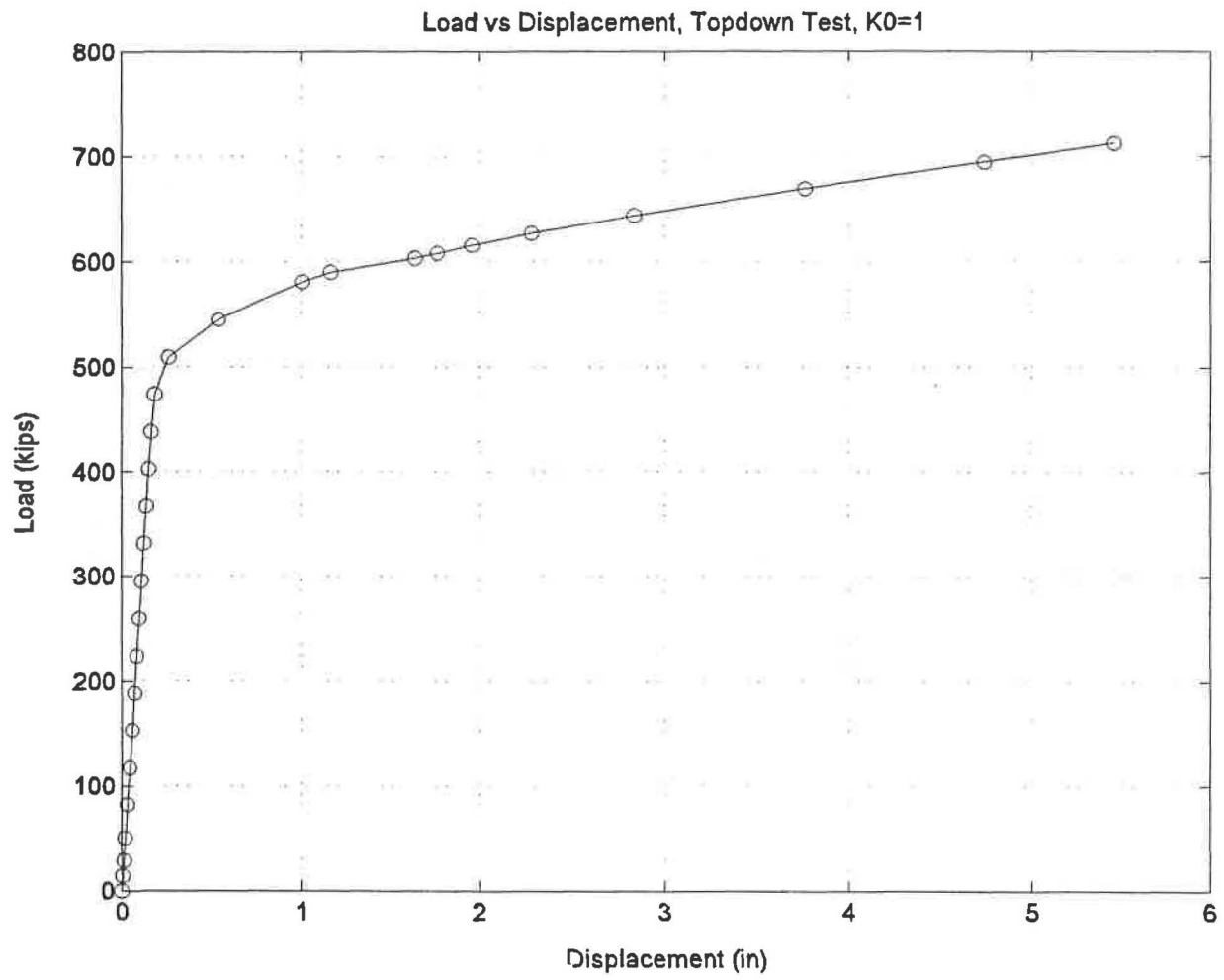
Figure A-18 Load-Displacement Curve, Topdown Test, $K_0=1$
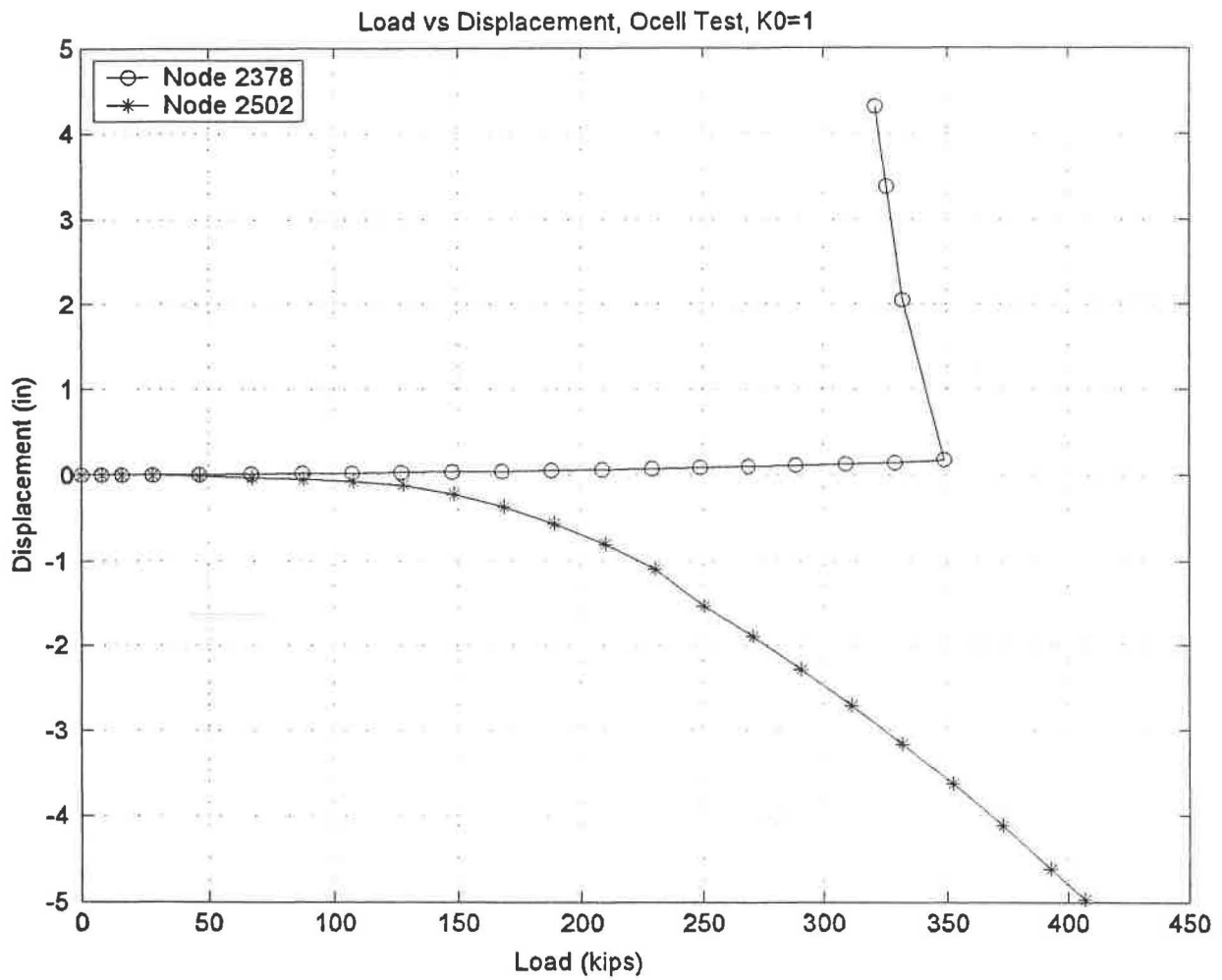
Figure A-19 Load-Displacement Curve, O-cell Test, $K_0=1$
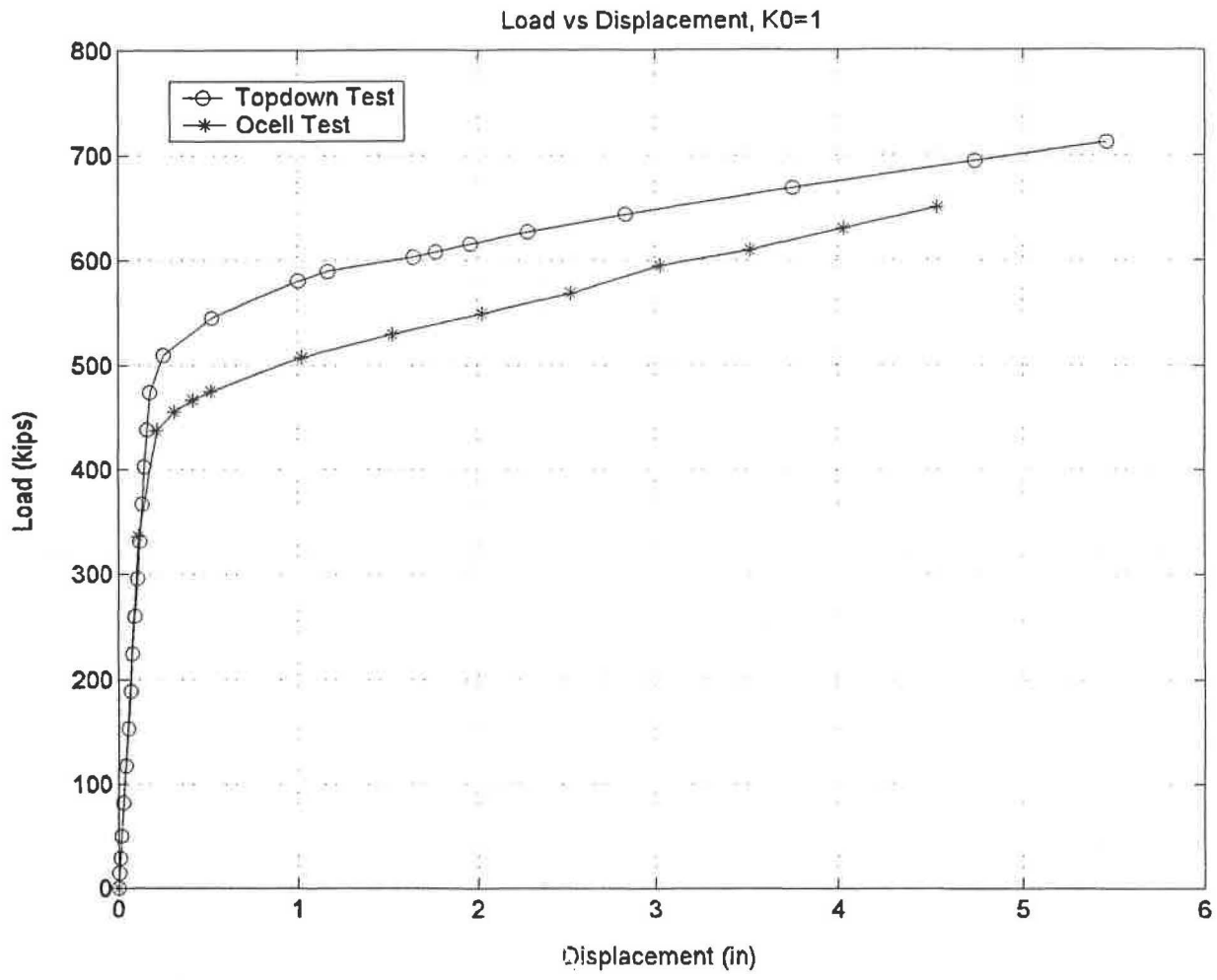
Figure A-20 Comparison of Topdown Test and O-cell Test, $K_0=1$
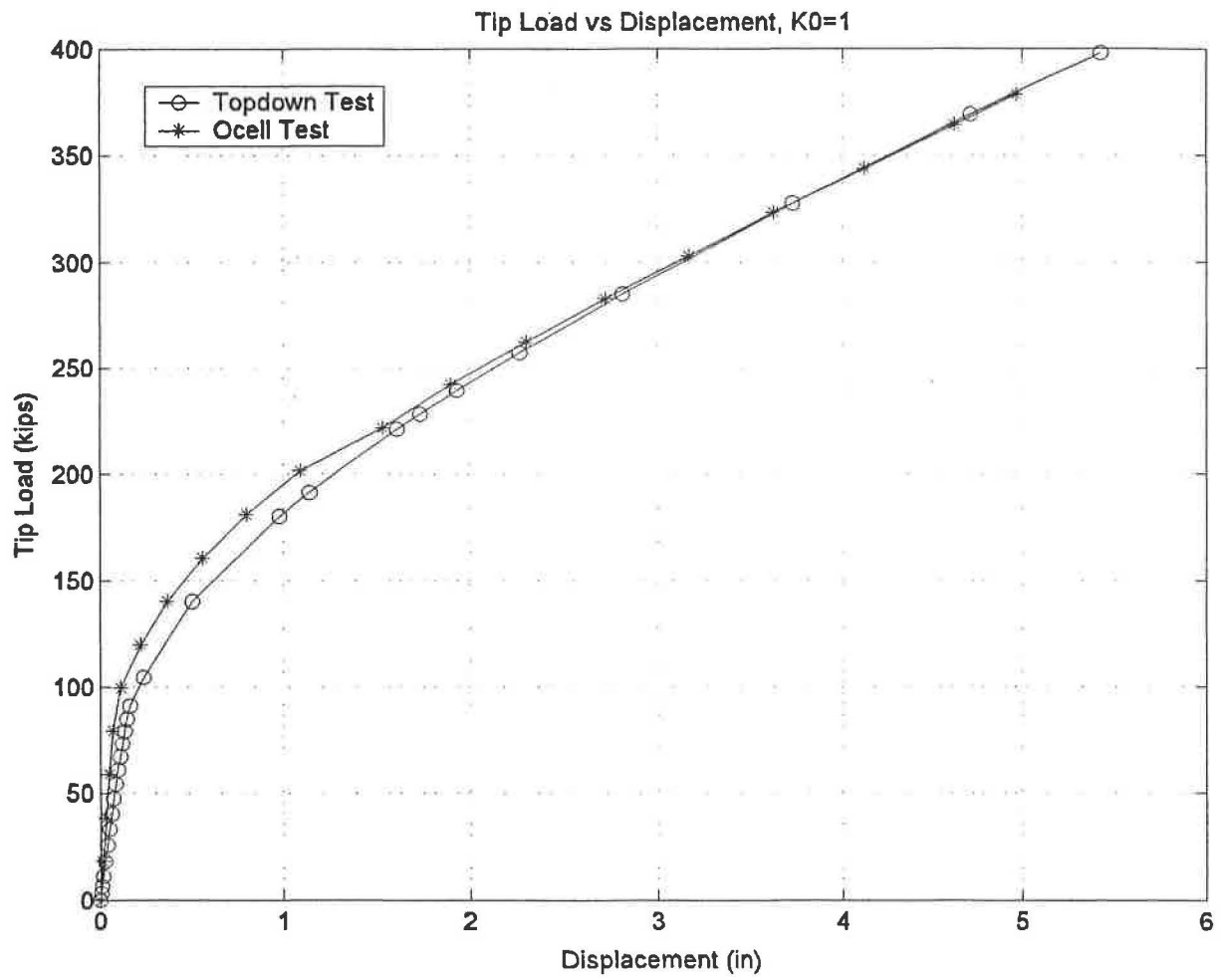
Figure A-21 Tip Load vs Displacement Curve, $K_0=1$
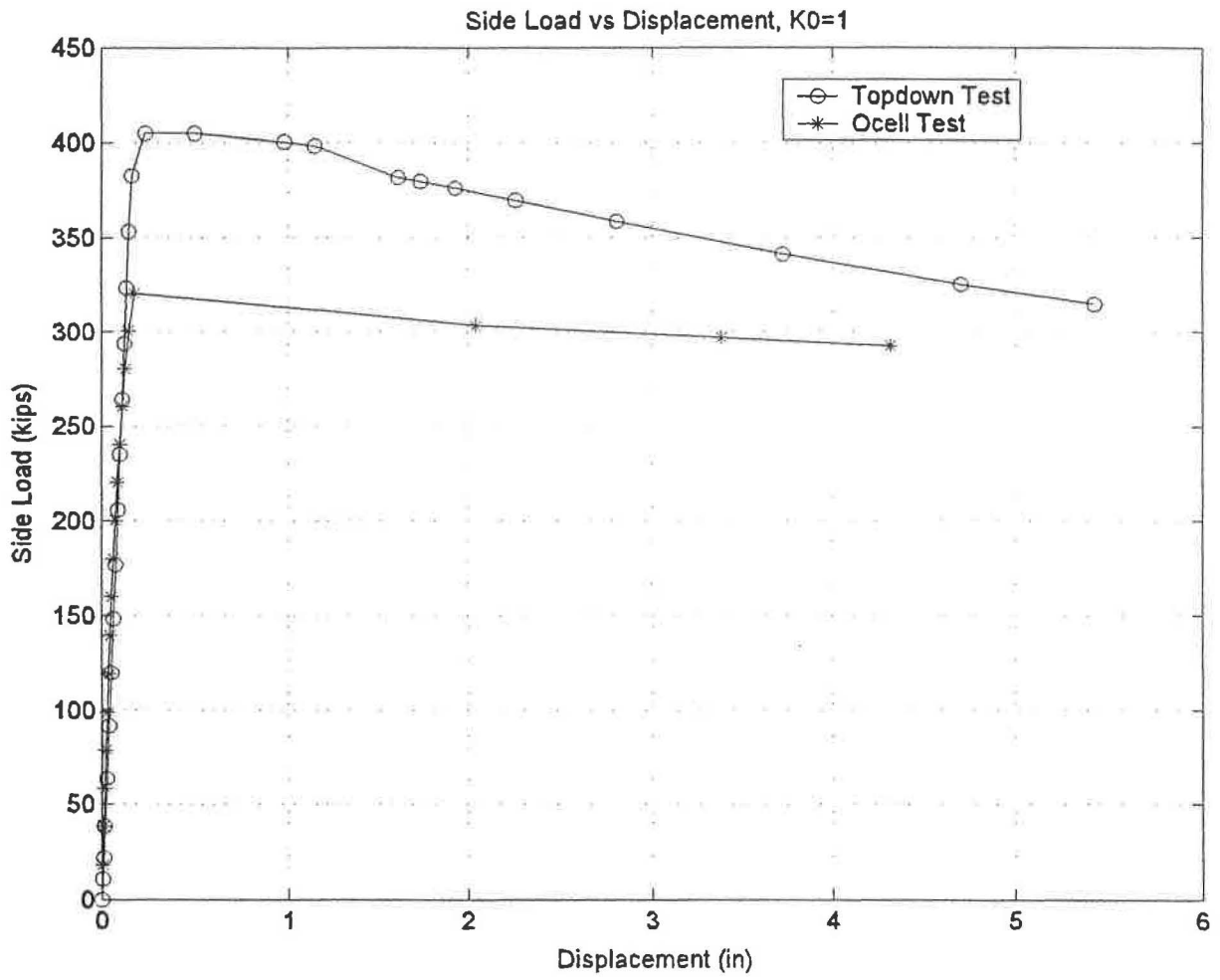
Figure A-22 Side Load vs Displacement Curve, $K_0=1$
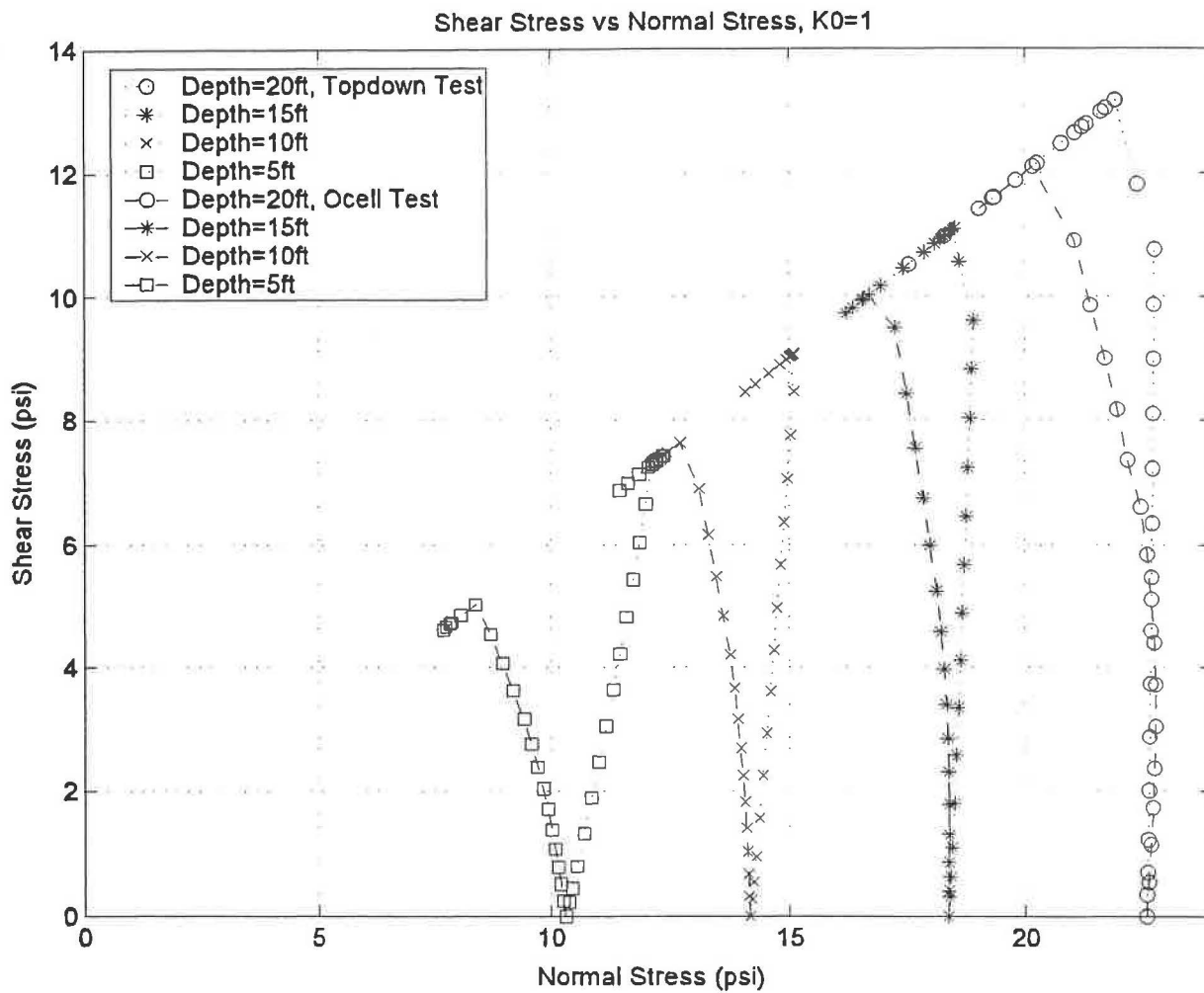
Figure A-23 Stress Path at Different Nodes on Soil-Pile Interface, $K_0=1$
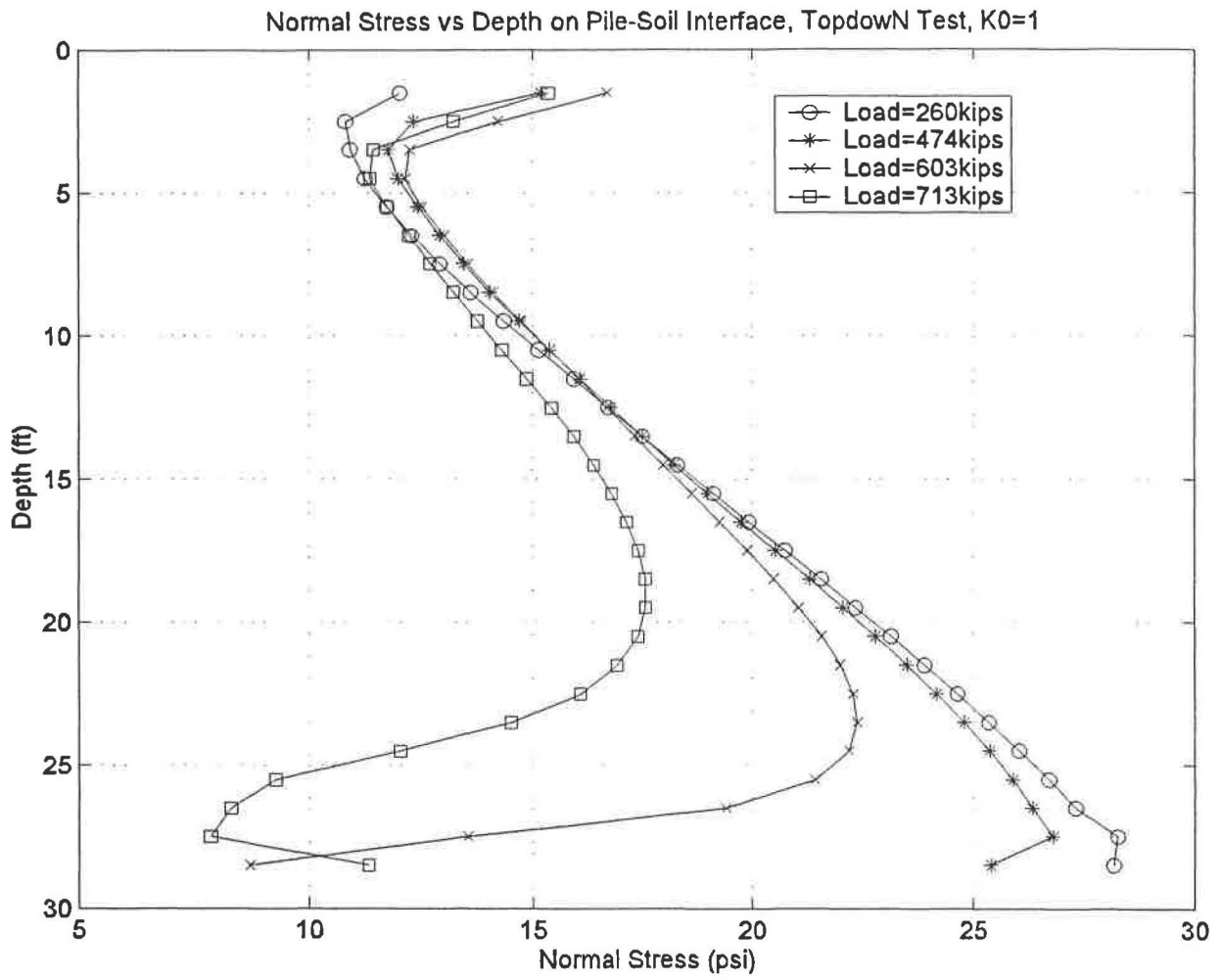
*Figure A-24 Normal Stress vs Depth Curve, Topdown Test, $K_0=1$*
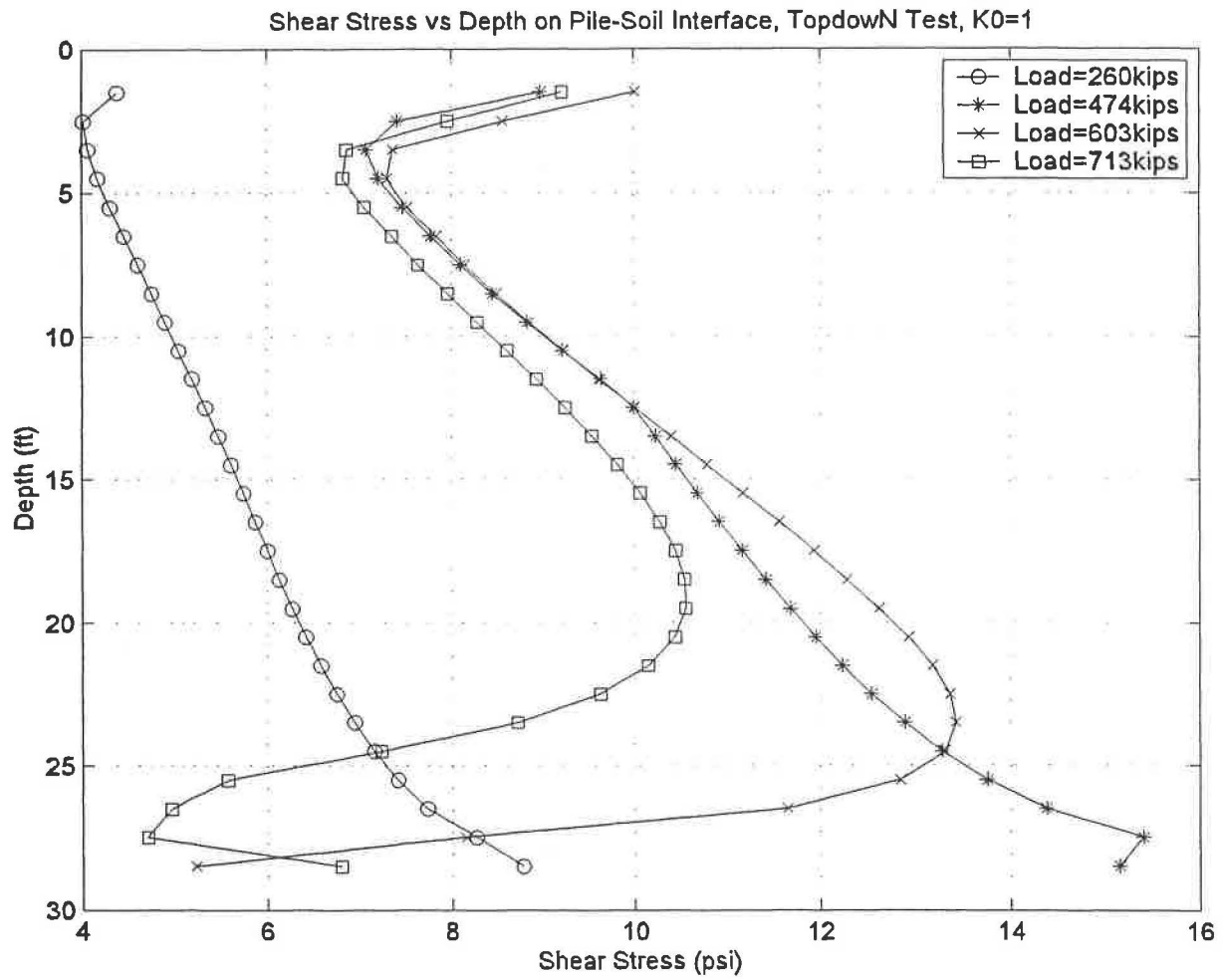
Figure A-25 Shear Stress vs Depth Curve, Topdown Test, $K_0=1$
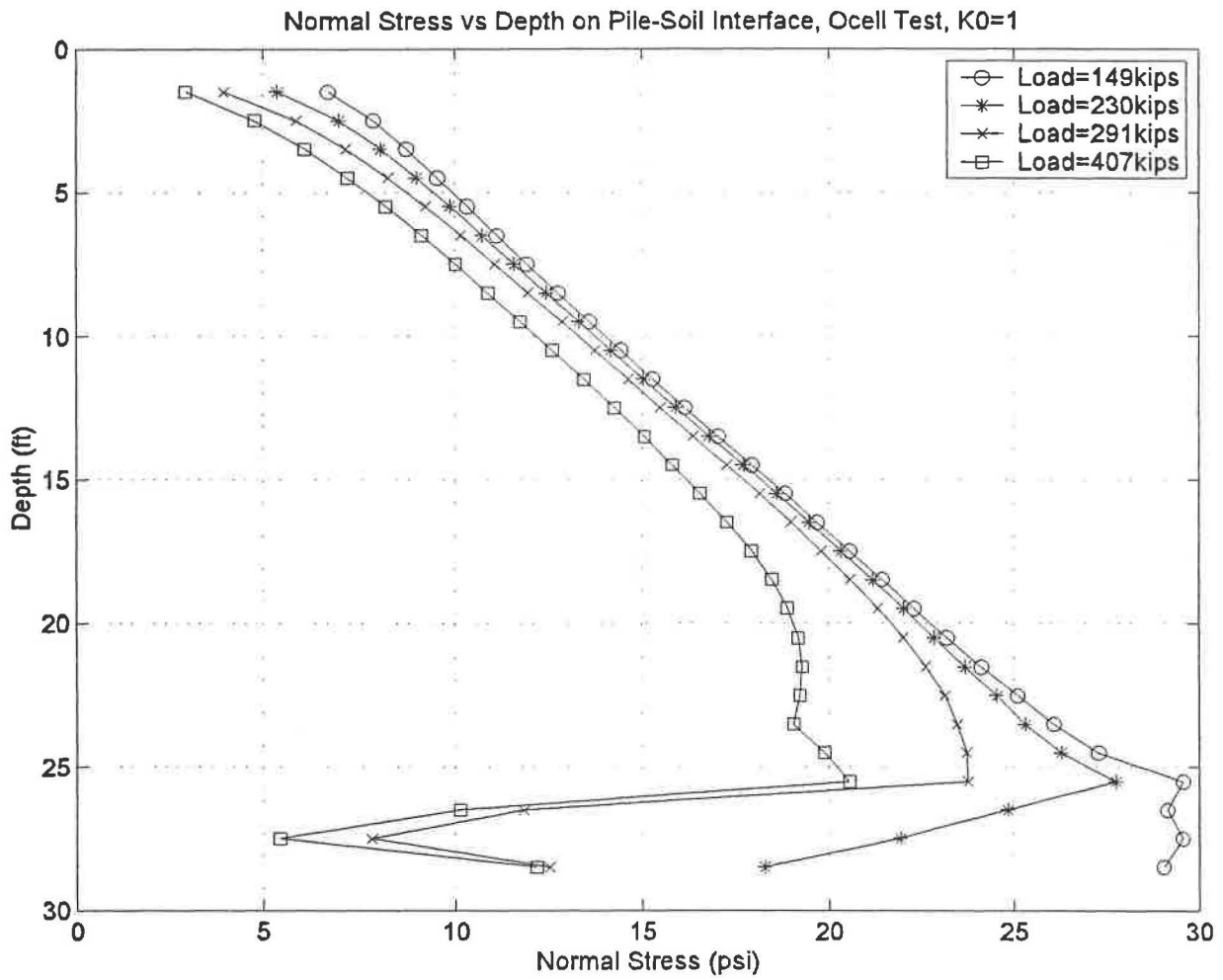
Figure A-26 Normal Stress vs Depth Curve, O-cell Test, $K_0=1$
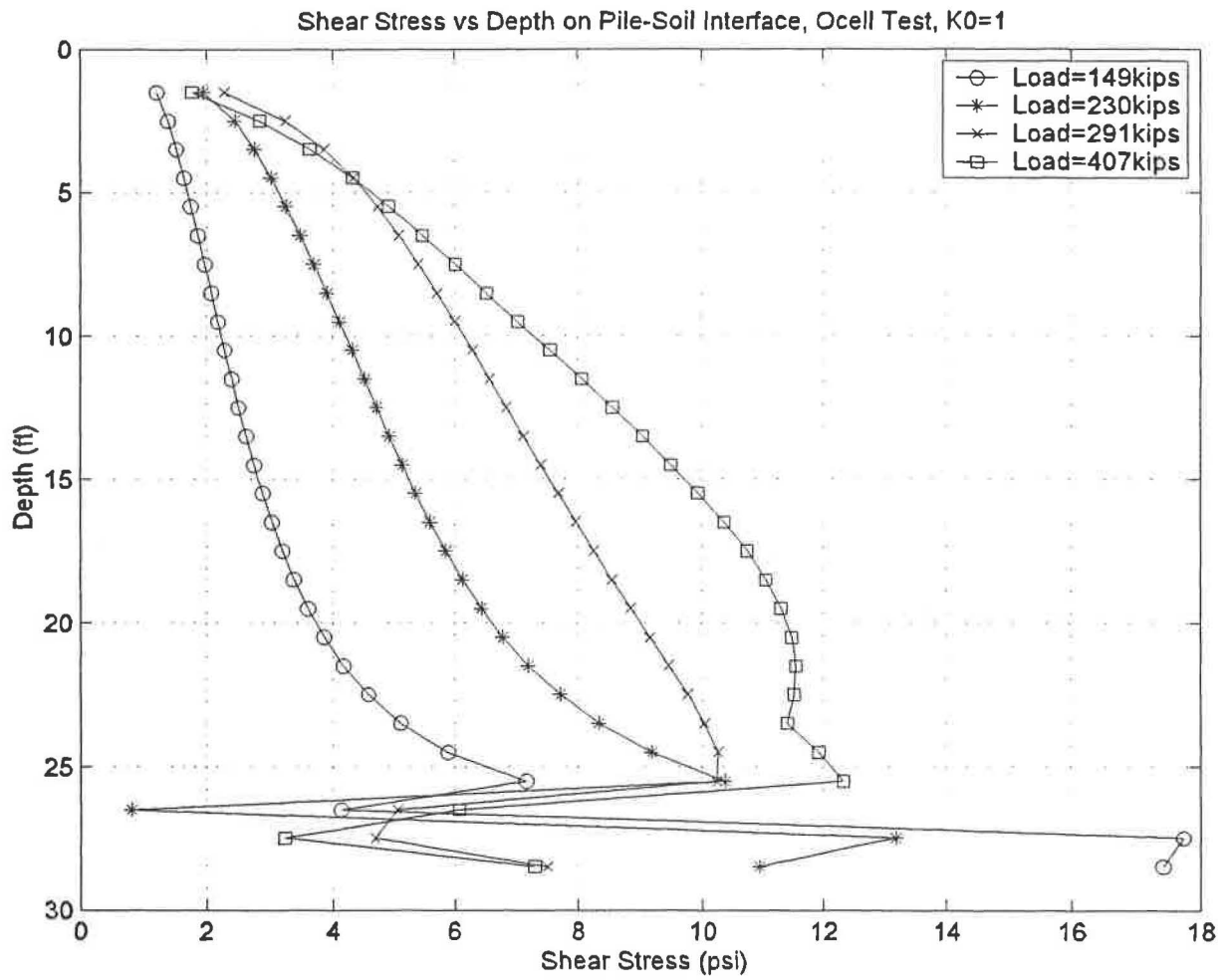
*Figure A-27 Shear Stress vs Depth Curve, O-cell Test, $K_0=1$*
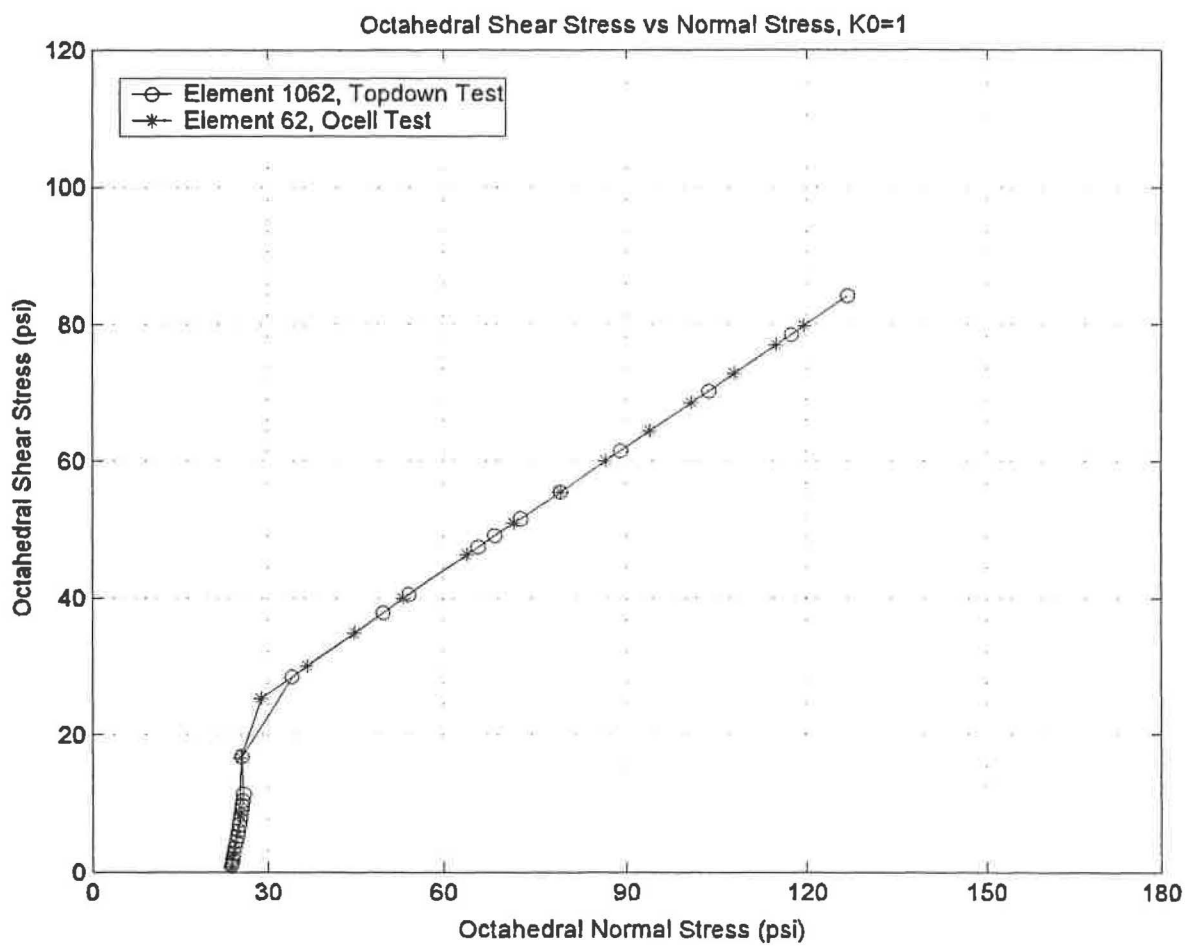
Figure A-28 Stress Path of Soil Element, $K_0=1$
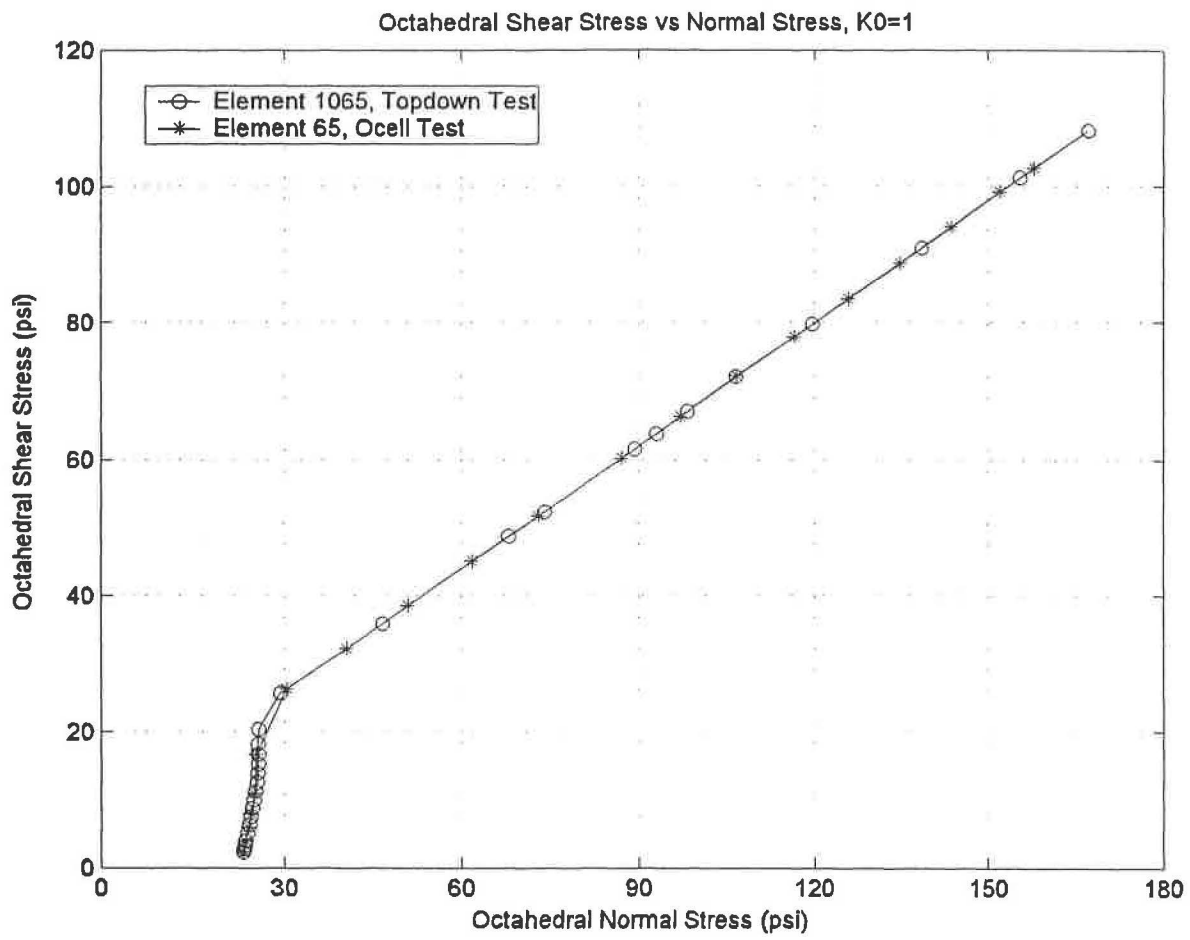
Figure A-29 Stress Path of Soil Element, K₀=1
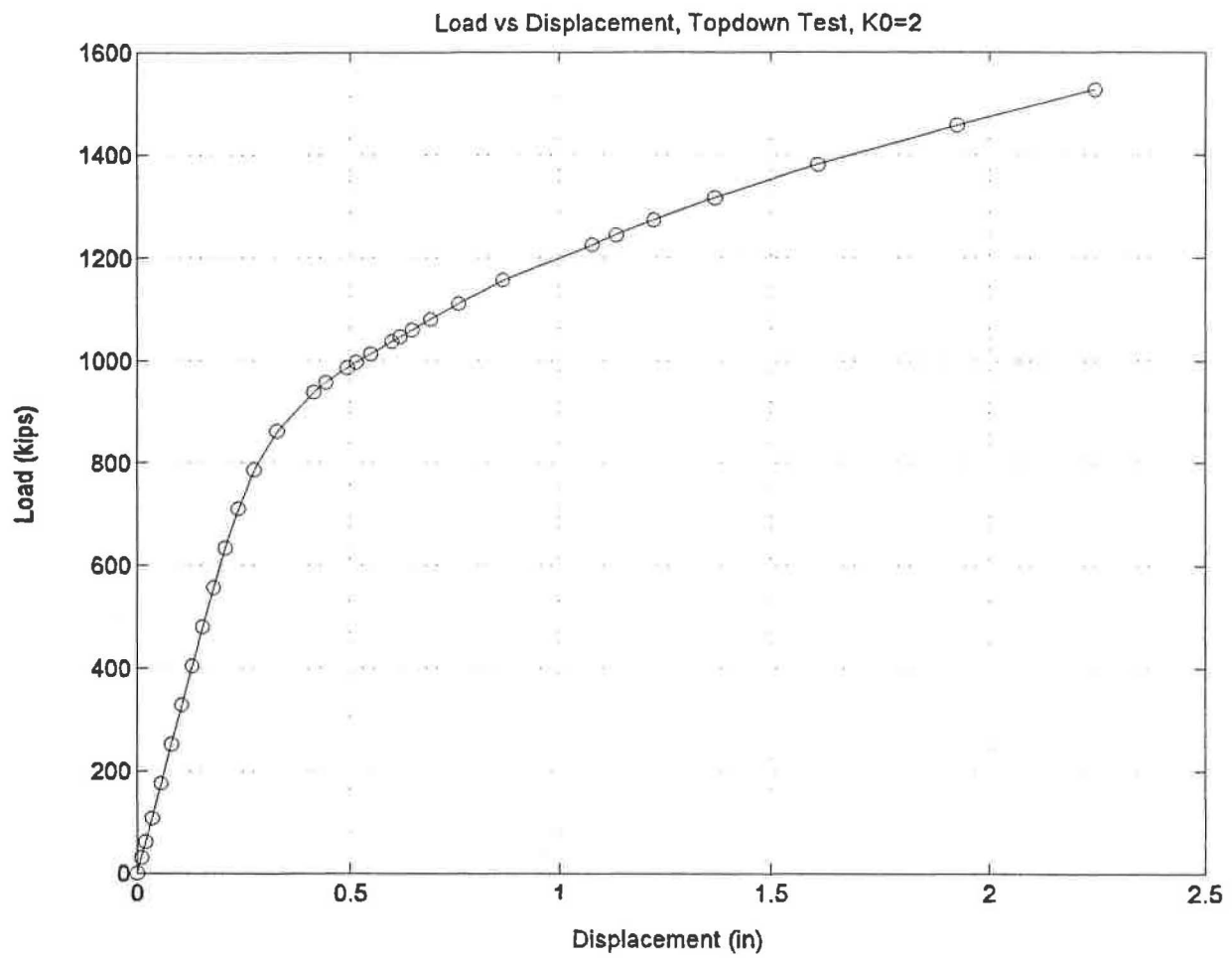
Figure A-30 Load-Displacement Curve, Topdown Test, $K_0=2$

A-48
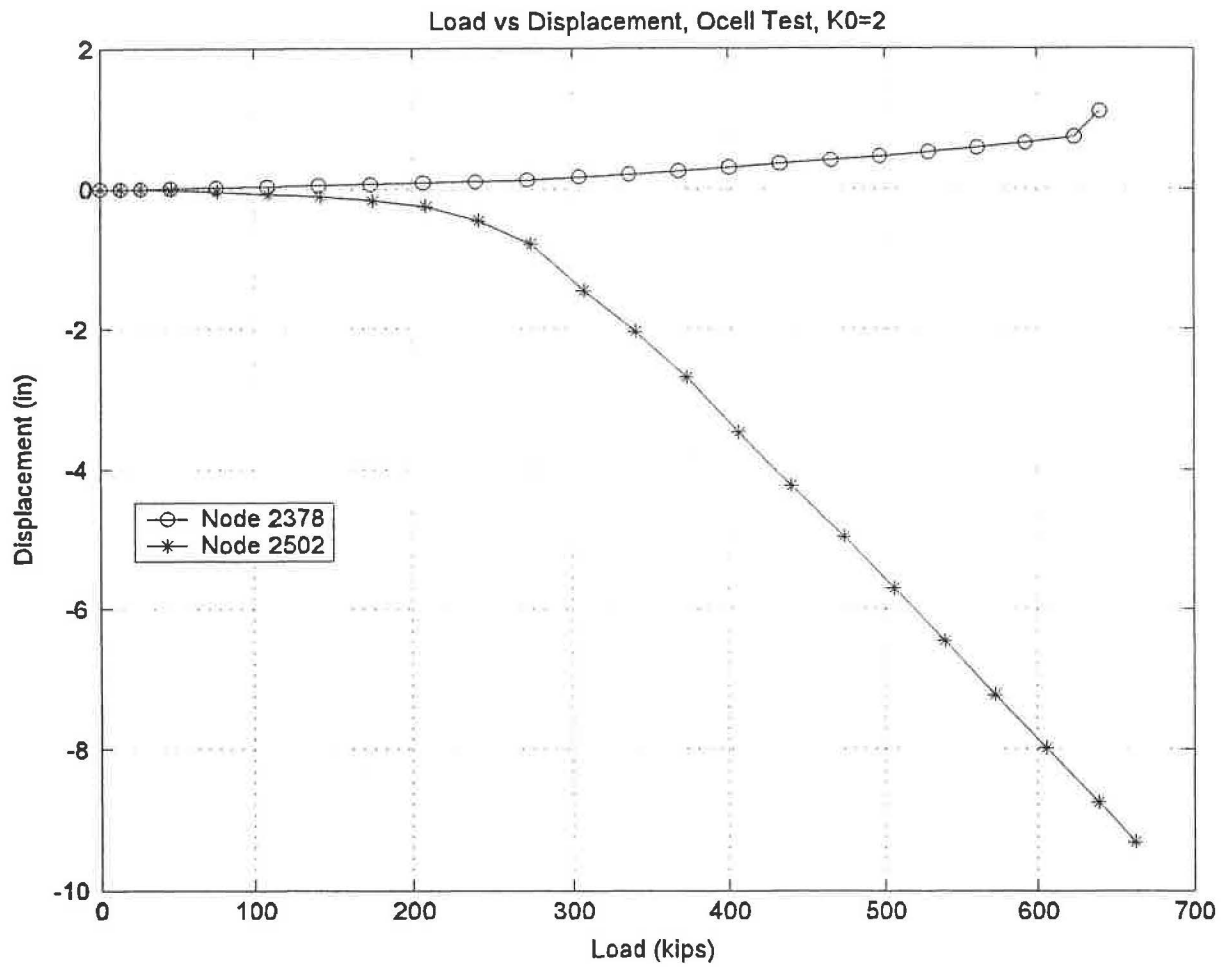
Figure A-31 Load-Displacement Curve, O-cell Test, $K_0=2$
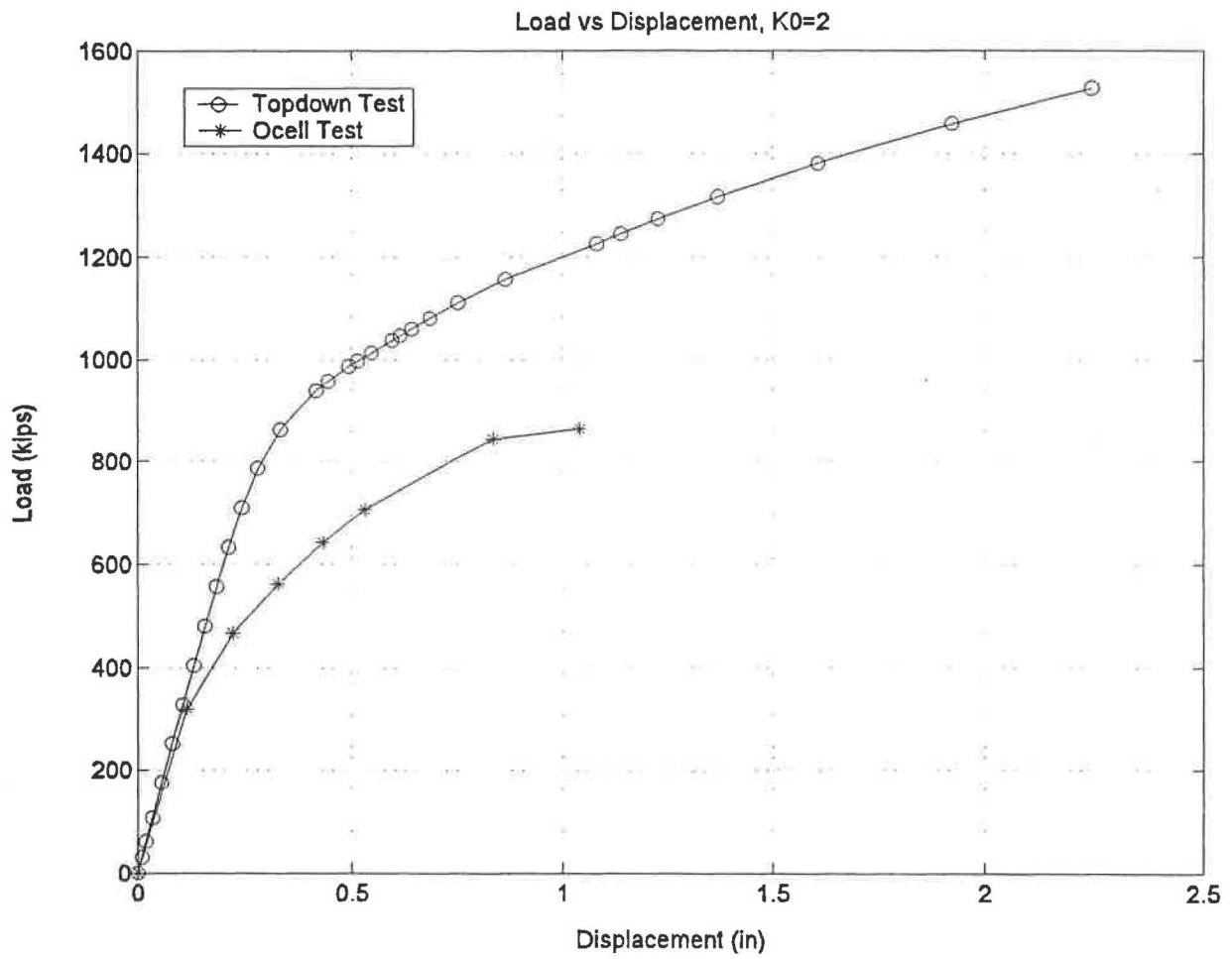
Figure A-32 Comparison of Topdown Test and O-cell Test, $K_0=2$

A-50
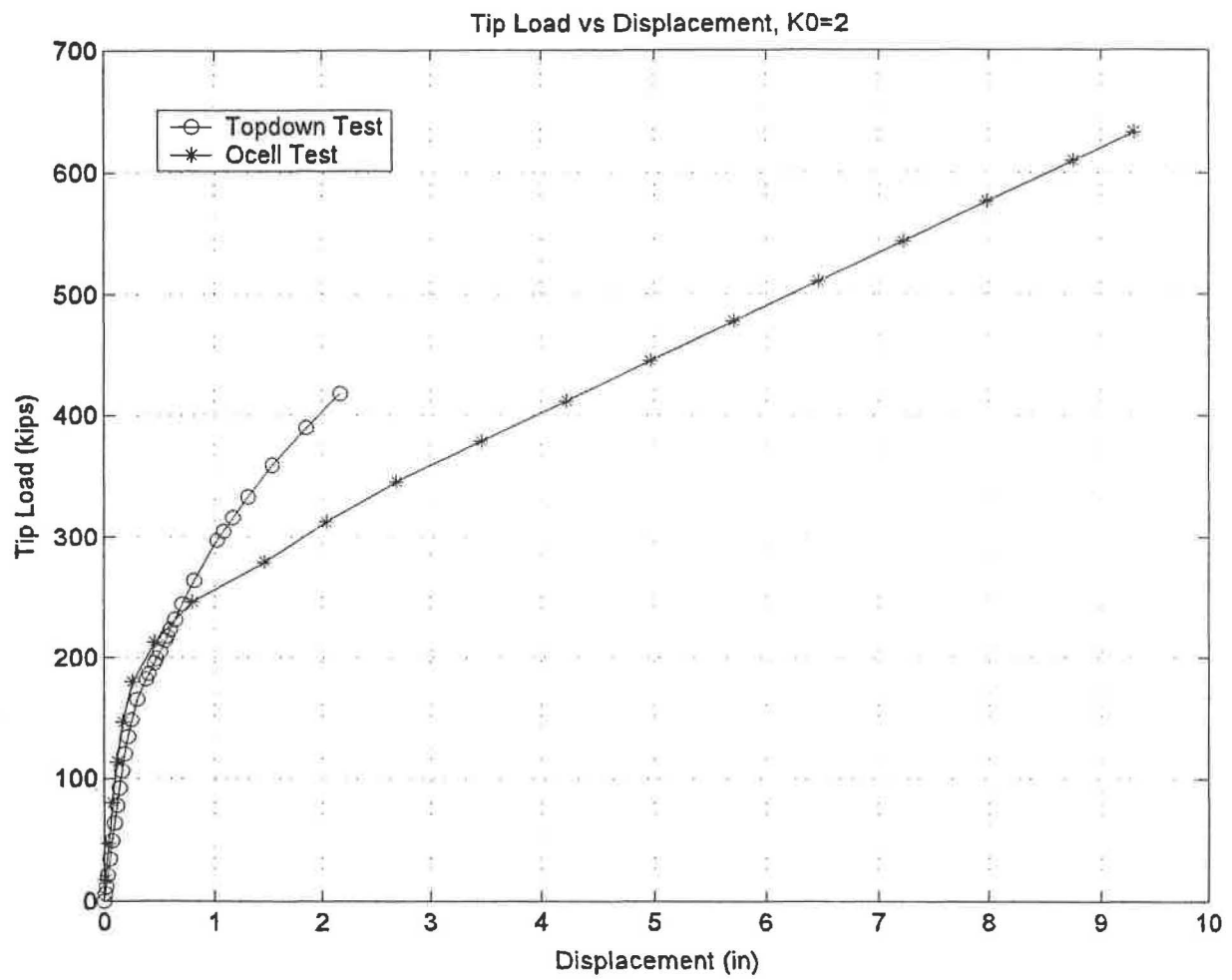
Figure A-33 Tip Load vs Displacement Curve, $K_0=2$
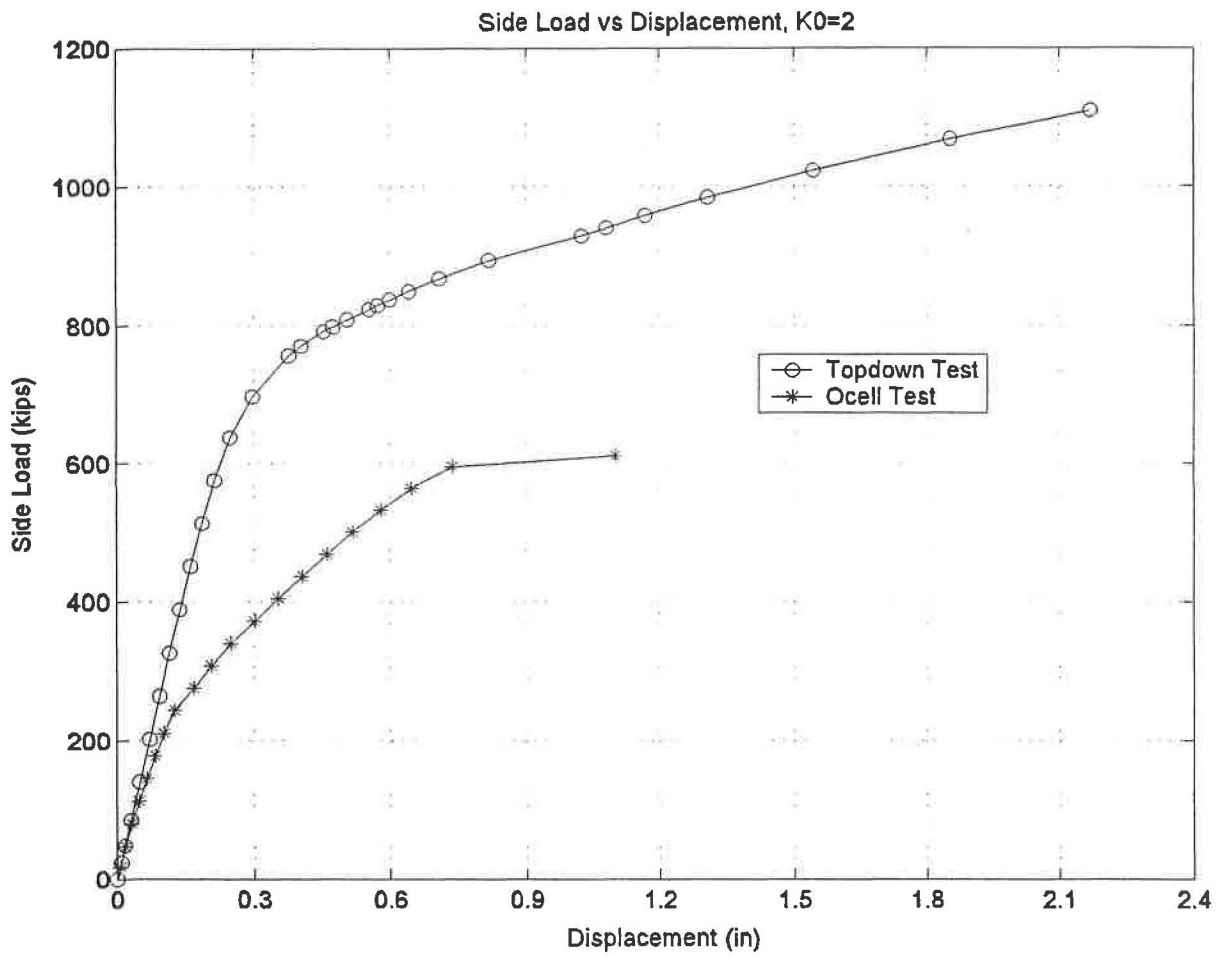
Figure A-34 Side Load vs Displacement Curve, $K_0=2$
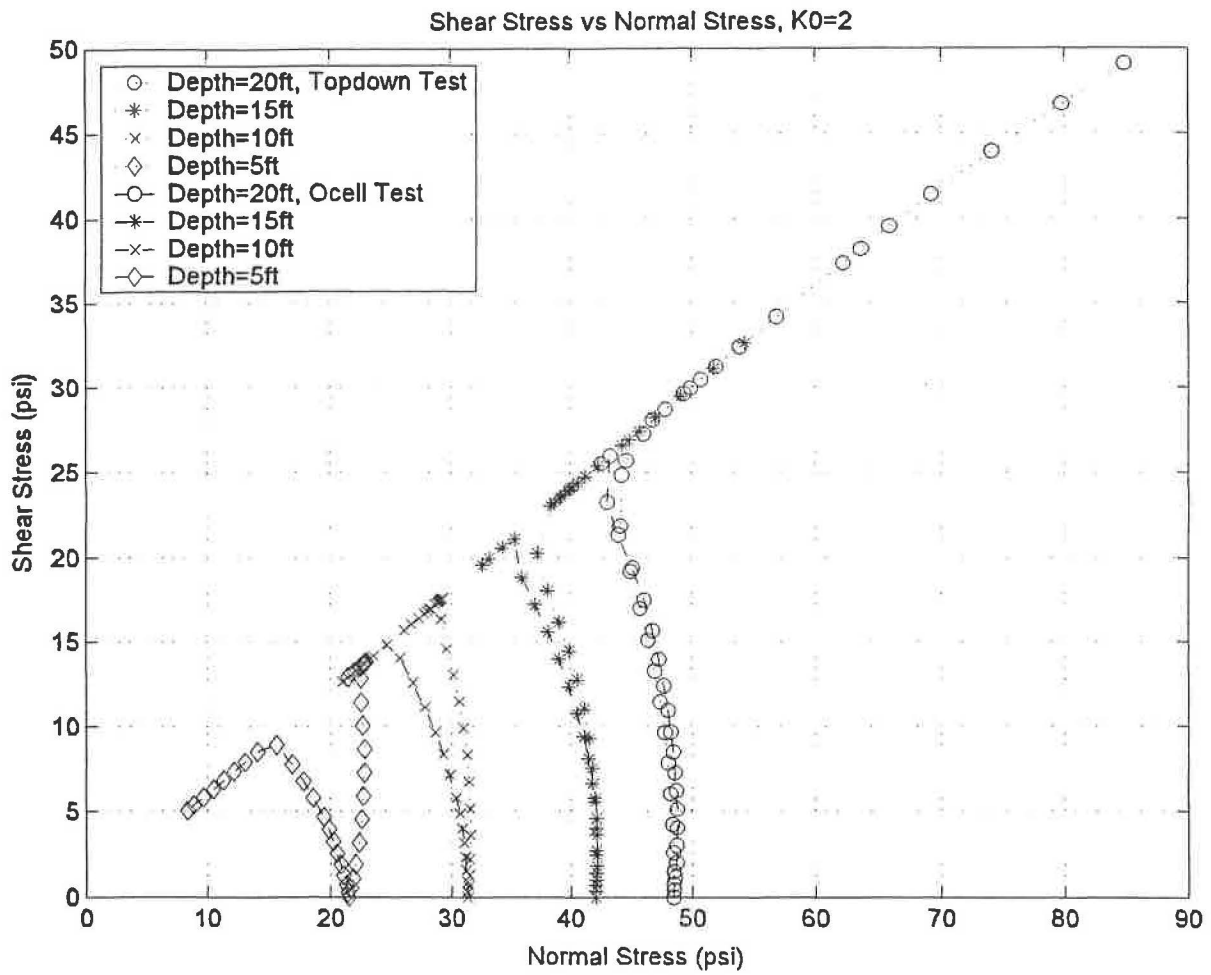
Figure A-35 Stress Path at Different Nodes on Soil-Pile Interface, $K_0=2$
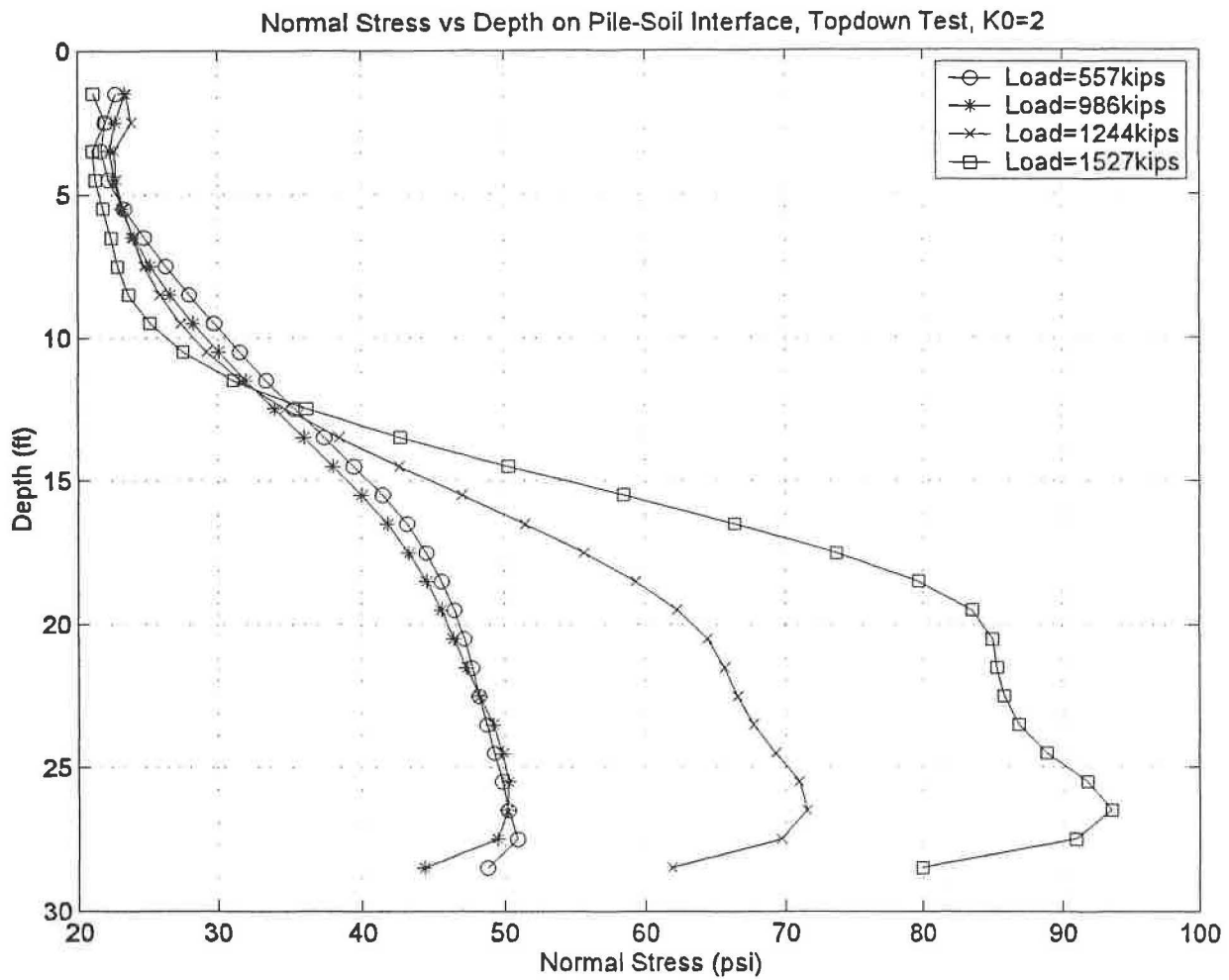
Figure A-36 Normal Stress vs Depth Curve, Topdown Test, $K_0=2$
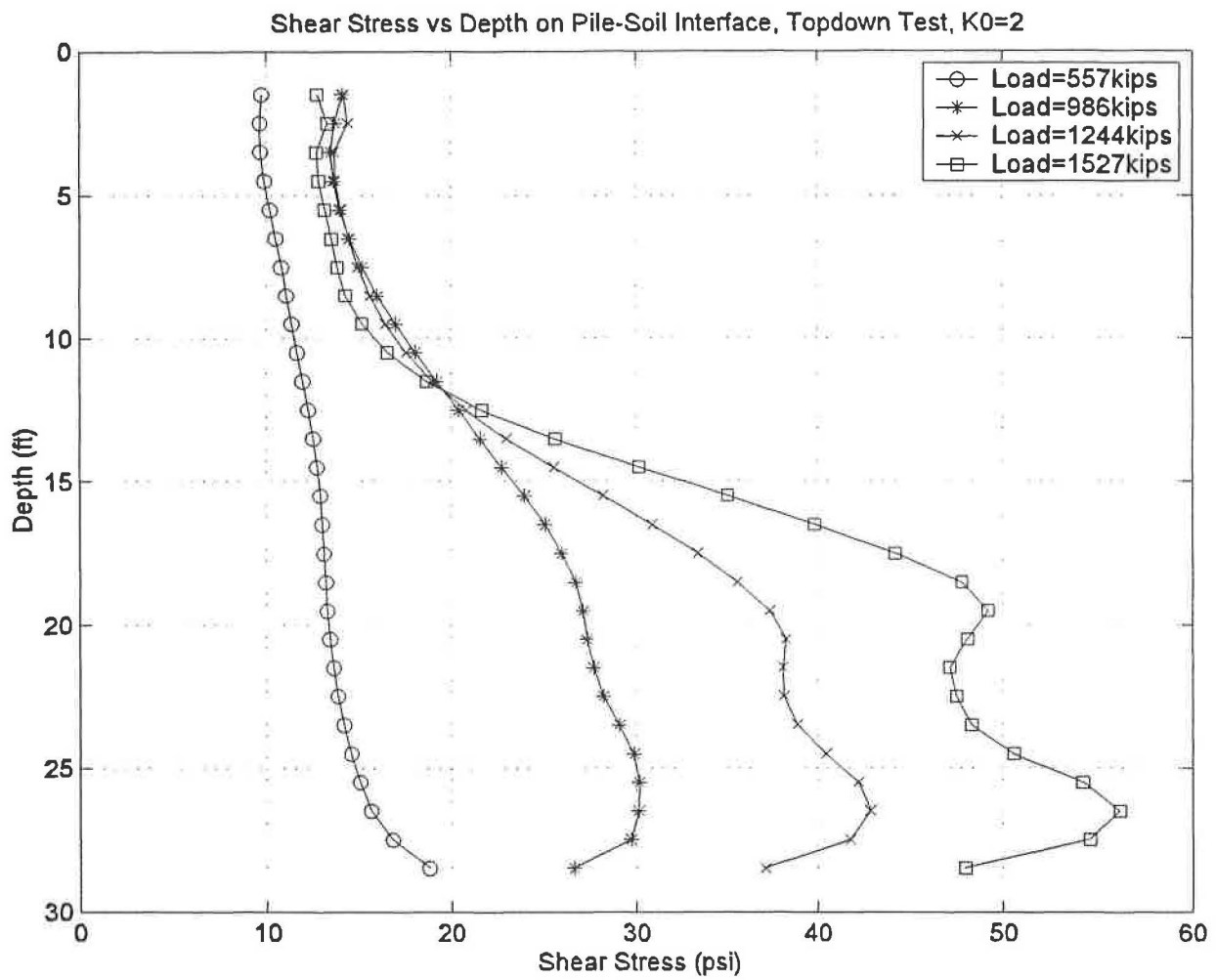
Figure A-37 Shear Stress vs Depth Curve, Topdown Test, $K_0=2$
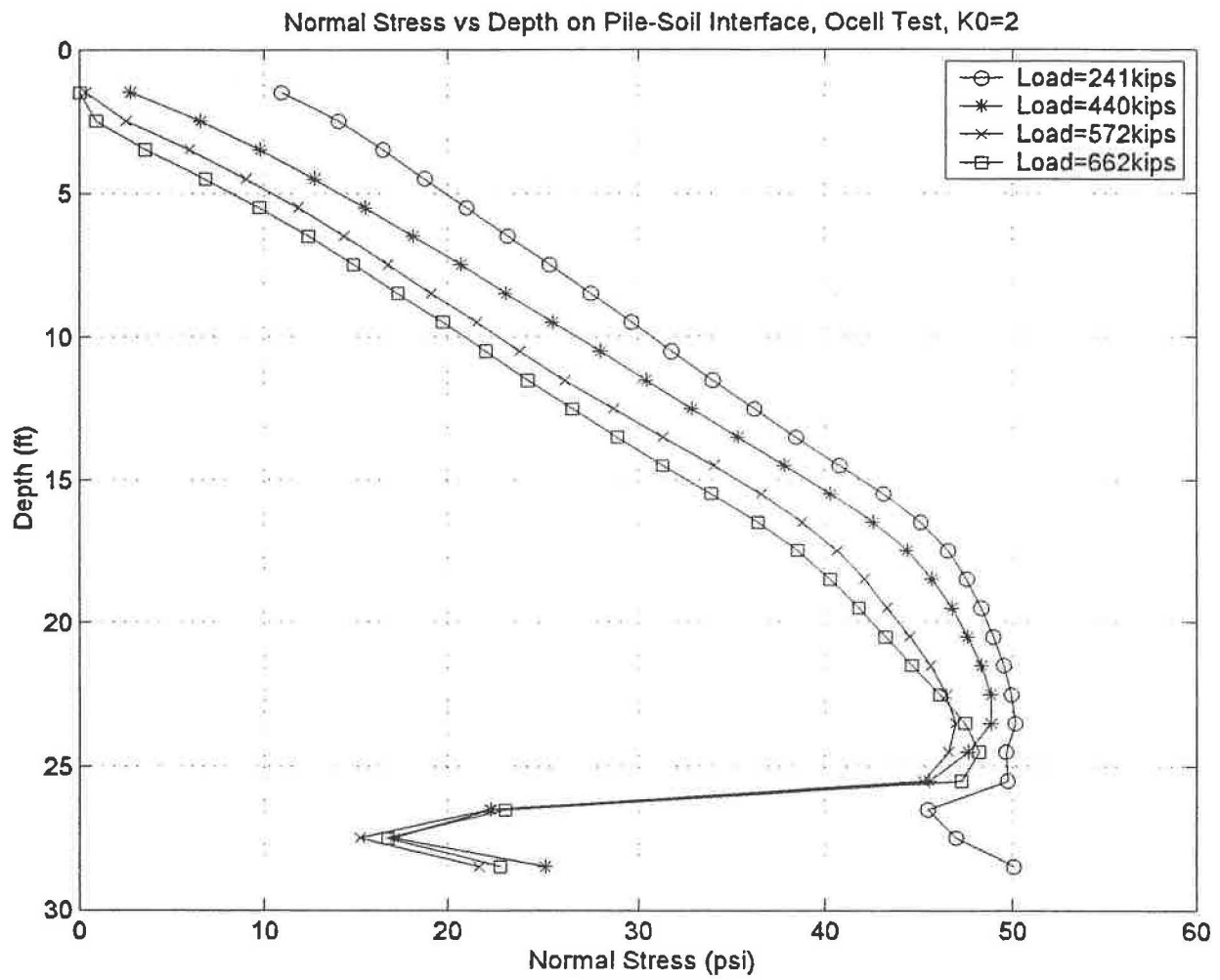
Figure A-38 Normal Stress vs Depth Curve, O-cell Test, $K_0=2$
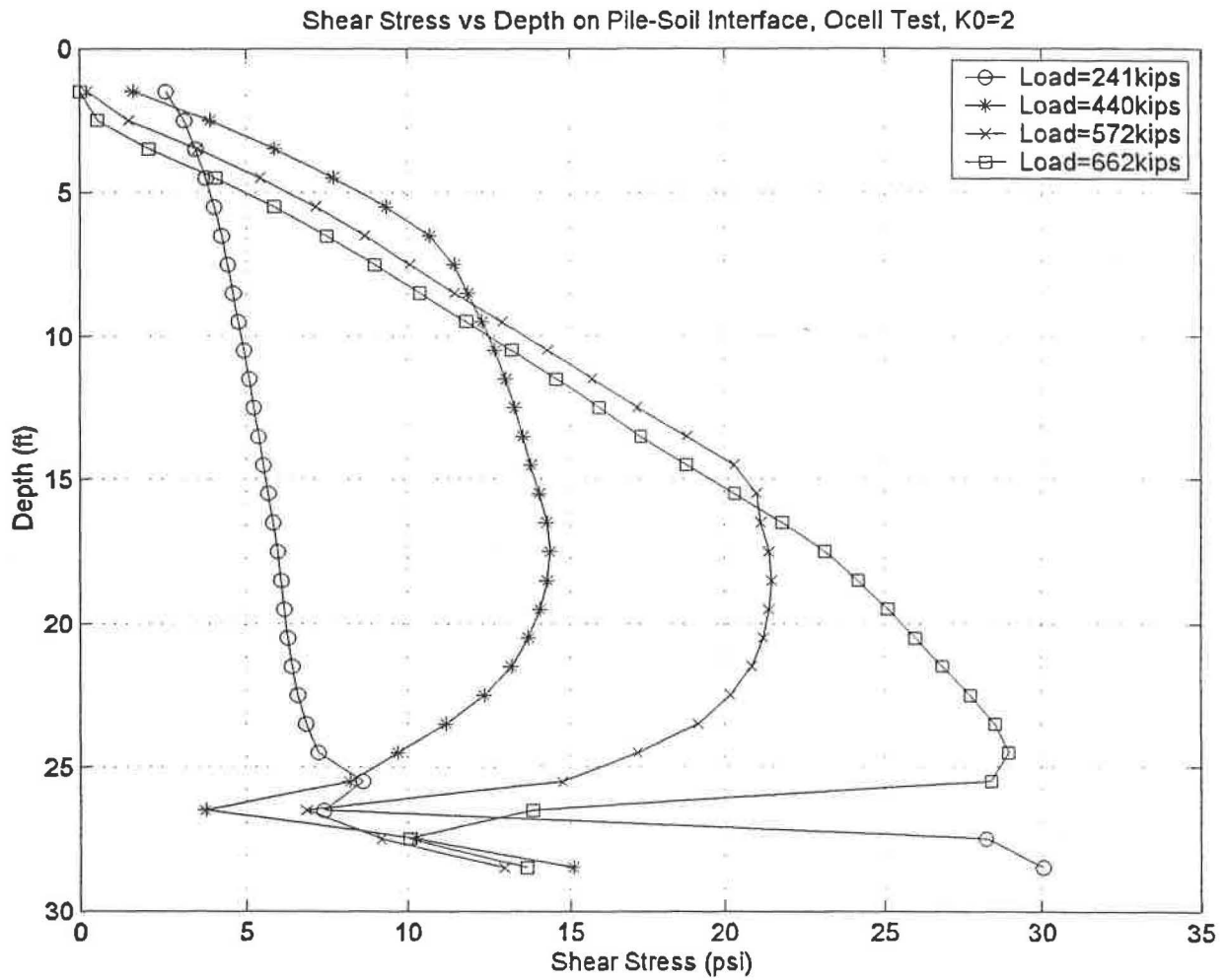
Figure A-39 Shear Stress vs Depth Curve, O-cell Test, $K_0=2$
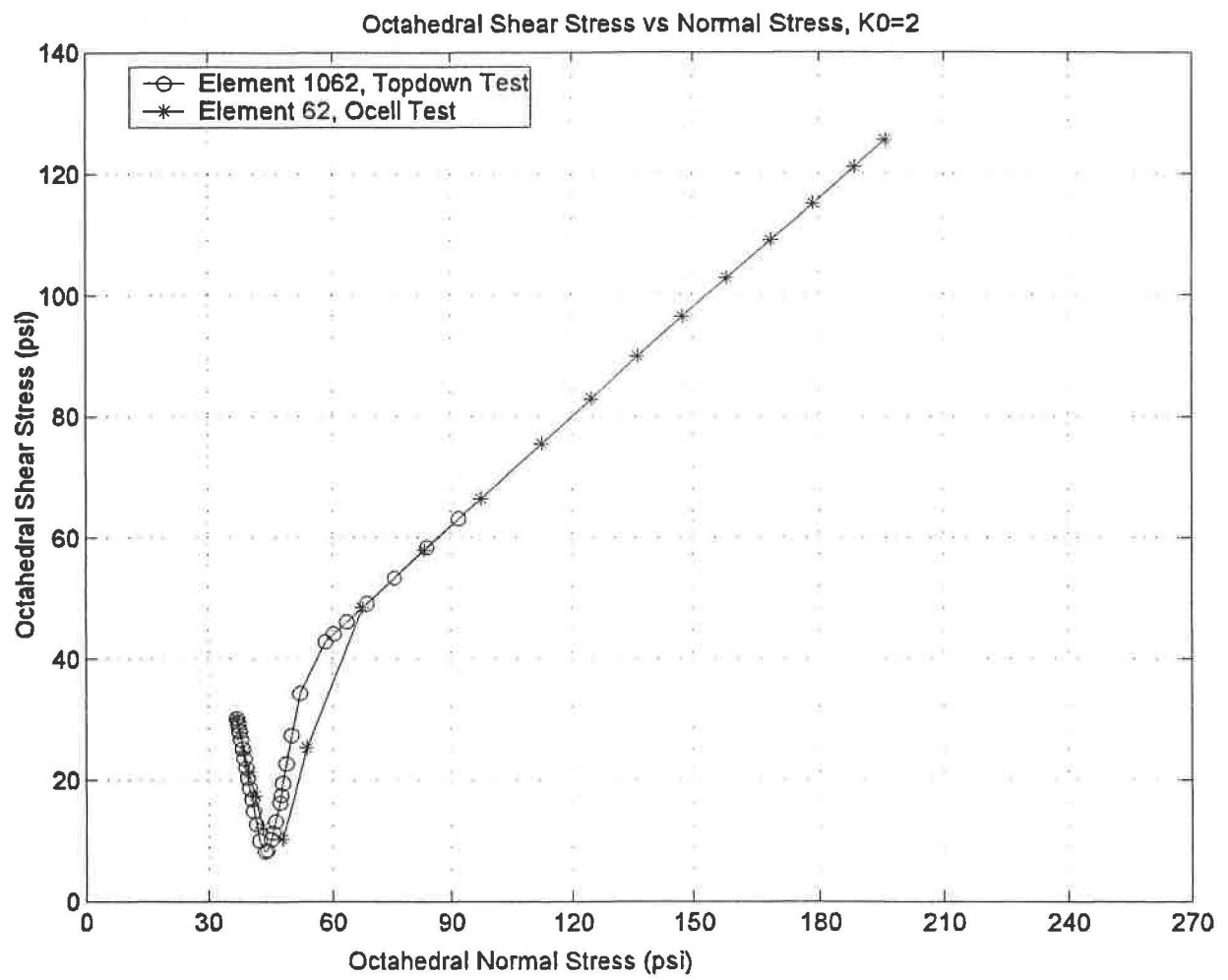
Figure A-40 Stress Path of Soil Element, $K_0=2$
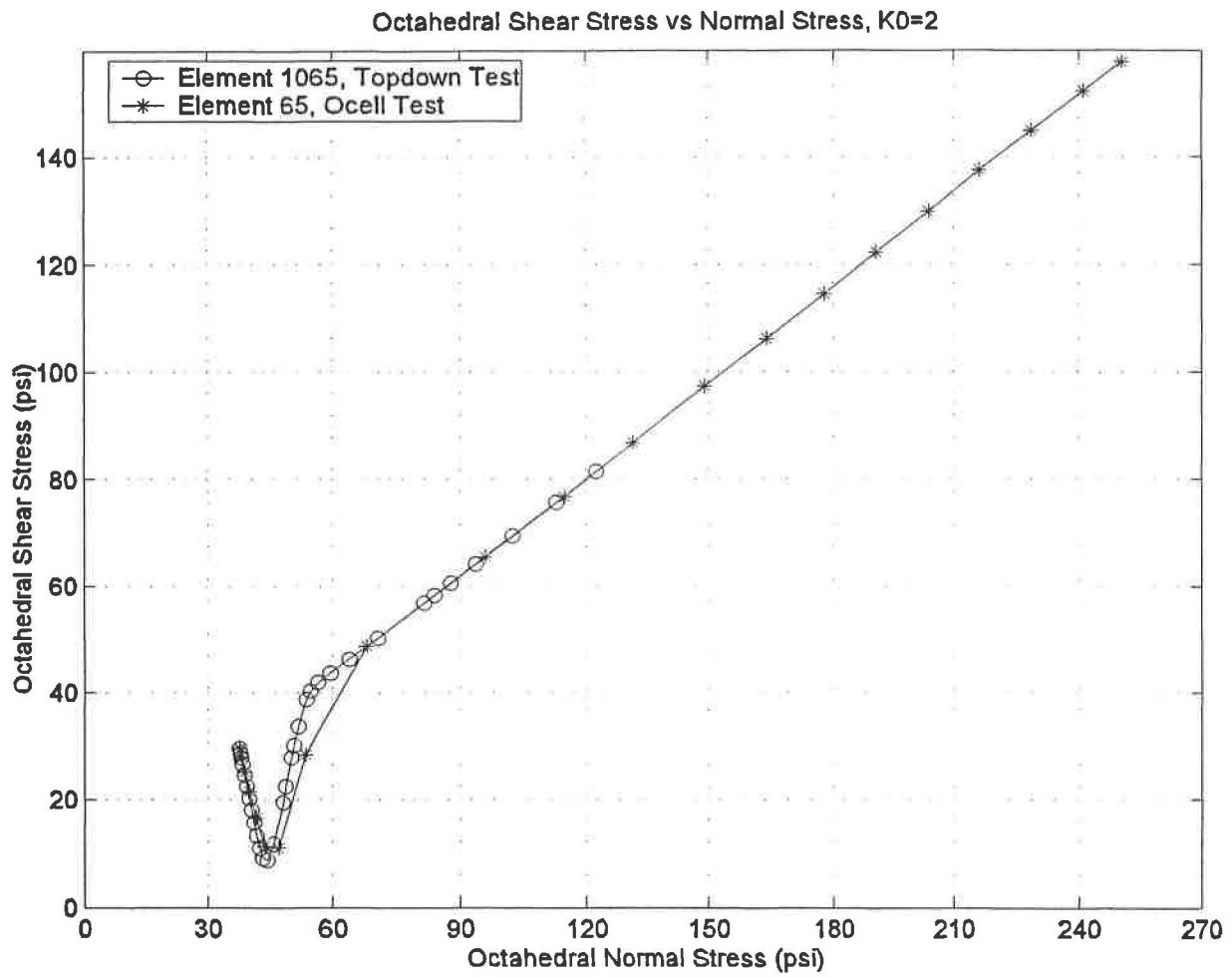
Figure A-41 Stress Path of Soil Element, $K_0=2$
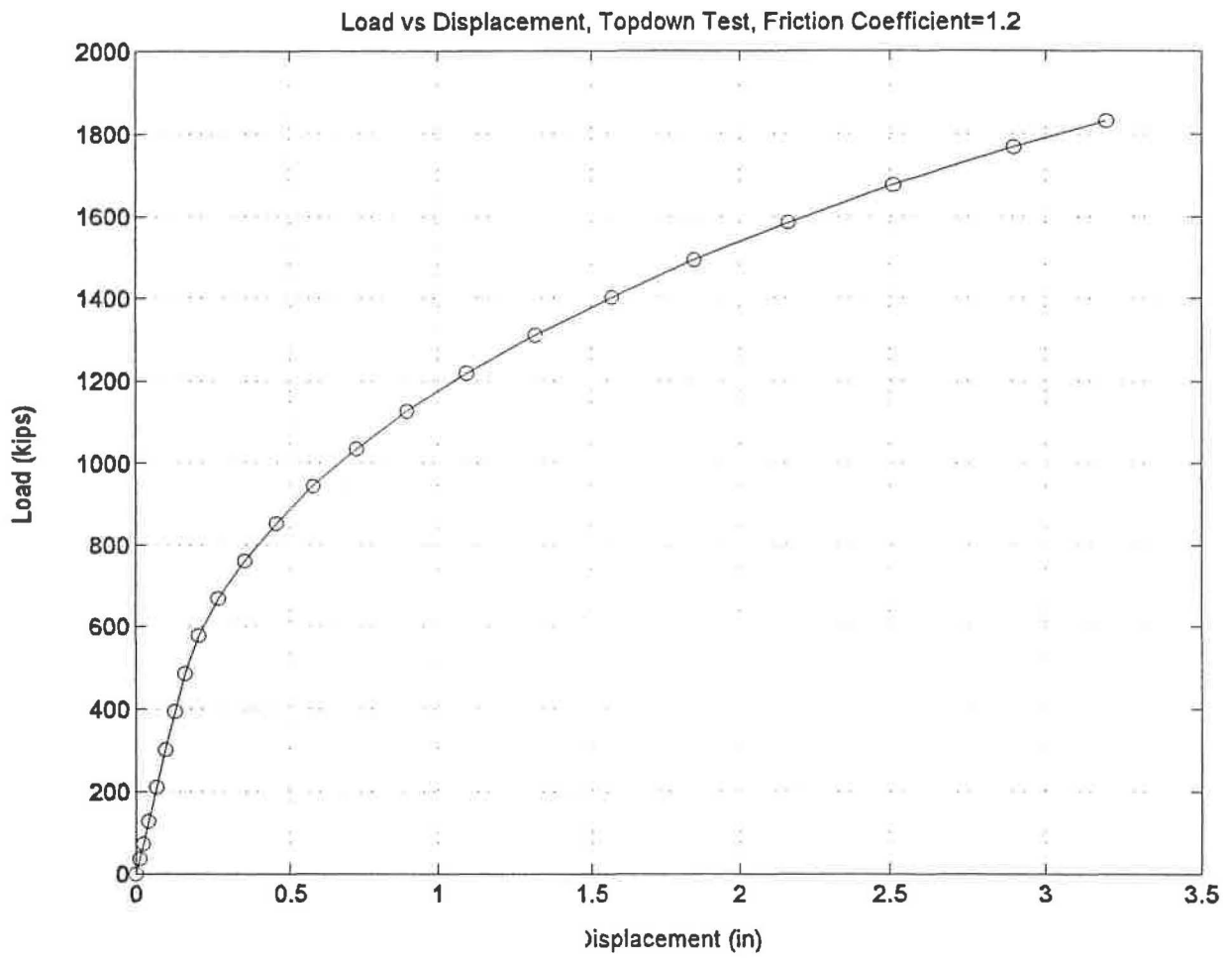
Figure A-42 Load-Displacement Curve, Topdown Test, μ=1.2
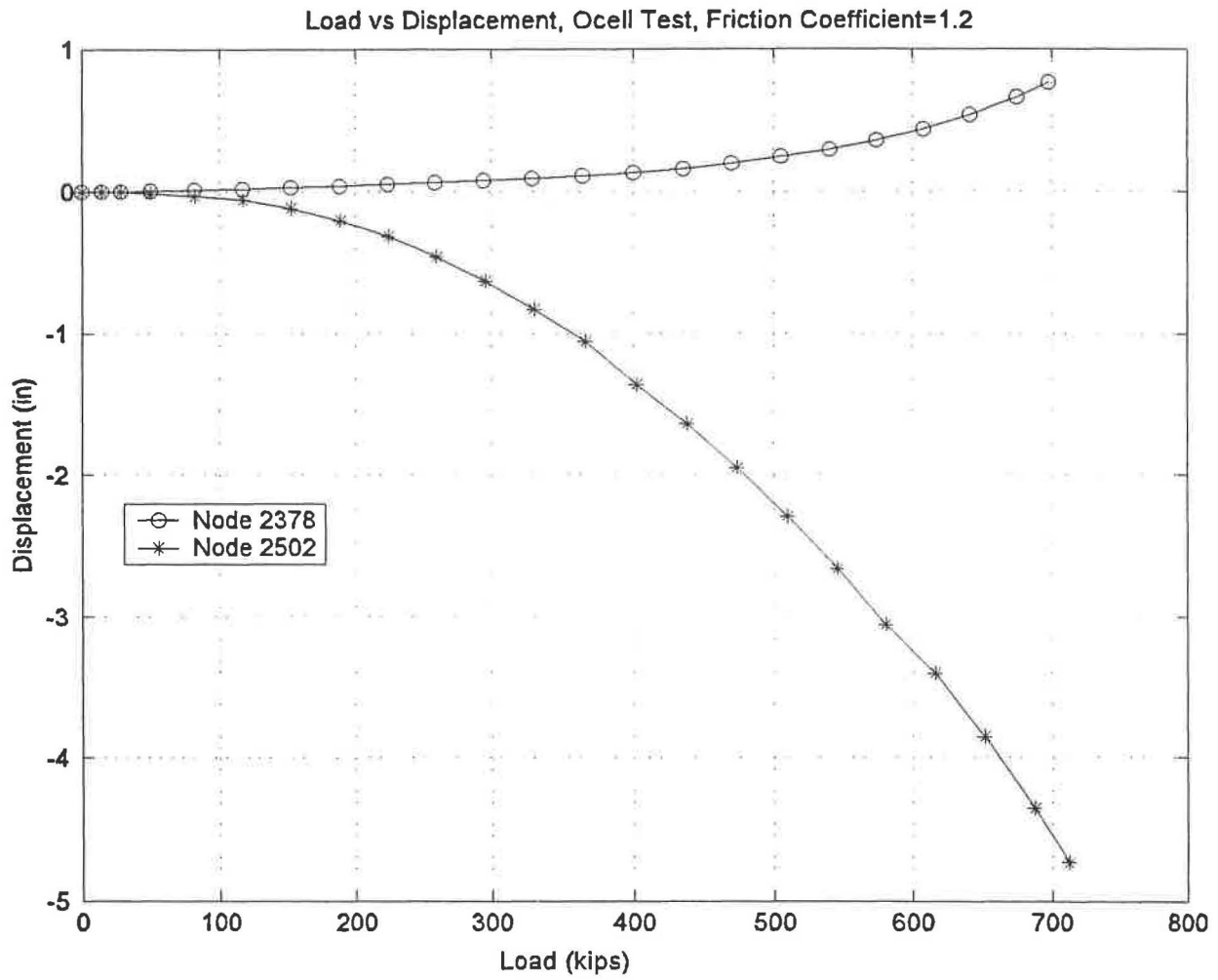
Figure A-43 Load-Displacement Curve, O-cell Test, $\mu=1.2$

Load vs Displacement, Topdown Test, Friction Coefficient=1.2
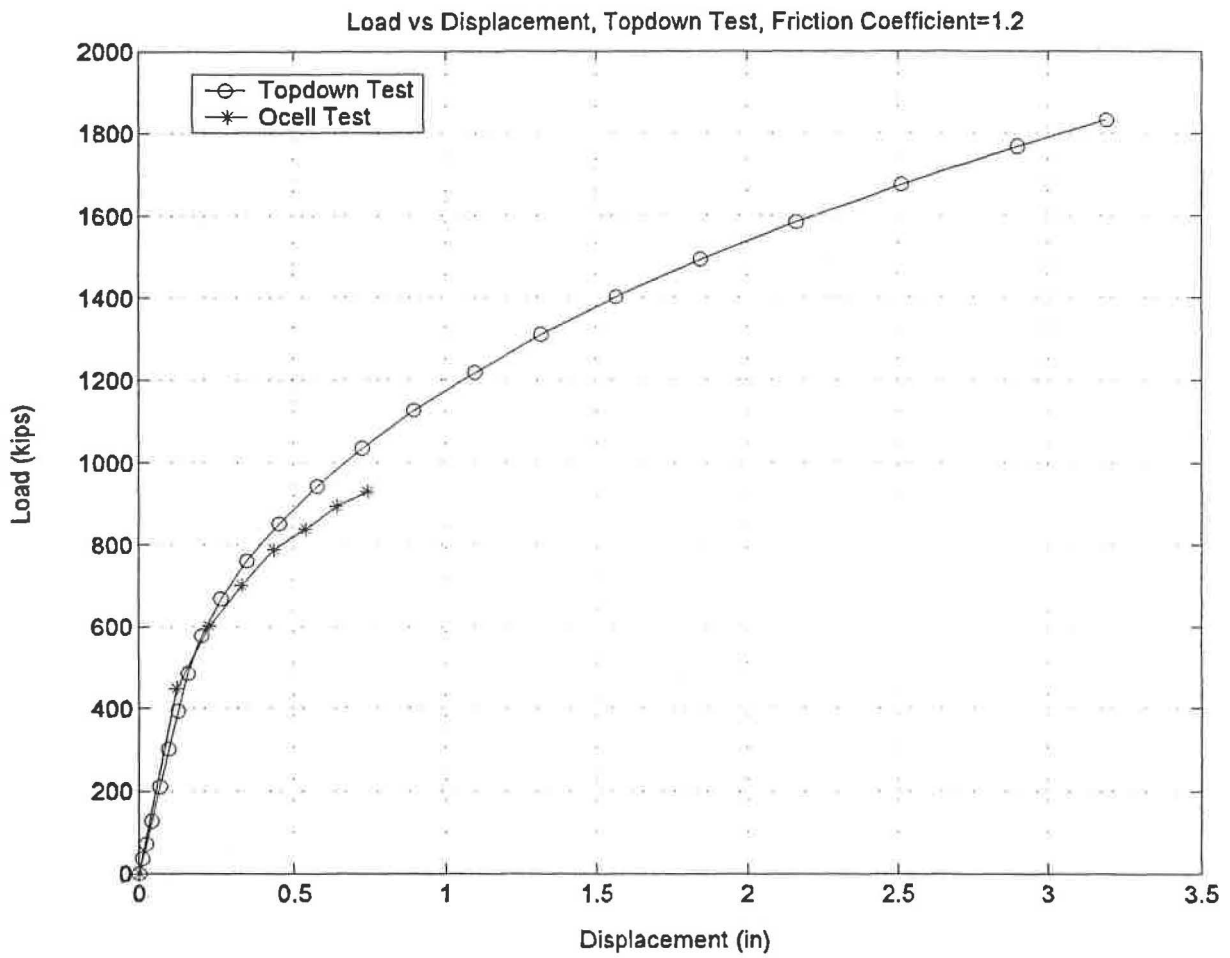
Figure A-44   Comparison of Topdown Test and O-cell Test, $\mu = 1.2$
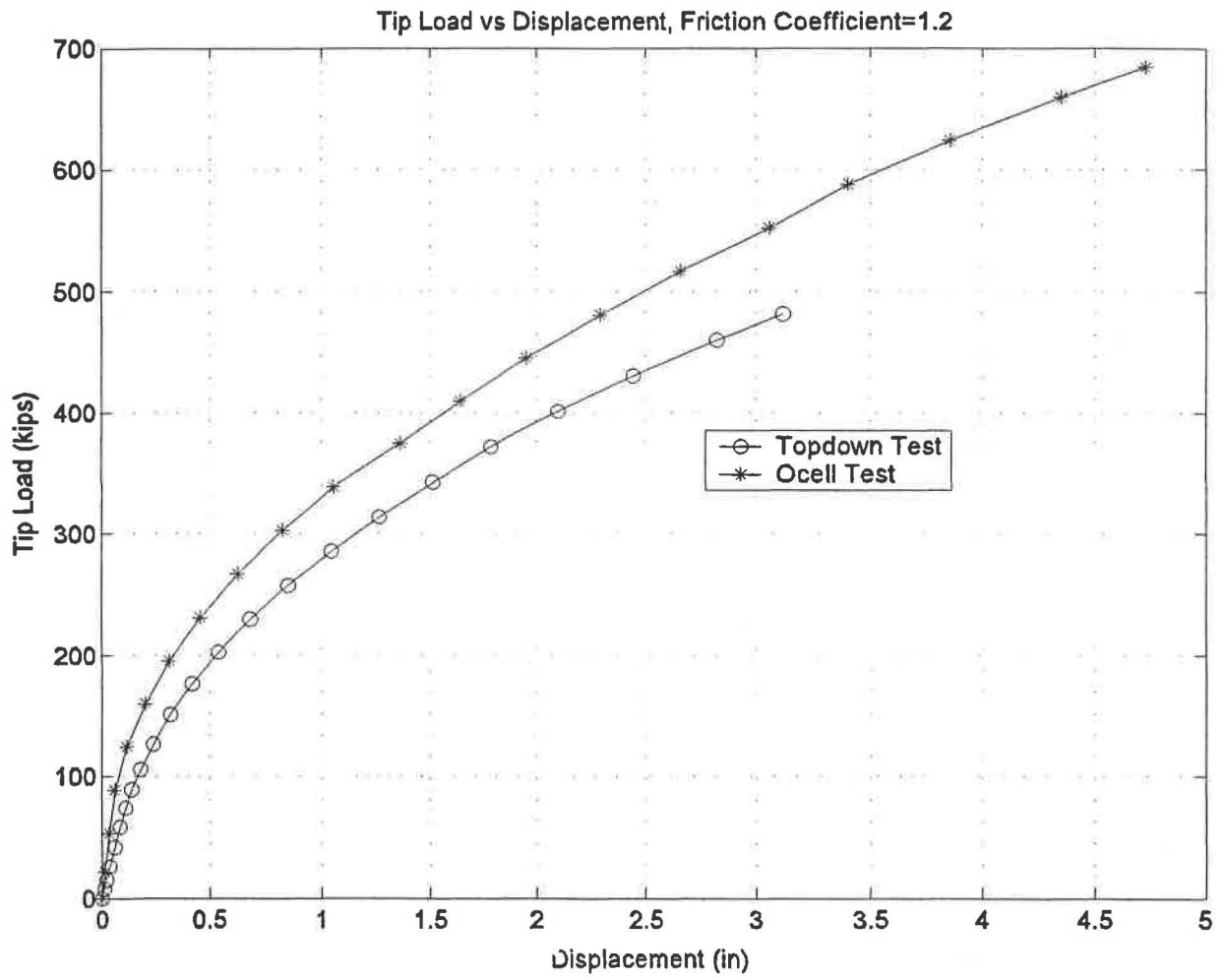
Figure A-45 Tip Load vs Displacement Curve, $\mu = 1.2$
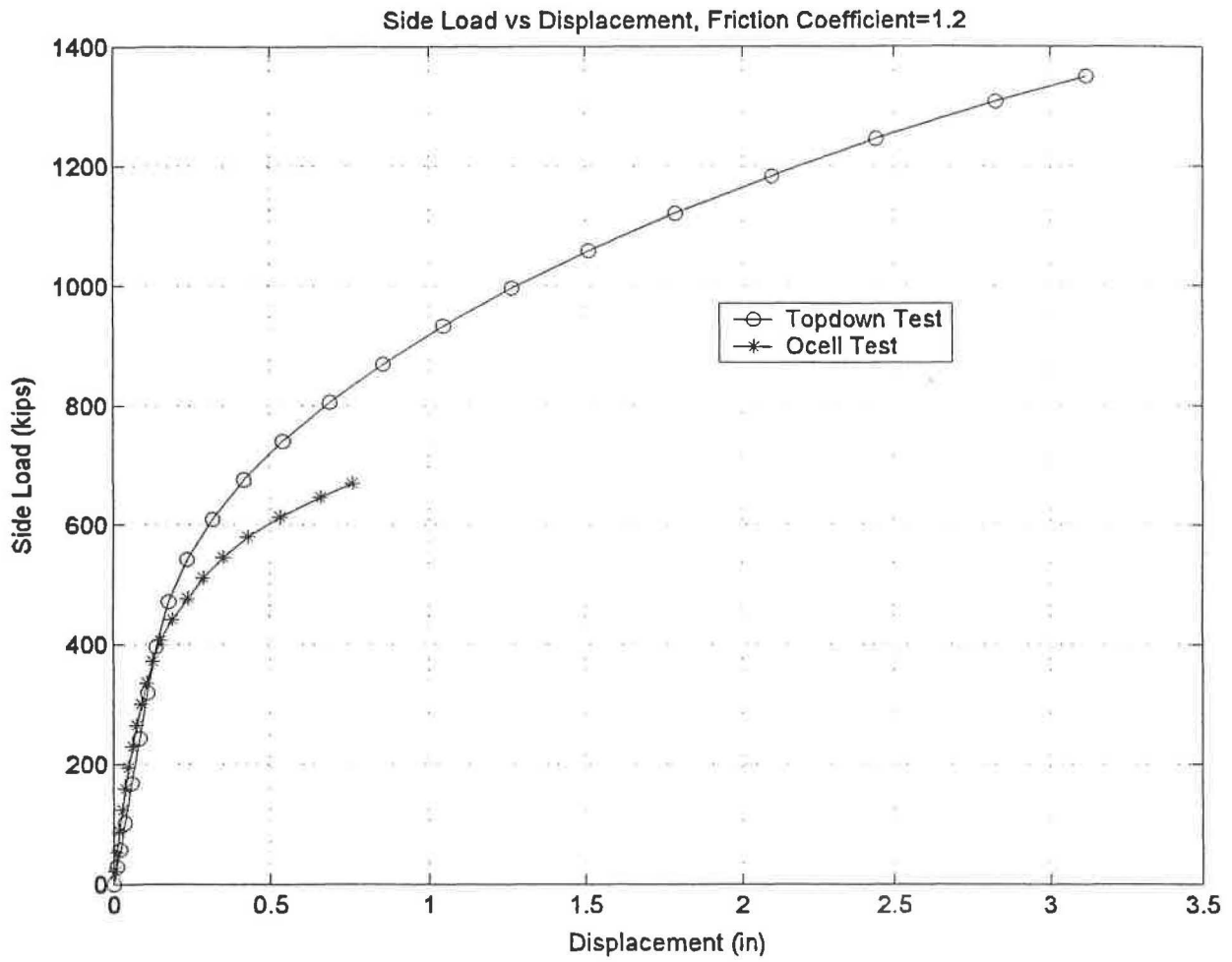
Figure A-46 Side Load vs Displacement Curve, $\mu = 1.2$
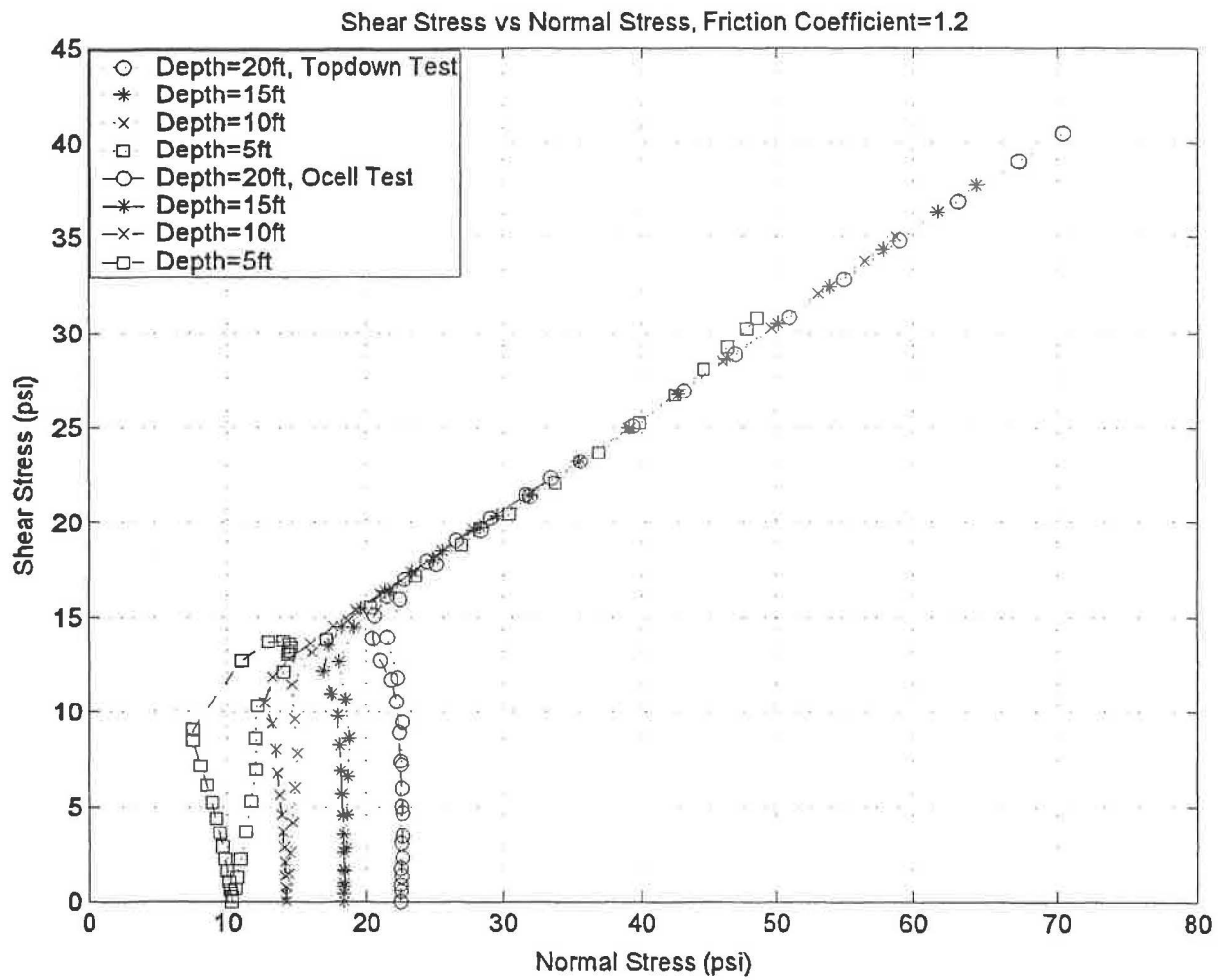
Figure A-47 Stress Path at Different Nodes on Soil-Pile Interface, μ=1.2
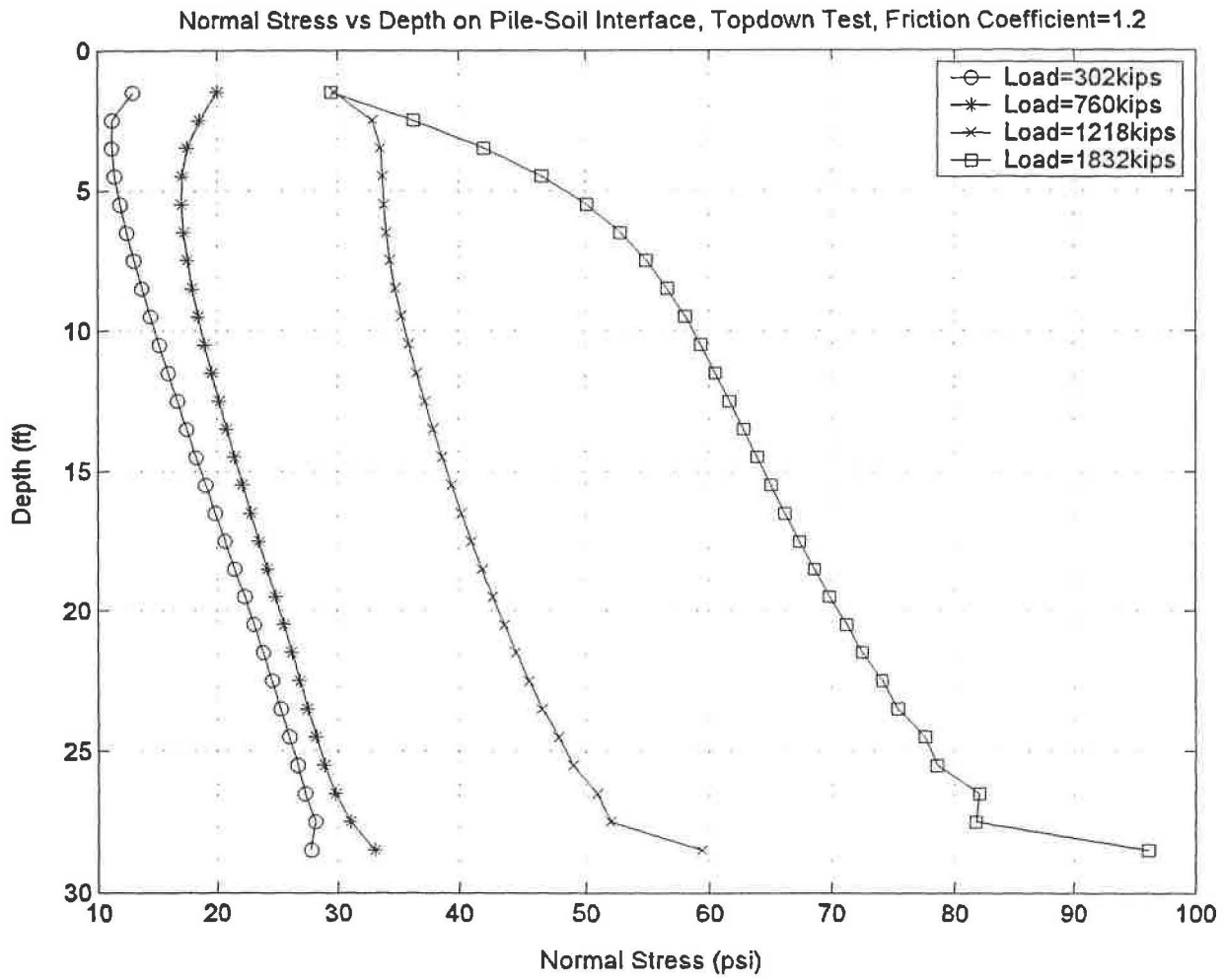
Figure A-48 Normal Stress vs Depth Curve, Topdown Test, $\mu = 1.2$
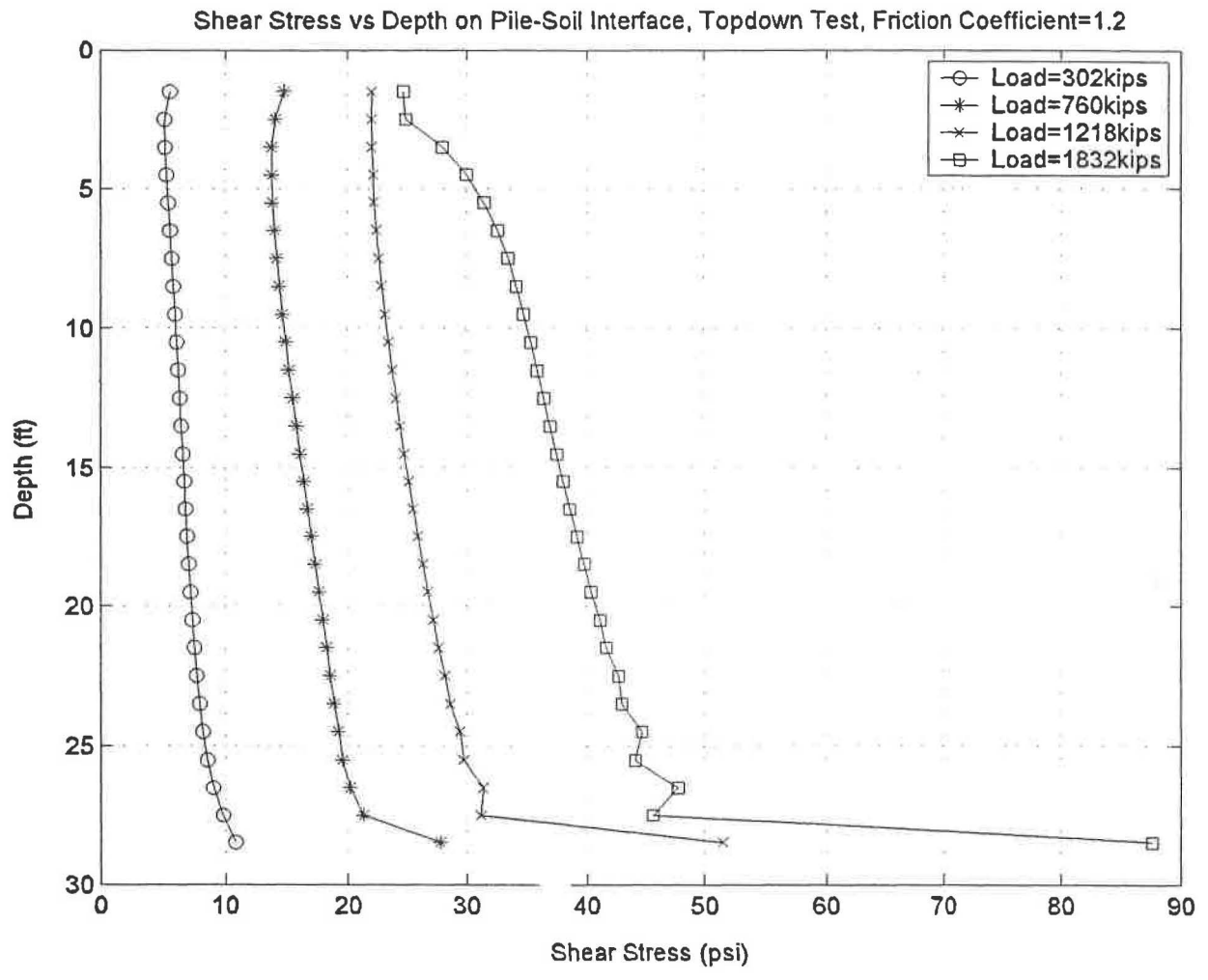
Figure A-49 Shear Stress vs Depth Curve, Topdown Test, $\mu=1.2$

A-67
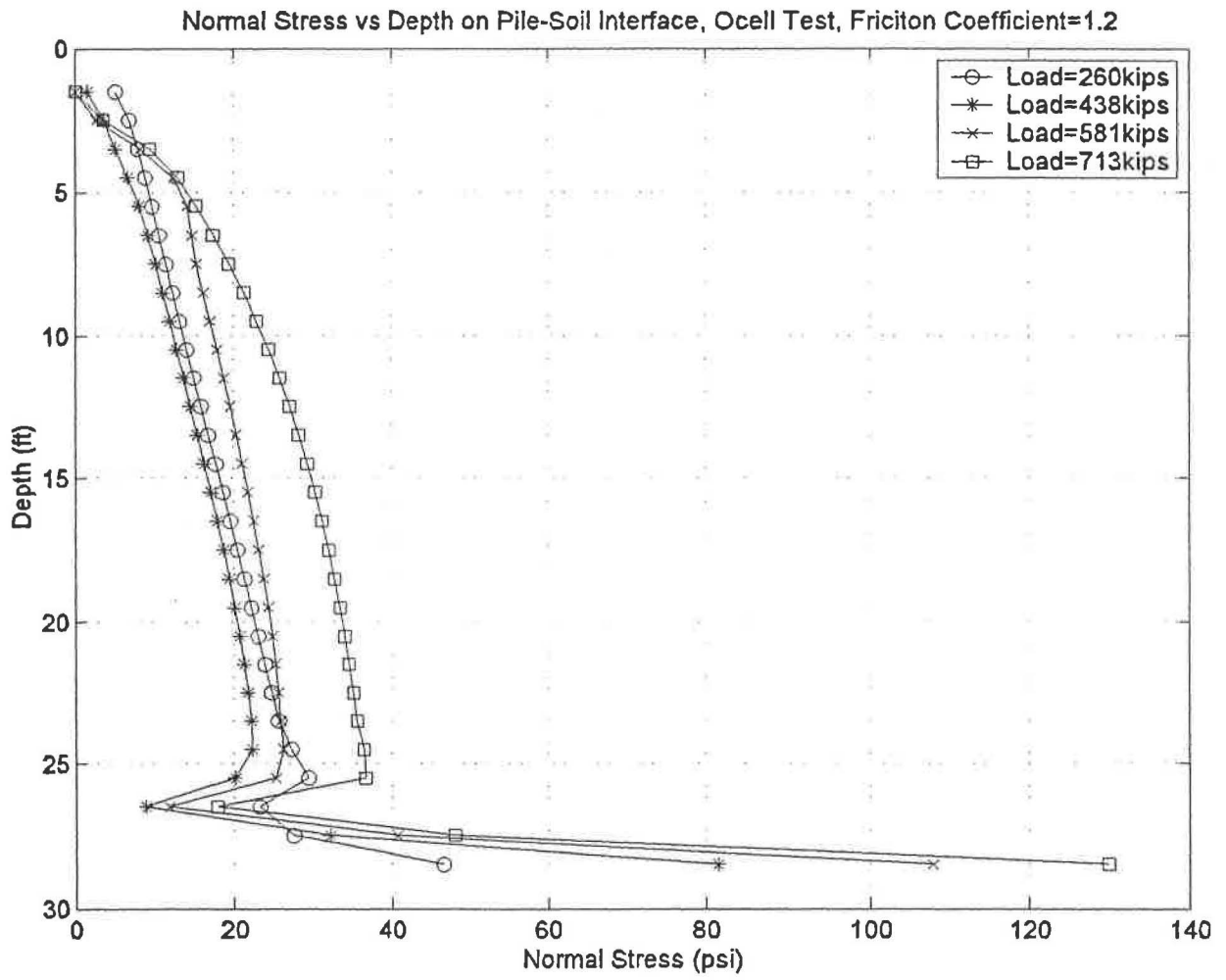
Figure A-50 Normal Stress vs Depth Curve, O-cell Test, $\mu = 1.2$
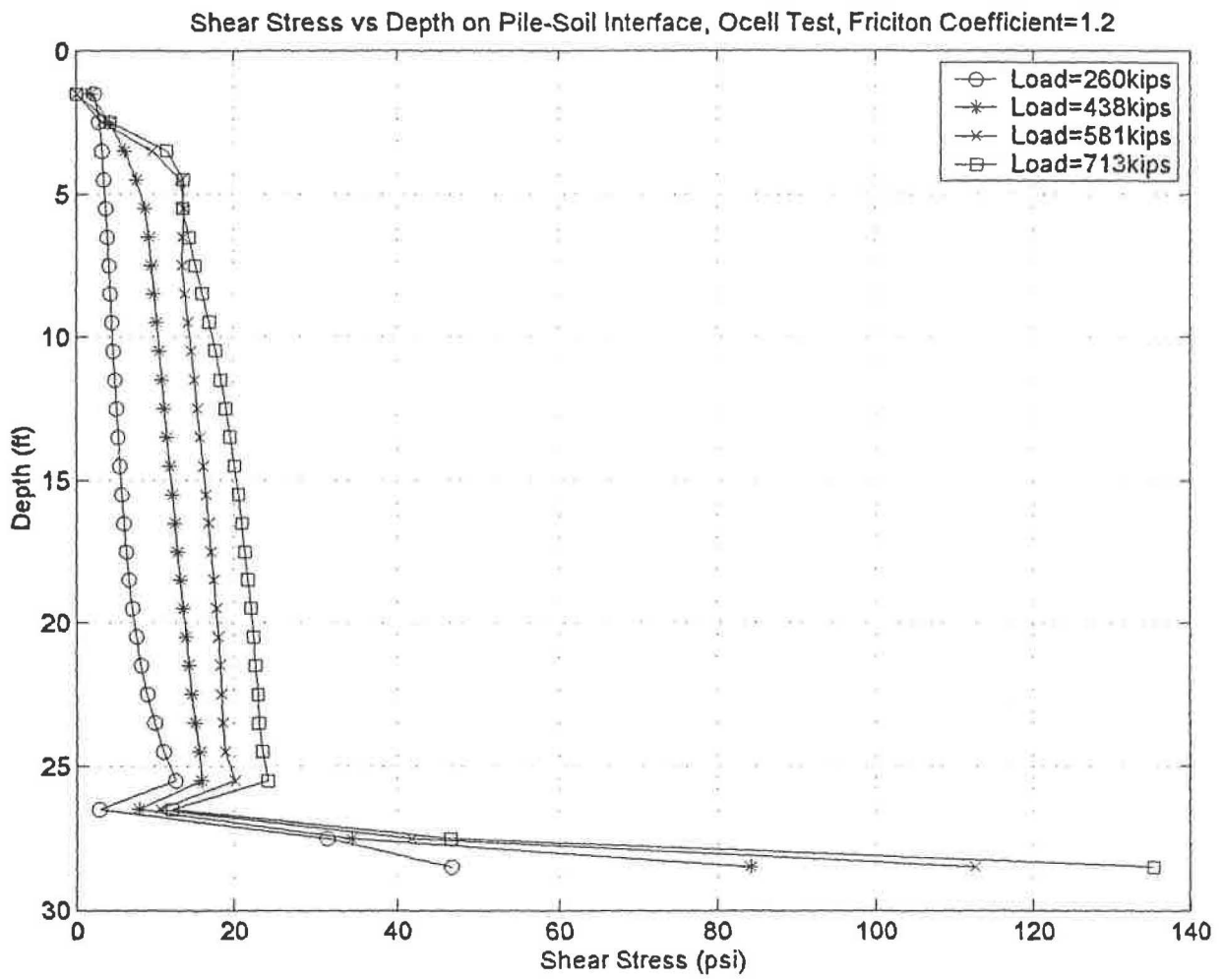
Figure A-51 Shear Stress vs Depth Curve, O-cell Test, $\mu = 1.2$
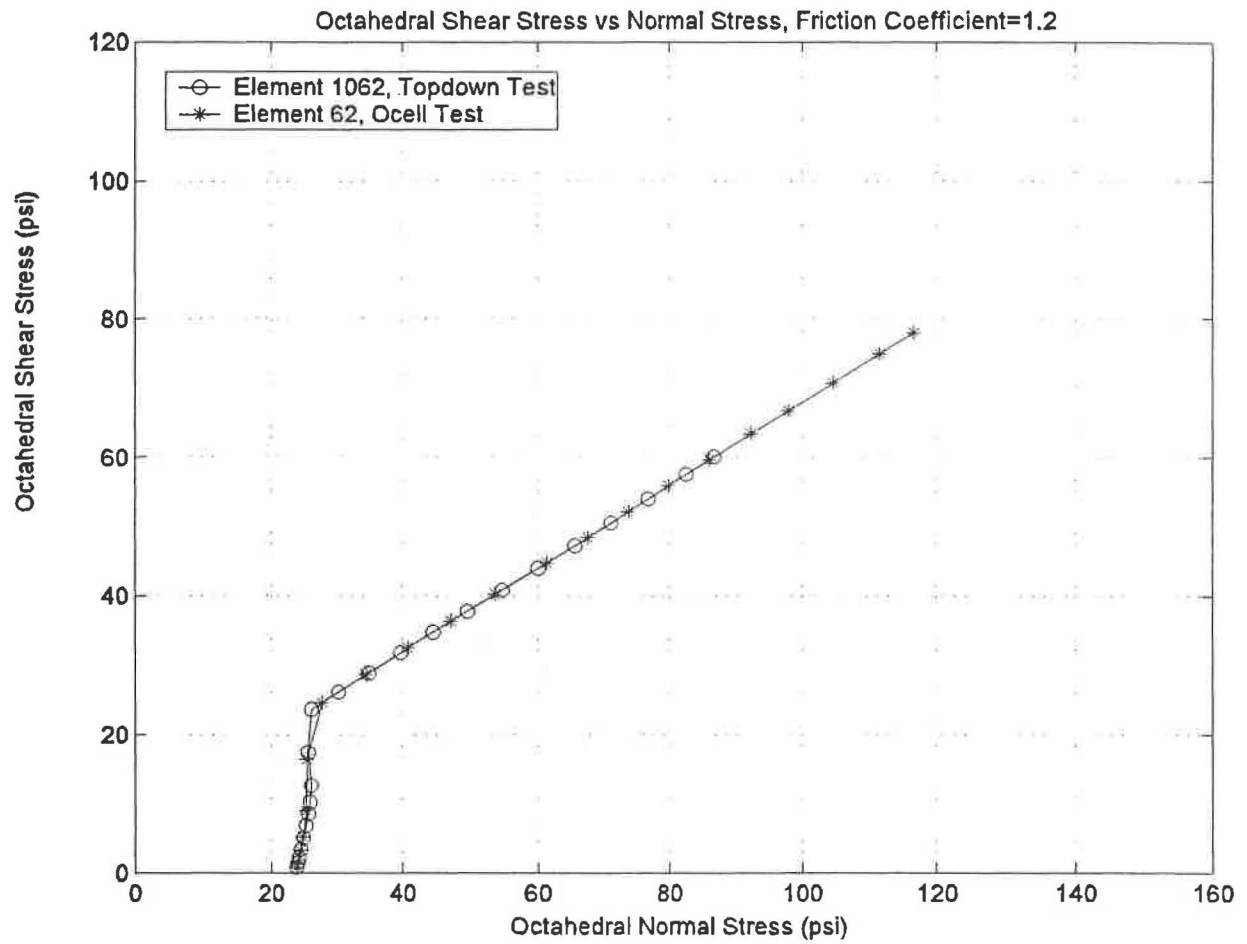
Figure A-52 Stress Path of Soil Element, μ=1.2

A-70
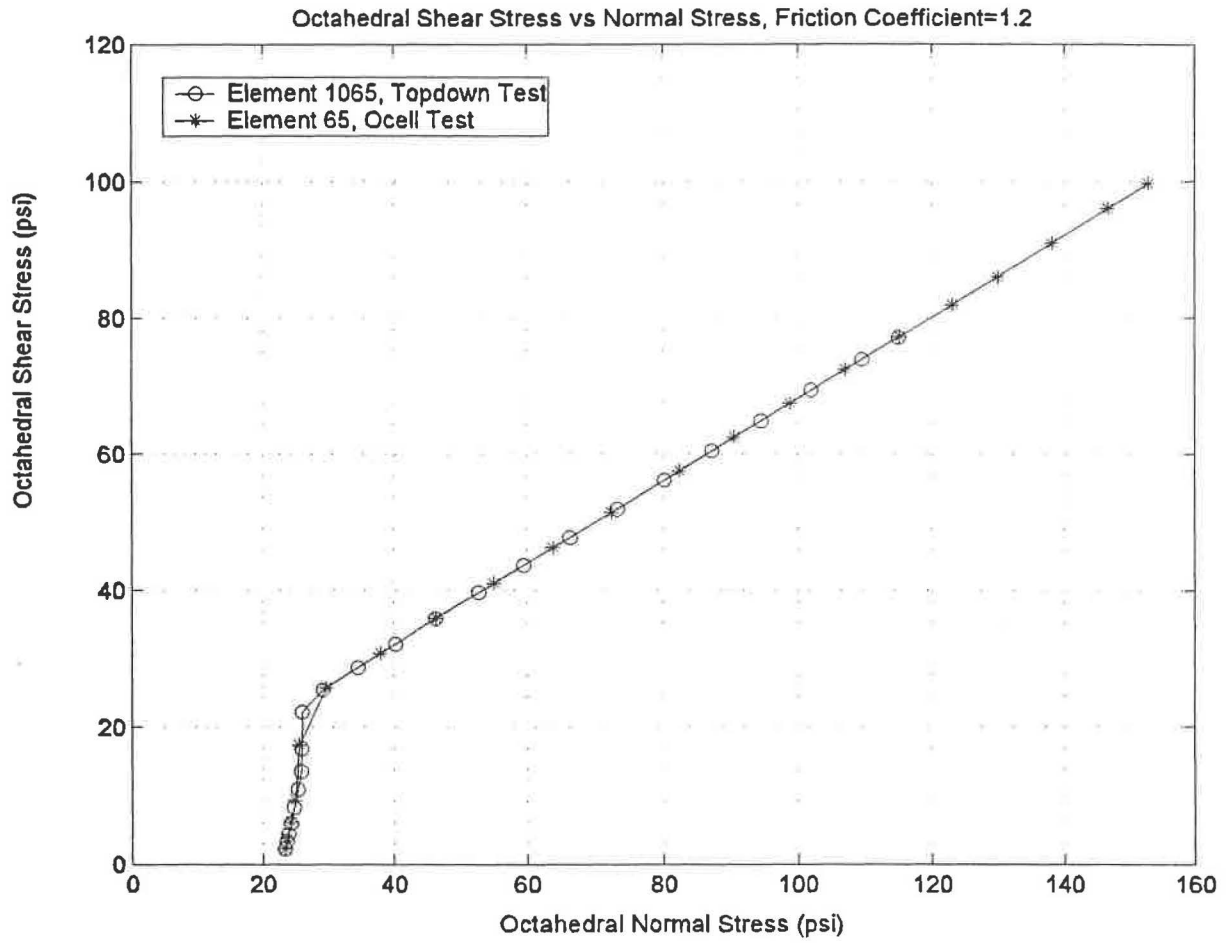
Figure A-53 Stress Path of Soil Element, $\mu = 1.2$

A-71
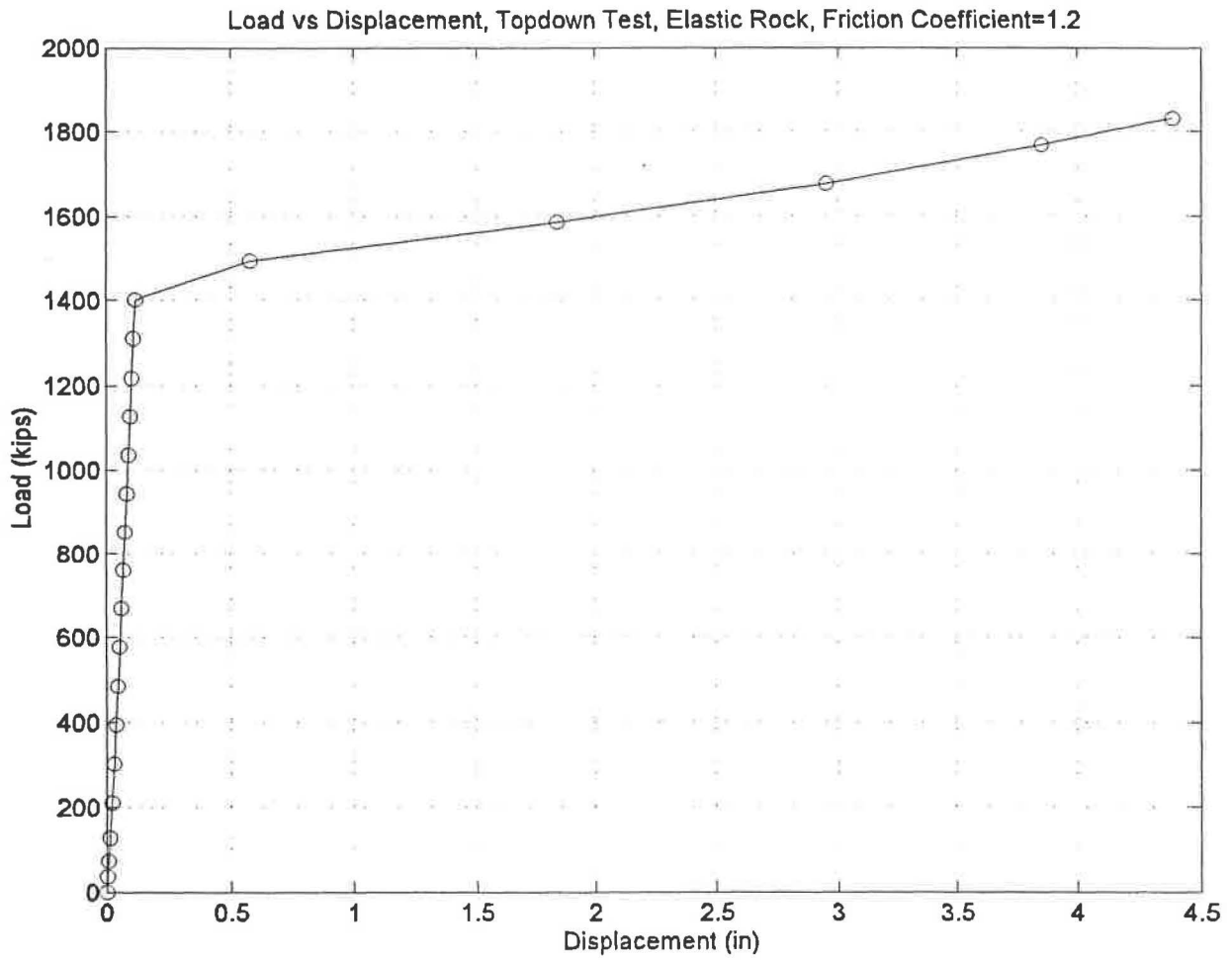
Figure A-54 Load-Displacement Curve, Topdown Test, Elastic Rock, $\mu = 1.2$
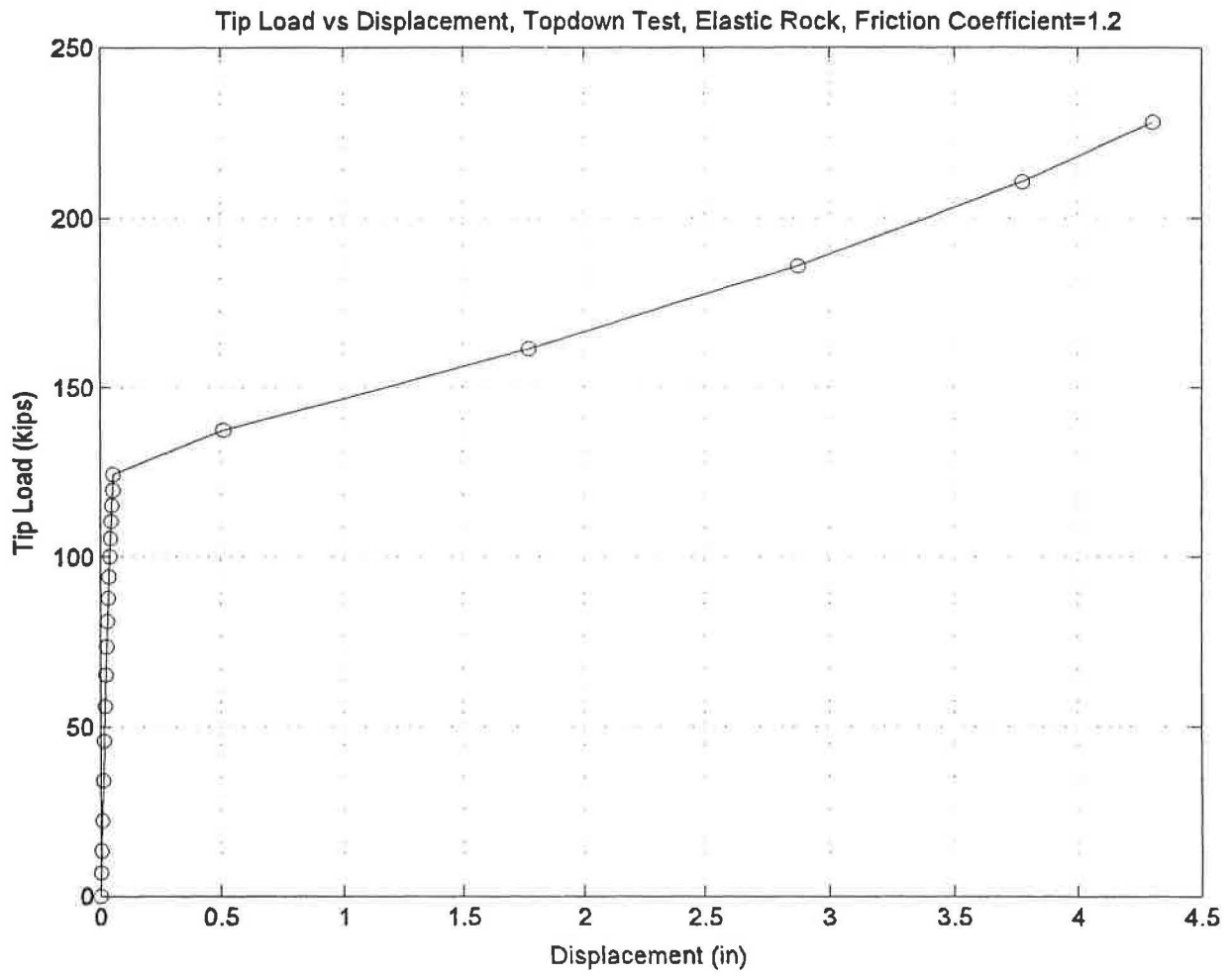
Figure A-55 Tip Load vs Displacement Curve, Topdown Test, Elastic Rock, μ=1.2
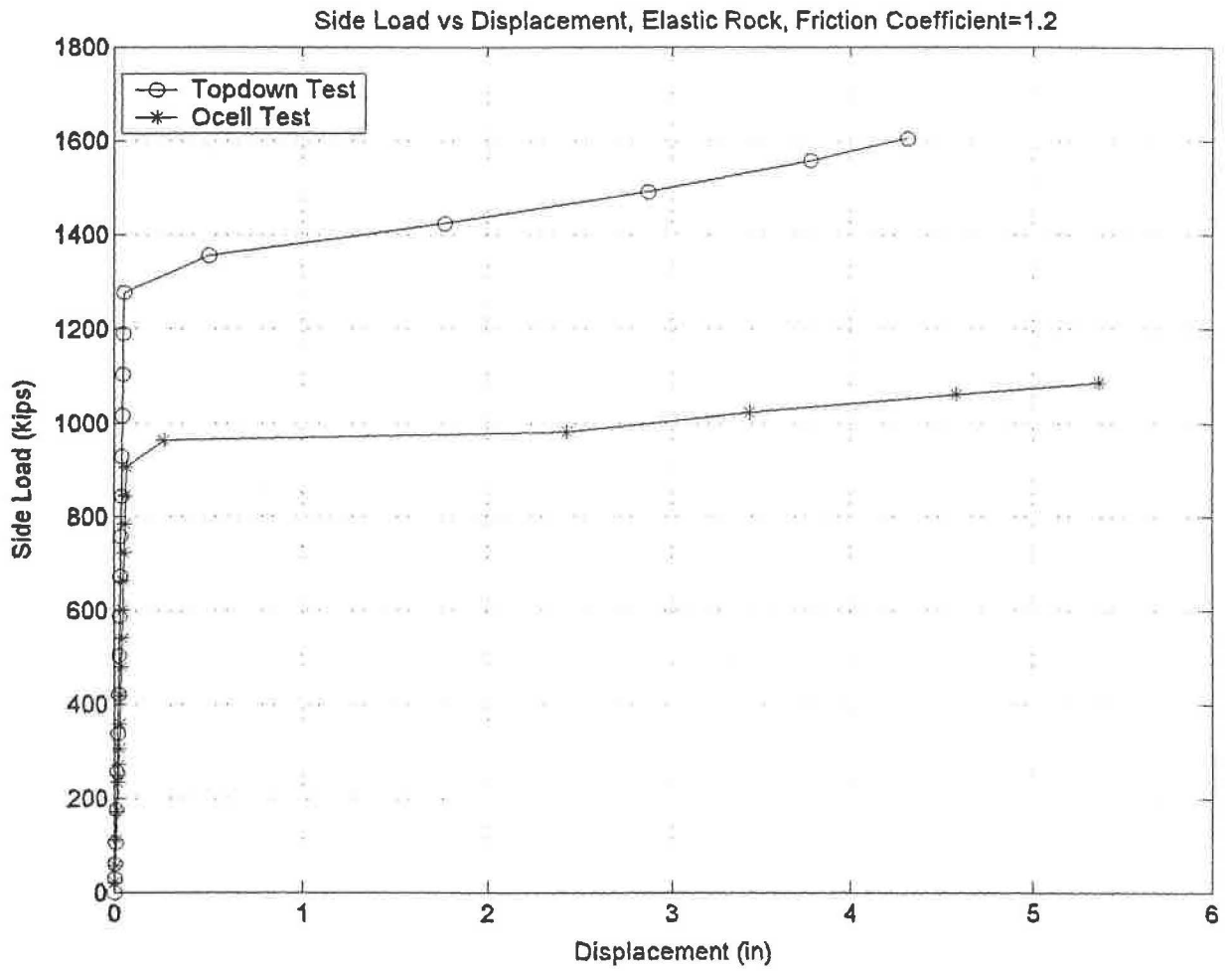
Figure A-56 Side Load vs Displacement Curve, Elastic Rock, μ=1.2
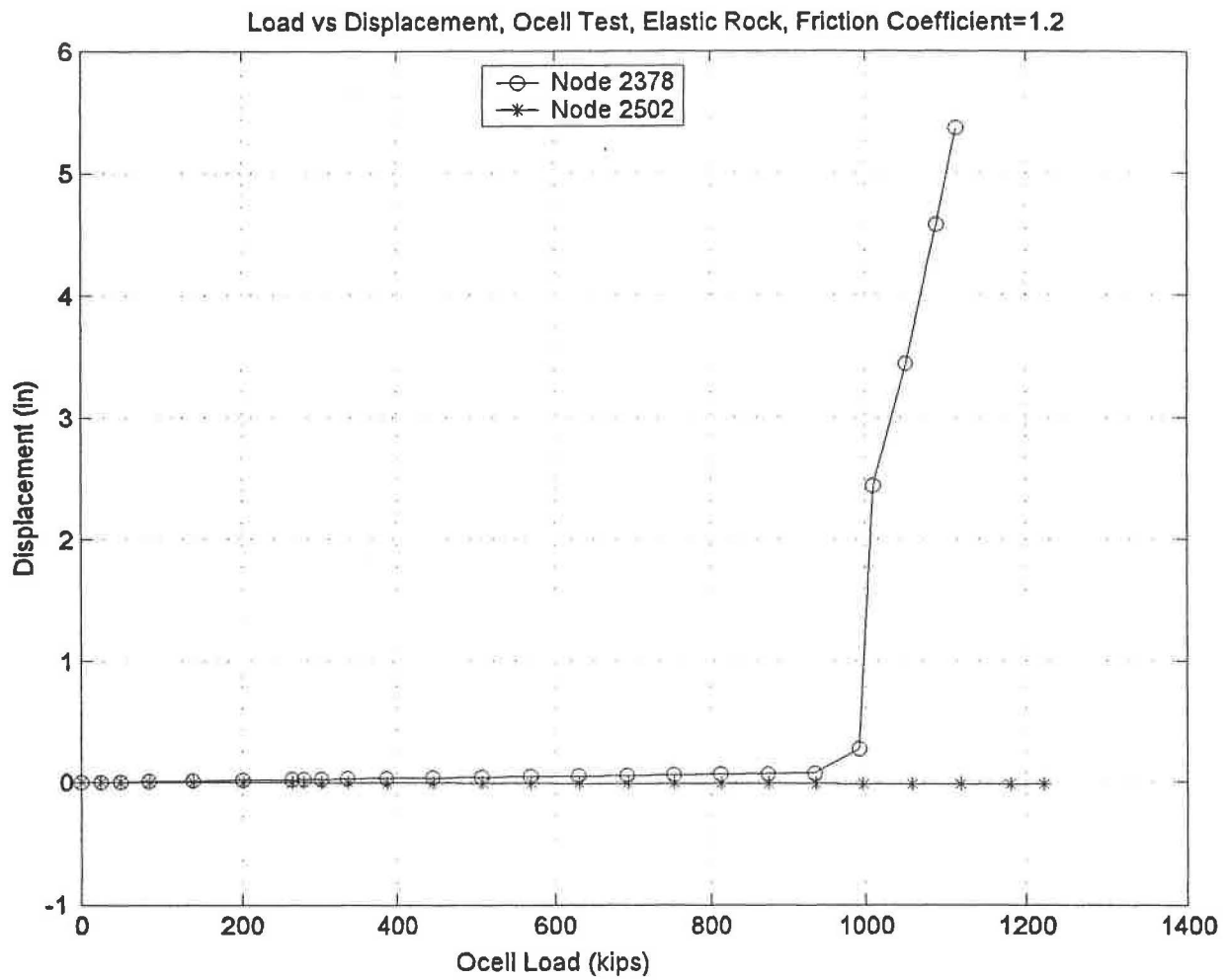
Figure A-57 Load-Displacement Curve, O-cell Test, Elastic Rock, μ=1.2
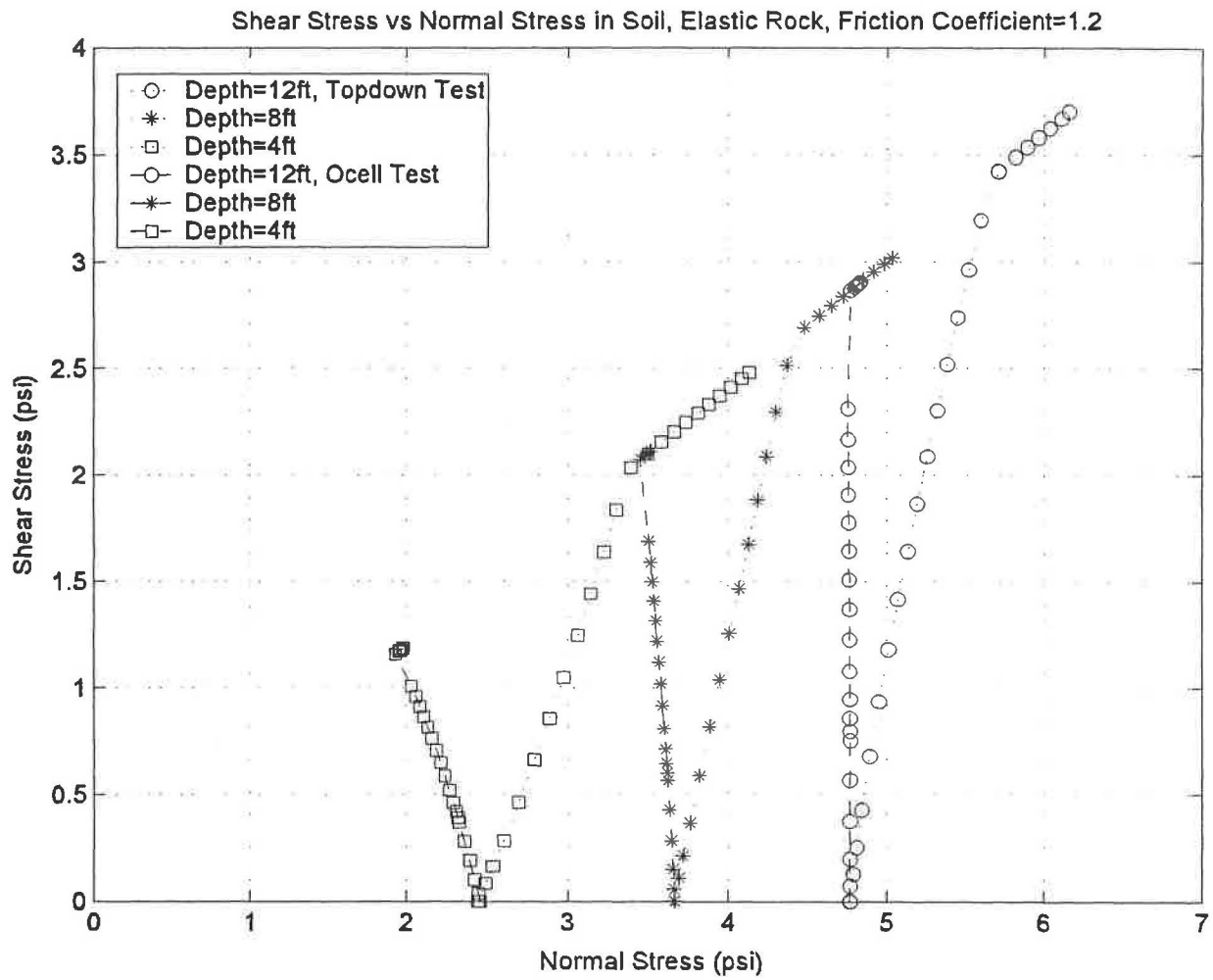
Figure A-58 Stress Path at Different Nodes on Soil-Pile Interface in Soil,

Elastic Rock, μ =1.2
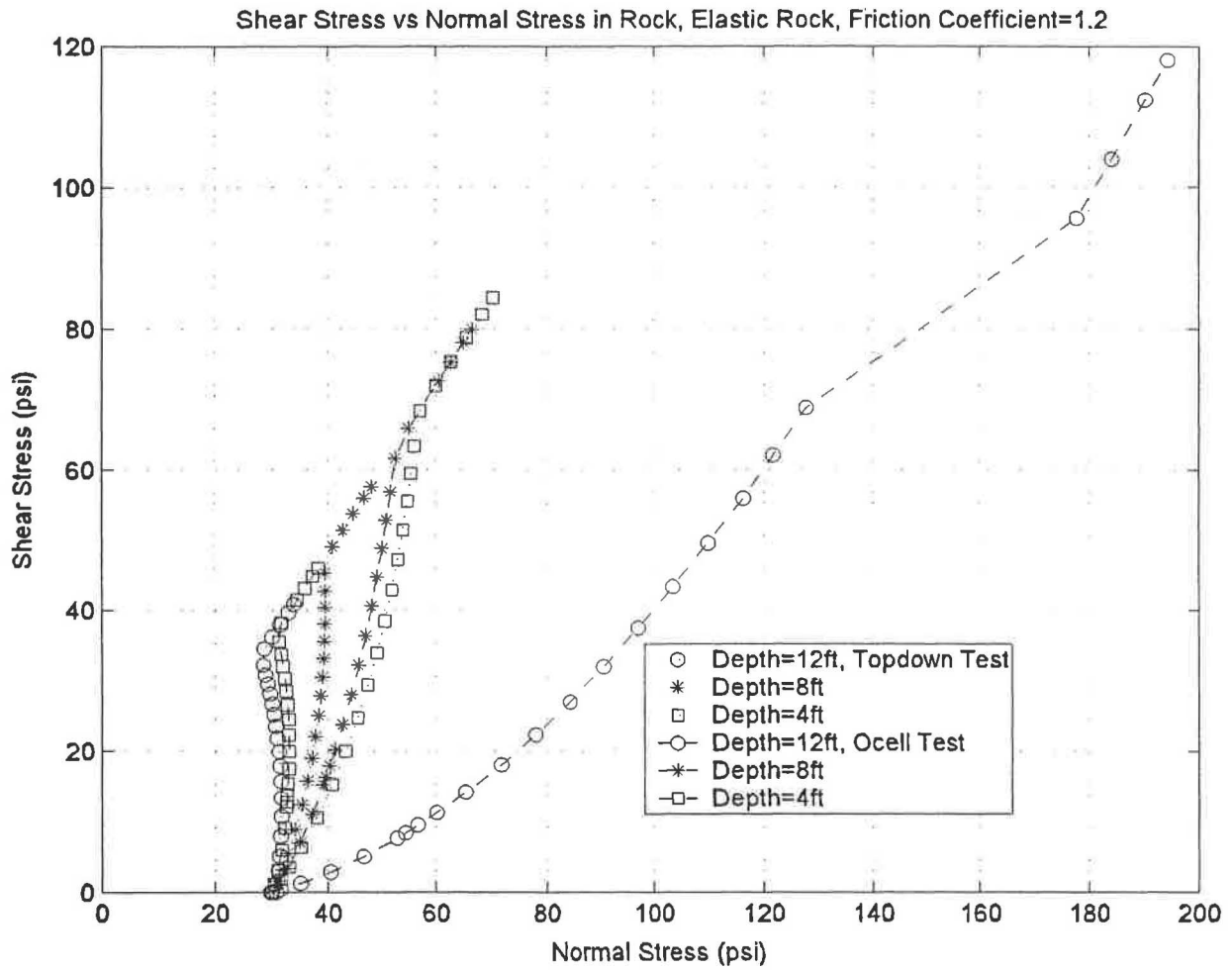
Figure A-59 Stress Path at Different Nodes on Soil-Pile Interface in Rock,

Elastic Rock, $\mu = 1.2$
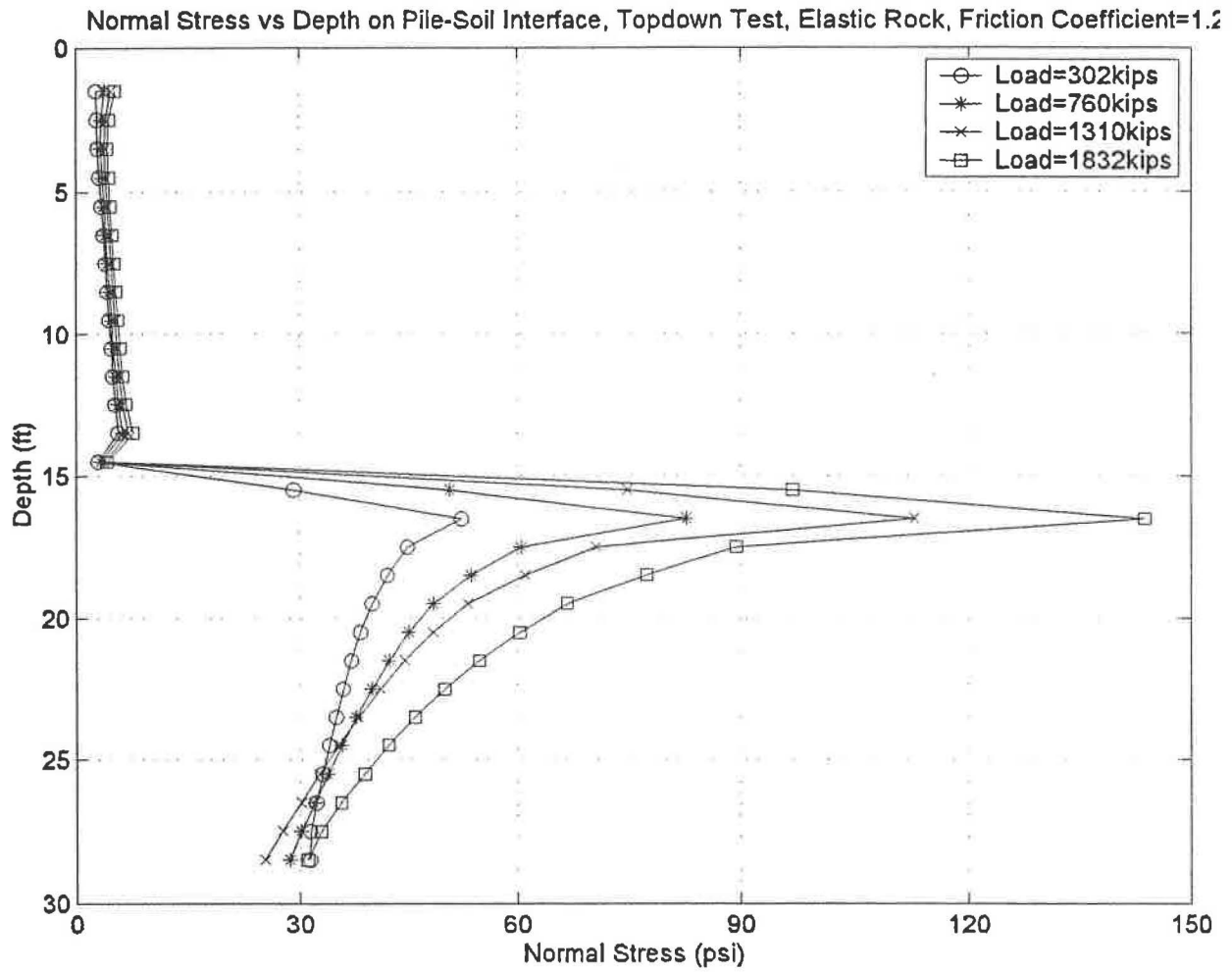
Figure A-60 Normal Stress vs Depth Curve, Topdown Test,
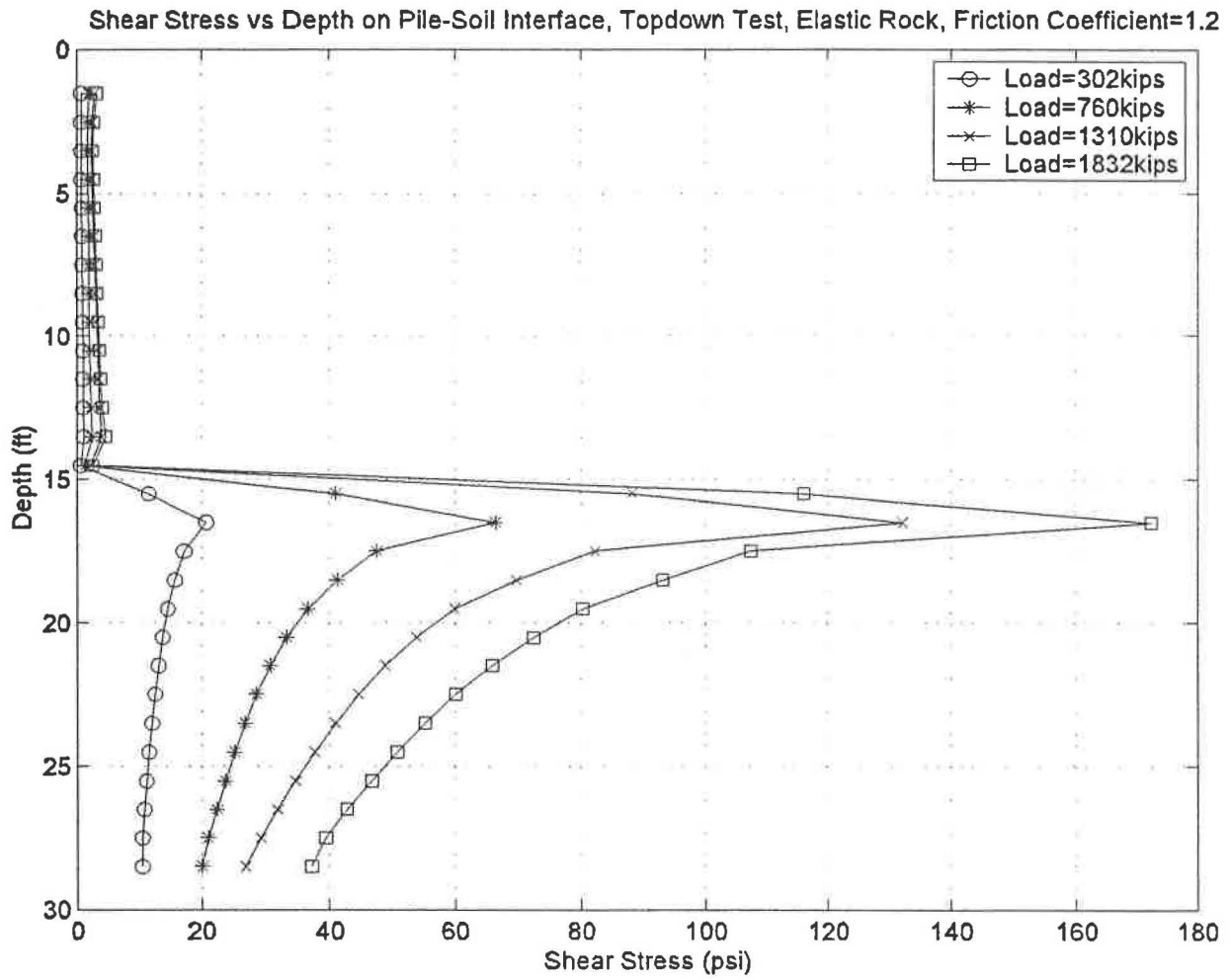
Elastic Rock, μ=1.2

Figure A-61 Shear Stress vs Depth Curve, Topdown Test,
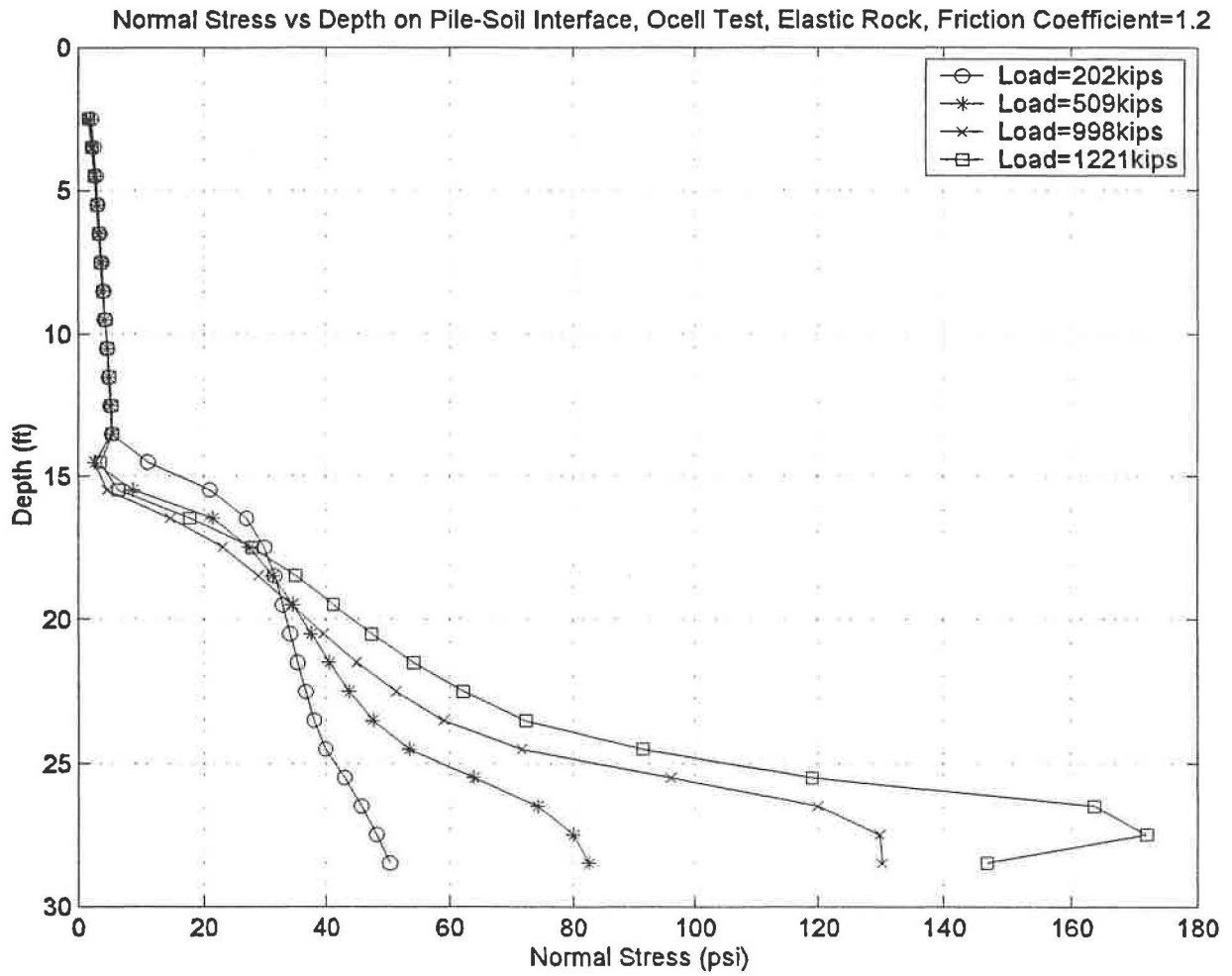
Elastic Rock, μ=1.2

Figure A-62 Normal Stress vs Depth Curve, O-cell Test,
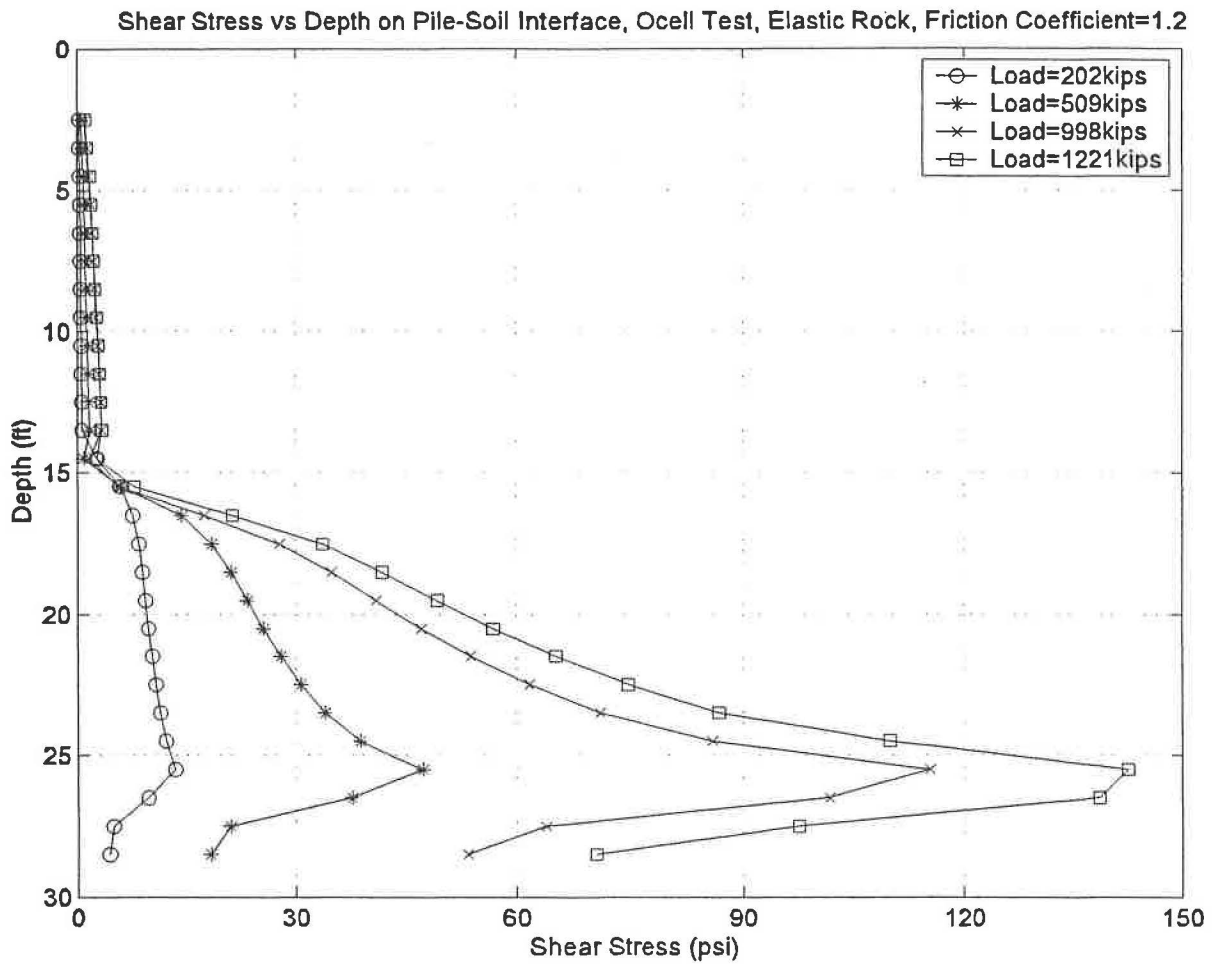
Elastic Rock, μ=1.2

Figure A-63 Shear Stress vs Depth Curve, O-cell Test,

Elastic Rock, μ=1.2